Title

The study of seasonal composition and dynamics of wetland ecosystems and wintering bird habitat at Poyang Lake, PR China using object-based image analysis and field observations

Author

Dronova, Iryna

Publication Date

2012

Peer reviewed|Thesis/dissertation

The study of seasonal composition and dynamics of wetland ecosystems and wintering bird habitat at Poyang Lake, PR China using object-based image analysis and field observations

By

Iryna Dronova

A dissertation submitted in partial satisfaction of the

requirements for the degree of

Doctor of Philosophy

in

Environmental Science, Policy and Management

in the

Graduate Division

of the

University of California, Berkeley

Committee in charge:

Professor Peng Gong, Chair
Professor Steven R. Beissinger
Professor John Radke

Fall 2012

The study of seasonal composition and dynamics of wetland ecosystems and wintering bird habitat at Poyang Lake, PR China using object-based image analysis and field observations

by Iryna Dronova

ABSTRACT

The study of seasonal composition and dynamics of wetland ecosystems and wintering bird habitat at Poyang Lake, PR China using object-based image analysis and field observations

by

Iryna Dronova

Doctor of Philosophy in Environmental Science, Policy and Management

University of California, Berkeley

Professor Peng Gong, Chair

Wetlands are among the most productive ecosystems in the world which support critical ecological services and high biological diversity yet are vulnerable to climate change and human activities. Despite their tremendous economic and ecological value, substantial uncertainty still exists about wetland ecosystem function, habitats and response to natural and anthropogenic stressors worldwide. This uncertainty is further aggravated by constrained field access and surface heterogeneity which limit the accuracy of wetland analyses from remote sensing images. In this thesis, I investigated the capabilities of satellite remote sensing with medium spatial resolution and object-based image analysis (OBIA) methods to elucidate seasonal composition and dynamics of wetland ecosystems and indicators of habitat for wintering waterbirds in a large conservation hotspot of Poyang Lake, PR China.

I first examined changes in major wetland cover types during the low water period when Poyang Lake provides habitat to large numbers of migratory birds from the East Asian pathway. I used OBIA to map and analyze the transitions among water, vegetation, mudflat and sand classes from four 32-m Beijing-1 microsatellite images between late fall 2007 and early spring 2008. This analysis revealed that, while transitions among wetland classes were strongly associated with precipitation and flood-driven hydrological variation, the overall dynamics were a more complex interplay of vegetation phenology, disturbance and post-flood exposure. Remote sensing signals of environmental processes were more effectively captured by changes in fuzzy memberships to each class per location than by changes in spatial extents of the best-matching classes alone. The highest uncertainty in the image analysis corresponded to transitional wetland states at the end of the major flood recession in November and to heterogeneous mudflat areas at the land-water interface during the whole study period. Results suggest seasonally exposed mudflat features as important targets for future research due to heterogeneity and uncertainty of their composition, variable spatial distribution and sensitivity to hydrological dynamics.

I further explored the potential of OBIA to overcome the limitations of the traditional pixel-based image classification methods in characterizing Poyang Lake plant functional types (PFTs) from the medium-resolution Landsat satellite data. I assessed the sensitivity in PFT classification accuracy to image object scale, machine-learning classification method and hierarchical level of vegetation classes determined from ecological functional traits of the locally dominant plant

species. Both the overall and class-specific accuracy values were higher at coarser object scales compared to near-pixel levels, regardless of the machine-learning algorithm, with the overall accuracy exceeding 85-90%. However, more narrowly defined PFT classes differed in their highest-accuracy object scale values due to their unique patch structure, ecology of the dominant species and disturbance agents. To improve classification agreement between different levels of vegetation type hierarchy and reduce the uncertainty, future analyses should integrate spectral and geometric properties of vegetation patches with species' functional ecological traits.

In periodically flooded wetlands such as Poyang Lake, rapid short-term surface dynamics and frequent inundation may constrain detection of directional long-term effects of climate change, succession or alien species invasions. To address this challenge, I proposed to classify Poyang Lake wetlands into "dynamic cover types" (DCTs) representing short-term ecological regimes shaped by phenology, disturbance and inundation, instead of static classes. I defined and mapped Poyang Lake DCTs for one flood cycle (late summer 2007-late spring 2008) from combined time series of medium-resolution multi-spectral and radar imagery. I further assessed sensitivity of DCTs to hydrological and climatic variation by comparing results with a hypothetical change scenario of a warmer wetter spring simulated by substituting spring 2008 input images with 2007 ones. This analysis identified the major steps in seasonal wetland change driven by flooding and vegetation phenology and spatial differences in change schedules across the heterogeneous study area. Comparison of DCTs from the actual flood season with the hypothetical scenario revealed both directional class shifts away from expanding permanent water and more complex location-specific redistributions of vegetation types and mudflats. These outcomes imply that changes in flooding may have non-uniform effects on different ecosystems and habitats and call for a thorough investigation of the future change scenarios for this landscape. The possibility to disentangle short-term ecological "regimes" from longer-term landscape changes via DCT framework suggests a promising research strategy for landscape ecosystem modeling, conservation and ecosystem management.

Following the assessments of Poyang Lake dynamics in the low water season, I further examined which landscape characteristics of the permanent sub-lakes and their 500-m neighborhoods extracted from 30-m Landsat satellite imagery could explain non-uniform spatial distribution of waterbird diversity and abundance in the ground bird survey of December 2006. I hypothesized that the indicators of habitat size, spectral greenness, spectral and geometric patch heterogeneity would be positively associated with bird diversity and abundance, while the proportions of cover types approximating human disturbance would be negatively related to response variables. In the best-fit regression models selected using the Akaike Information Criterion, on average higher bird diversity and abundance were associated with larger sub-lake size, higher spectral greenness of emergent grassland and lower spectral greenness of mudflat as well as lower proportion of flooded/aquatic vegetation. At the same time, predictive performance of the best-fit models was penalized by large amounts of unexplained variation and inconsistencies among bird survey and remote sensing data from another year. Significant spatial autocorrelation in linear regression models raised concerns about missing predictor variables and the utility of sub-lakes as spatial units for diversity analysis, but it also suggested new hypotheses on spatial ecological interactions in bird community variables and habitat characteristics among sub-lakes. Research challenges identified in this study suggest that future monitoring programs should take more rigorous steps to standardize the protocols of bird surveys and improve spatial and temporal frequency of both bird and habitat observations.

Rapid short-term surface variation and problematic field access will likely continue to limit remote sensing-based analyses of Poyang Lake wetlands and their habitats by traditional, static-class approaches. Using "dynamic" classes representing characteristic wetland transitions and disturbance regimes may provide more ecologically informative targets for management, conservation and modeling of ecosystem change. Object-based image analysis is a potentially powerful and promising approach to enhance classification accuracy of remote sensing data and ecologically informative interpretations of complex, heterogeneous wetland surfaces such as the study area. However, this methodology should be developed further to allow for more automated optimization of landscape object properties to capture vegetation patch structure and quantitatively assess propagation of the uncertainty among different spatial scales of the analysis. Finally, future studies should explore new ways of overcoming the limitations of problematic field access and frequent cloudiness obstructing the view of remote sensors by more rigorous utilization of in situ wireless sensors to record environmental conditions and surface composition and by introducing airborne lake-wide imaging programs for periods of prolonged cloudiness.

To my Mom and Dad

TABLE OF CONTENTS

INTRODUCTION

This dissertation investigated seasonal composition and dynamics of wetland ecosystems and indicators of habitat for wintering waterbirds in Poyang Lake, the largest freshwater lake in PR China and a unique biodiversity conservation hotspot under Ramsar Convention since 1992 (Ramsar 2012). This research was motivated, first of all, by the urgent need to improve the basic scientific understanding of Poyang Lake environment to facilitate conservation and management in the face of changing climate, numerous anthropogenic pressures and hydrological interventions in the region. I was also interested in enhancing the remote sensing-based methodology of landscape analysis and ecological inference for areas with heterogeneous and dynamic surface, limited field access and scarce records of historical data, such as the study area.

My specific objectives were to: 1) describe and investigate patterns of seasonal change in Poyang Lake wetland cover and assess the uncertainty of their classification from medium-resolution remote sensing data; 2) assess the benefits of the object-based image analysis (OBIA) framework over traditional pixel-based approaches to characterize and map functional diversity of Poyang Lake wetland vegetation with remote sensing; and 3) examine the extent to which spatial variation in waterbird diversity and abundance could be explained by landscape characteristics of their wintering habitat extracted from the satellite imagery. Below I summarize the key research needs which inspired my study and the structure of this thesis.

Research needs for wetland environments and their analyses with remote sensing

Wetlands are among the most ecologically diverse and productive ecosystems in the world that have been severely impacted by human activities. Global losses of wetland areas, increasing anthropogenic pressures on remaining sites and the uncertainty of climate change effects create an urgent need for sustainable wetland conservation and management strategies (Gibbs 2000, Dudgeon et al. 2006, Gong et al. 2010). Yet, scientific understanding of the linkages among wetland ecosystem functioning, biodiversity and multi-faceted ecological services is often still insufficient for sustainable ecosystem management and reliable projection of future change scenarios. Comprehensive field surveys in wetlands may be constrained by difficult on-site access due to soft waterlogged soil, dense vegetation, the risk of disturbing vulnerable habitats and species, and sometimes – large size and infectious disease agents (Chen and Lin 2004, McCarthy et al. 2005, Tuxen and Kelly 2008, Feng et al. 2012). This limitation has stimulated the use of remote sensing platforms for the analyses of wetland cover types, ecological habitats and biophysical parameters describing ecosystem function. The primary benefits of remote sensing for wetland research include the opportunities to capture vast and/or inaccessible areas at the same states of vegetation phenology and flooding, regular revisits, spectral sensitivity of instruments to surface composition and lower cost of data compared to frequent field visits (Johnston and Barson 1993, Ozesmi and Bauer 2002, McCarthy et al. 2005, Gong et al. 2010).

At the same time, the accuracy of wetland analyses from remote sensing data is frequently challenged by spatio-temporal heterogeneity of wetland surface resulting from high species diversity and fine-scale variation in topography, hydrology and disturbance (Johnston and Barson 1993, Ozesmi and Bauer 2002, Hestir et al. 2008). This may lead to spectral confusion among cover types, unreliable estimates of ecosystem variables and the infamous “salt-and-pepper” speckle in wetland maps where image pixels from the same cover type become assigned to different classes (Yu et al. 2006, Kim et al. 2011). One strategy to address these challenges is to revise the design of classification schemes to make the latter more conducive for

interpretations based on remotely collected information. For instance, landscape classifications of vegetation may be facilitated by incorporating plant functional traits which affect not only differences in their ecological performance but also biophysical, structural and spectral contrasts (DeFries et al. 1995, Bonan et al. 2002, Ustin and Gamon 2010). In some cases, heterogeneity of wetland surface may be caused by periodic inundation and high magnitude of flood-driven short-term variation of spectral reflectance. Characterizing such areas in terms of their common transitions may be a more useful and ecologically informative approach than trying to disentangle static land cover classes (Hess et al. 2003, McCleary et al. 2008, Crews 2008).

Another promising strategy for improving wetland cover interpretation from remote sensing data is the object-based image analysis (OBIA) which allows incorporating spatial structure of landscape patches into image classification (Blaschke and Strobl 2001, Benz et al. 2004, Blaschke 2010). With OBIA, cover type classification is preceded by image segmentation where the pixels are grouped into "objects" approximating meaningful landscape entities, patches or patch primitives. The primary benefits of this approach include: 1) reduced likelihood of "salt-and-pepper" speckle in the output due to smoothing of the local noise at the object level; 2) the possibility of using object shape, texture and "contextual" relationships with spatial neighbors as class discriminating features in addition to spectral values and 3) the possibility of hierarchical landscape analyses with nested different-scale object layers to incorporate relationships between ecosystem mosaics and broader topographic, hydrological and/or administrative units (Yu et al. 2008, Blaschke 2010, Liu and Xia 2010, Kim et al. 2011).

However, despite more than a decade of OBIA applications in environmental studies, the strengths of this framework have been relatively under-explored in continuous-cover landscapes, including heterogeneous wetlands, and with medium-resolution imagery. An important caveat with OBIA applications, particularly with the popular software, is high user flexibility to customize algorithms and steps of image analysis. This offers the benefit of achieving close match between image processing and ground targets; however, overly subjective rule sets may be difficult to generalize and apply among different image dates and locations (Rokitnicki-Wojcik et al. 2011). This issue may be addressed by 1) integration of OBIA with advanced machine-learning algorithms to enhance the quality of automated classifications and 2) developing spatially explicit quantitative methods for addressing the uncertainty in image analysis and its change with spatial scale of mapping units. Recent studies have started to explore these strategies (Yu et al. 2008, Liu and Xia 2010, Richmond 2011, Kim et al. 2011), but to date their utility for analyses of large heterogeneous wetland landscapes has not been fully assessed.

Poyang Lake wetlands and gaps in scientific understanding

My dissertation research focused on seasonal composition, dynamics and ecological attributes of Poyang Lake region in the central Yangtze River basin of PR China. This periodically inundated wetland area is a unique biodiversity hotspot hosting hundreds of thousands of wintering migratory waterbirds from the East Asian Flyway (Wu and Ji 2002, Ji et al. 2007, Ramsar 2012). Multiple concerns have been raised about the future of Poyang Lake ecosystems in the face of changing climate, shifting hydrological regimes due to operation of the Three Gorges Dam upstream Yangtze River (Guo et al. 2012), controversial projects for local hydrological dams (Barzen et al. 2009, Finlayson et al. 2010, Harris and Hao 2011), pollution and other anthropogenic pressures (Fang et al. 2006, Fox et al. 2011). While the severity of these threats has been increasingly recognized (Li 2009, Fox et al. 2011, Zhao et al. 2012, Guo et al. 2012), resolving these problems and optimizing the conflicting objectives among conservation efforts

and various users of Poyang Lake ecosystem services is still hampered by the lack of scientific understanding of this wetland environment and specific drivers of its dynamics.

Historically, comprehensive assessments of Poyang Lake ecosystems have been constrained by large size of wetland areas and difficult field access, the risk of water-borne infectious disease (Chen and Lin 2004) and the lack of high-resolution basin-wide bathymetric and digital elevation data. Temporal frequency of high-quality optical remote sensing images is often limited by the cloudiness in the region. Many of the previous remote sensing studies at Poyang Lake focused on single-date assessments of selected cover types (de Leeuw et al. 2006, Chen et al. 2007, Zeng et al. 2007, Michishita et al. 2008, Liu 2009), while multi-temporal basin-wide analyses addressed mainly the dynamics of inundation (Andreoli et al. 2007, Hui et al. 2008, Wu 2008, Zhao et al. 2011, Feng et al. 2012), and rarely vegetation or habitat features (Liu 2009, Wang et al 2012). Recent studies have started to discuss ecosystem components controlling Poyang Lake biogeochemical cycles and bird habitats (Wu 2008, Wang et al. 2012), but these efforts have not yet thoroughly addressed seasonal and inter-annual wetland dynamics. Furthermore, the utility of remote sensing to highlight landscape indicators of waterbird abundance and diversity at Poyang Lake and provide cost-effective habitat proxies has been largely unexplored, except for a few studies focusing on individual bird species or foraging guilds (de Leeuw et al. 2006, Wu 2008, Kwaiser 2009). There is an urgent need for a more rigorous assessment of spatio-temporal variation in bird community characteristics and suitable habitat features to inform ecosystem management and conservation and to reconcile conflicting land and natural resource use goals in the area (Burnham 2007, Barzen et al. 2009, Finlayson et al. 2010, de Boer et al. 2011).

Thesis structure

This dissertation is organized as follows. Chapter 1 investigated the change among major Poyang Lake wetland cover types and their classification uncertainty during the low water season from late fall 2007 to early spring 2008. During this period, landscape composition and dynamics directly affect wintering habitat of migratory birds, but surface cover types are much more heterogeneous than at high flood stages in the summer. I used OBIA to classify the landscape into major general cover types (water, mudflat, vegetation and sand) and proposed a new approach to allocate training samples despite limited field data using multi-temporal histograms of class-specific spectral indices. I further examined class changes among four Beijing-1 microsatellite images with 32-m spatial resolution. I quantified the changes among 1) spatial extents of the highest-likelihood classes assigned by the "hard" classification; and 2) fuzzy membership values to each class per location, regardless of the relative class ranks. Finally, I proposed a new method for quantifying classification uncertainty and compared it among different classes, image dates and fuzzy cutoff thresholds to assess the sensitivity of classification outcomes to the timing of available cloud-free imagery.

Chapter 2 more closely examined potential benefits of OBIA to enhance classification accuracy of Poyang Lake vegetation of the low water season relative to pixel-based methods. For this analysis, I first developed a classification scheme of plant functional types (PFTs) based on the dominant vegetation species traits related to morphology, physiology, seasonality and inundation tolerance. I hypothesized that using image objects as minimum mapping units approximating primitive patches of PFTs would enhance classification accuracy relative to pixels even with medium-resolution 30-m Landsat data. To investigate this hypothesis, I compared object-based PFT classification results among several "small" object segmentation scales representing different sizes of primitive vegetation patches, six different statistical machine-

learning algorithms and two levels of PFT ecological hierarchy. The primary objectives of this analysis were: 1) to determine whether an "optimal" segmentation scale can be found that would maximize classification accuracy for all PFTs and 2) to assess the agreement between ecological hierarchy of PFTs and class allocation based on the spectral and geometric properties of class objects and mapped patches.

In Chapter 3, I used the new understanding of the low water season dynamics and spatial distribution of PFTs to develop an alternative framework for assessing change in this rapidly varying landscape. Traditional change detection approaches may not be effective for Poyang Lake, because continuous variation in flooding and phenology often produces transitional states and sub-pixel or sub-objects mixtures of different classes. Instead, I proposed using "dynamic cover types" (DCTs) to characterize the landscape in terms of its common transitions representing short-term ecological regimes shaped by phenology, disturbance and inundation. I demonstrated how DCTs could be defined and mapped for one Poyang Lake flood cycle (late summer 2007-late spring 2008) from complementary time series of multi-spectral and radar images using OBIA and machine-learning classification algorithms. I also assessed potential sensitivity of DCTs to hydrological and climatic variation by comparing results with a hypothetical quasi-experimental change scenario of a warmer wetter early spring simulated by substituting spring 2008 input images with 2007 ones. Finally, I outlined the critical considerations for extending DCT framework to long-term change assessments, including temporal frequency and spatial resolution of the data, the choice of sensor(s), validation requirements and applicability to landscape ecosystem modeling and management.

Finally, Chapter 4 applied the generated understanding of the Poyang Lake environment and OBIA to examine which landscape characteristics were most closely associated with non-uniform spatial distribution of wintering waterbird diversity and abundance across this landscape. Using ground bird survey data from December 2006 and a temporally close Landsat TM image, I performed an object-based wetland cover type classification for 500-m neighborhoods of the surveyed sub-lakes within the "natural" wetland area. I then applied an information-theoretic model selection approach (Burnham and Anderson 2002) to determine the strongest and most consistent statistical predictors of several bird diversity and abundance metrics among candidate variables representing sub-lake area, proportions of habitat cover types, their spectral greenness, heterogeneity of their spectral and shape properties and classes associated with human disturbance. I further examined the potential importance of spatial autocorrelation in multivariate regression models and whether correcting for it improved model predictive strength. This analysis represented the first effort to explain spatio-temporal variation in the aggregate waterbird community characteristics at Poyang Lake with remote sensing. I also discussed the limitations of the available survey data and model performance and outlined the key challenges that need to be addressed by the future monitoring efforts and spatial analyses of waterbird diversity and habitat in this wetland.

ACKNOWLEDGEMENTS

I am very grateful to many colleagues, professors, organizations, friends and family who have helped me in my research and academic progress towards this PhD degree. I would like to first thank my PhD advisor, Professor Peng Gong, for his guidance and support along my path as a graduate student in UC Berkeley. My work and academic growth have been tremendously facilitated by his generous advice, research support, insight and great collaboration opportunities. I am also extremely grateful to him for encouraging me to think widely outside of the bounds of my immediate research area and to dare to seek new creative research venues for challenging questions.

I thank Professor Steve Beissinger, my qualifying exam and dissertation committee member, for his invaluable advice and encouragement and for teaching me to identify and appreciate the connections among ecology, conservation science and geospatial disciplines. I also thank my qualifying exam and dissertation committee member Professor John Radke for his advice, support and for teaching me to think critically about the meaning of space and scale in the environmental science.

My dissertation research would not be possible without the generous help from my colleagues in the State Key Laboratory of Remote Sensing Science (Beijing, China), the Center of the Earth Systems Science, Tsinghua University (Beijing, China), Jiangxi Normal University (Nanchang, China) and Poyang Lake Ecological Station for Environment and Health (Duchang, China). I am deeply thankful to Dr. Lin Wang for valuable help with obtaining and processing field and remote sensing data and wetland analysis. I thank Professors Shuhua Qi and Ying Liu from the Jiangxi Normal University for organizing wetland field surveys and to Professor Wan Wenhao from the Nanchang University for teaching me about Poyang Lake vegetation. I am very grateful to Dr. Huang Lingguang from the Center for Remote Sensing/GIS Application of Jiangxi Province (Nanchang, China) for the help with field spectral data collection. Finally, I thank Qiming Zheng, Wei Fu, Xuelin Zhou, Xiaoli Liu, Zhan Li and Shaoqing Shen for their invaluable assistance and great company during Poyang Lake field visits.

I also thank James Burnham from the International Crane Foundation for sparking my interest in unique and precious Poyang Lake wetland ecosystems and for continually helping me to learn more about them. Our discussions on the Poyang Lake ecology, human-nature interactions, research questions and challenges have greatly stimulated my research motivation and fascination with wetlands and waterbirds. James also provided advice on Chapter 4 of this thesis.

My dissertation work has tremendously benefited from the support of many colleagues at UC Berkeley. I am grateful to Professor Greg Biging for advice, support and encouragement of my research and future career. I also thank him for an exciting series of joint lab meetings with our group, which have broadened my understanding of environmental remote sensing and spatial analysis. I also thank my UC Berkeley colleagues and friends from the Gong and Biging research groups, especially Nick Clinton, Lu Liang, Liheng Zhong, Yanlei Chen, Kyle Holland and Yu-Ting Huang for their research advice, comments, help and moral support. I thank Professor Maggi Kelly for her guidance as my qualifying exam committee member and for sparking my interest in the object-based image analysis (OBIA). I am very grateful to Kevin Koy, Mark O'Connor and UC Berkeley's Geospatial Innovation Facility for the opportunity to learn and apply OBIA software which helped to form an exciting research direction for my thesis.

I am very grateful to many professors in the Department of Environmental Science, Policy and Management for their guidance, advice, support and for being outstanding role models to graduate students. I thank Professor Dennis Baldocchi for his advice and for teaching me to

appreciate the complex multi-scale biometeorological linkages in our environment. Taking his courses, communicating with his research group and working with him as a teaching assistant for Ecosystem Ecology and student representative on the faculty search committee has greatly enriched my understanding of ecosystem science and inspired my future research and career goals. I thank my graduate academic advisor, Professor Kevin O'Hara, for support and for guiding me through the academic requirements towards my degree. I also thank Professor Todd Dawson for being on my qualifying exam committee and providing useful research advice at the early stage of my study. I also thank Professor Whendee Silver for being a terrific teacher and scientist role model and for inspiring me to think about ecosystem ecology in new and broader ways. I also thank Professor Katharine Suding and her lab for inspiring me to think about new research perspectives on landscape-scale vegetation ecology. Finally, I thank the whole ESPM department – professors, administration, staff and students, for providing a fantastic stimulating intellectual environment for the studies, research and communication over these years.

I am very grateful for the financial support of this research by the National Aeronautics and Space Administration (NASA) Earth and Space Science Student Fellowship 2009-2012 (NNX09AO27H), additional support from the grant from the National High Technology Programme of China (2009AA12200101) and funding from the University of California, Berkeley.

I am also very grateful to many family members, relatives and friends who supported me throughout my graduate school journey. I thank my dear Mom for her immense love and encouragement of my aspirations. She passed away during the first year of my PhD following a tough battle with cancer, but her love and advice have continued to support me on this path and into the future. I thank my Dad for his love and help and for sparking my curiosity about nature and quantitative methods from my early childhood. I am deeply thankful to my parents-in-law, my sister-in-law and her family for all their love and enormous help during these years and to my sister and my brother-in-law for their love and support. I also thank Lenochka, Tanyusha, Katyusha, Alice, YeS, Shasta, Lisa, Sarah, Lu, Yu-Ting and Siew Chin for lots of positive encouragement and precious friendship.

Finally, I cannot thank enough my dear husband Yuriy for all his help and for being my wonderful partner, friend and colleague. This all would not be possible without him and our dearest son who turned my PhD study into an exciting, joyful adventure and gave a new meaning to my career and entire life.

CHAPTER 1. Object-based analysis and change detection of major wetland cover types and their classification uncertainty during the low water period at Poyang Lake, China

This article has been published previously and is reproduced here with permission from the publisher, Elsevier

Dronova I, Gong P, Wang L. 2011. Object-based analysis and change detection of major wetland cover types and their classification uncertainty during the low water period at Poyang Lake, China. Remote Sensing of Environment 115: 3220-3236.

Abstract

Productive wetland systems at land-water interfaces that provide unique ecosystem services are challenging to study because of water dynamics, complex surface cover and constrained field access. We applied object-based image analysis and supervised classification to four 32-m Beijing-1 microsatellite images to examine broad-scale surface cover composition and its change during November 2007-March 2008 low water season at Poyang Lake, the largest freshwater lake-wetland system in China (>4000 km^2). We proposed a novel method for semi-automated selection of training objects in this heterogeneous landscape using extreme values of spectral indices (SIs) estimated from satellite data. Dynamics of the major wetland cover types (Water, Mudflat, Vegetation and Sand) were investigated both as transitions among primary classes based on maximum membership value, and as changes in memberships to all classes even under no change in a primary class. Fuzzy classification accuracy was evaluated as match frequencies between classification outcome and a) the best reference candidate class (MAX function) and b) any acceptable reference class (RIGHT function). MAX-based accuracy was relatively high for Vegetation (≥90%), Water (≥82%), Mudflat (≥76%) and the smallest-area Sand (≥75%) in all scenes; these scores improved with the RIGHT function to 87-100%. Classification uncertainty assessed as the proportion of fuzzy area within a class at a given fuzzy threshold value was the highest for all classes in November 2007, and consistently higher for Mudflat than for other classes in all scenes. Vegetation was the dominant class in all scenes, occupying 41.2-49.3% of the study area. Object memberships to Vegetation mostly declined from November 2007 to February 2008 and increased substantially only in February-March 2008, possibly reflecting growing season conditions and grazing. Spatial extent of Water both declined and increased during the study period, reflecting precipitation and hydrological events. The "fuzziest" Mudflat class was involved in major detected transitions among classes and declined in classification accuracy by March 2008, representing a key target for finer-scale research. Future work should introduce Vegetation sub-classes reflecting differences in phenology and alternative methods to discriminate Mudflat from other classes. Results can be used to guide field sampling and top-down landscape analyses in this wetland.

Introduction

Natural interfaces between terrestrial and aquatic environments often host wetland systems which support important ecosystem services, high productivity and biodiversity yet may be vulnerable to climate change, human activities and alien species invasions (Nicholls et al. 1999, Gibbs 2000, Mitch and Gosselink 2000, Zedler and Kercher 2004, Dudgeon et al. 2006, Houlahan et al. 2006). One of the first steps in uncovering the complexity of wetland surface

cover and its temporal variation is studying the context in which biotic components of wetland ecosystems such as vegetation interact with physical environment including atmosphere, hydrology, soil and geomorphology. At the broad landscape scales these relationships can be manifested in spatio-temporal associations between vegetation and non-vegetated cover types at a given location following water fluctuations (Gilmore et al. 2008, Wang et al. 2012).

In this study we specifically consider freshwater lake-wetland systems characterized by seasonal and interannual fluctuations of the water extent due to hydrological and/or climatic cycles such as seasonal change in river discharge, precipitation and human regulations of the water levels. Such spatio-temporal variation produces complex changes in surface cover and vegetation across seasons and years which are further affected by wildlife grazing (Lodge 1991, Mitchell and Perrow 1998). In wetlands with seasonal flood cycle (such as in subtropical regions with monsoonal climate), periods of low water levels are particularly important for establishment and productivity of emergent vegetation (Chen et al. 2007, Barzen 2008, Miller and Fujii 2010) and thus for seasonal nutrient cycling. Studying these dynamics is essential for understanding wetland productivity, the source-sink distribution for nutrients and greenhouse gases as well as associated wildlife habitats and hazard risks (Davidson and Janssens 2006, Dudgeon et al. 2006, Jiang et al. 2008, Niu et al. 2009, Barzen et al. 2009, Marie et al. 2010).

However, comprehensive assessments of such lake-wetland systems may be challenging due to limited on-site access to inundated areas, complexity of cover type and ecosystem composition, sometimes vast system dimensions and the risk of infectious disease (Marie et al. 2010). For these reasons, remote sensing provides useful sensors and methods to investigate large wetland systems and monitor their change over time (e.g., Johnston and Barson 1993, Baker et al. 2006, Niu et al. 2009, Gong et al. 2010). Satellite-based remote sensing is especially useful due to simultaneous capture of large areas at the same phenology stage and the possibility of consistent revisit. In particular, moderate-resolution multispectral sensors such as Landsat, SPOT, and ASTER have been successfully used for studying the extent of flooding and affected land cover (Johnston and Barson 1993, Jiang et al. 2008, Hui et al. 2008, Qi et al. 2009), detecting presence and composition of wetlands in heterogeneous landscapes (Baker et al. 2006, Wright and Gallant 2007), extracting vegetation characteristics (Li and Liu 2002, Michishita et al. 2008) and monitoring invasive plant species (Laba et al. 2010). However, 10-30 m spatial resolution is sometimes too coarse for accurate discrimination of fine-scale mosaic in heterogeneous wetlands (Wright and Gallant 2007, Laba et al. 2010), which may necessitate fuzzy analysis and sub-pixel inference (Li et al. 2005, Gilmore et al. 2008). Novel microsatellite sensors combining multispectral capacity, medium spatial resolution, large-area coverage and frequent revisit time are promising for assessment of vast wetland areas (Wang et al. 2012).

Recently, Object-Based Image Analysis (OBIA) has been applied more frequently for image classification and change detection in wetland and inundated systems (Gilmore et al. 2008, Conchedda 2008, Laba et al. 2010). In contrast to pixel-based analysis, OBIA methods consider landscapes as aggregations of meaningful objects corresponding to ground entities and patches of surface cover (Blaschke et al. 2000, Benz et al. 2004, Arbiol et al. 2006). As a result, some OBIA advantages compared to pixel-based methods include: 1) adding object shape and context (e.g., neighborhood characteristics) to spectral and textural information in the analysis and 2) absence of "salt-and-pepper" pattern of closely located pixels assigned to different classes which is common in pixel-based classifications (Yu et al. 2006). Context is particularly important in classifications of wetlands (Wright and Gallant 2007) given their high spatial heterogeneity and

gradients of soil moisture and water depth. These features make OBIA a very useful research venue for both single-date and multitemporal wetland studies (Desclee et al. 2006, Conchedda 2008, Shen et al. 2008, Johansen et al. 2010).

However, OBIA has not yet been extensively applied in natural landscapes where continuous variation in vegetative cover "dilutes" the boundaries between potential "objects" thus creating challenges for cover type classifications (Dorren et al. 2003, Yu et al. 2006, Grenier et al. 2007, Mallinis et al. 2008, Yu et al. 2008). Previous studies in vegetated landscapes have reported both higher (e.g., Johansen et al. 2010, riparian and forest ecosystems) and lower (Dorren et al. 2003, mountainous forests) OBIA classification accuracies compared to pixel-based methods. Among wetland studies, Laba et al. (2010) demonstrated how the overall classification accuracy could be improved by incorporating texture variables generated via object-based classification. Gilmore et al. (2008) reported relatively high object-based classification accuracies for a number of wetland vegetation types and discussed sources of error resulting from multiple possible class memberships in heterogeneous wetland environment.

Typically OBIA involves two major steps: 1) segmentation of the image into objects representing groups of pixels at desired scale, shape and compactness criteria (Benz et al. 2004, Clinton et al. 2010) and 2) classification of the segments into categories of interest. In supervised classifications, training object data for the classes of interest also need to be specified prior to step 2. Previous vegetation analyses derived training objects from tree crowns and canopy gaps in woodlands (Bunting and Lucas 2006, de Chant and Kelly 2009), from patches of specific plant types traced either with GPS in the field or within fine-resolution images and aerial photos (Laliberte et al. 2004, Yu et al. 2006) and from field survey plots with known ground characteristics (Dorren et al. 2003, Yu et al. 2008). In heterogeneous and dynamic wetlands with limited ground access, however, such object-level training data may be difficult to obtain. To address this challenge, one solution may be in using very small spectrally homogeneous primitive or "prototype" objects in classification, rather than searching for larger objects exactly matching ground entities. "Prototype" objects can be classified analogous to pixels but with added shape and context information (Blaschke et al. 2000, Tzotsos 2006, Gilmore et al. 2008, Tian et al. 2008), and larger patches can be recovered in classification outcome. Another beneficial strategy is to use image spectral information to guide training object selection. Gilmore et al. (2008) used field vegetation type spectra and LiDAR canopy height data to generate rules guiding object-based wetland classification. In a forested landscape OBIA study (Chubey et al. 2006), IKONOS bands were thresholded according to the signal from different cover types to obtain training data for the land cover classification. Similarly, image-estimated spectral indices (SIs) which represent surface moisture, vegetation or soil brightness (Crist and Cicone 1984, Baret and Guyot 1991, McFeeters 1996) may provide useful information for training data selection but have not yet been extensively utilized in this respect.

In this study, we applied OBIA to examine broad-scale composition of the general surface cover types and their change during the low water season at the large dynamic freshwater lake-wetland system of Poyang Lake, People's Republic of China (Figure 1). Recent wetland research in China using geospatial technology have demonstrated the critical need for monitoring wetland systems and assessing their ecological components at multiple spatial scales (Niu et al. 2009, Gong et al. 2010). The evaluation and future decision on a recently proposed new dam project at the Poyang Lake outlet (Li 2009) require enhanced understanding of the present seasonal ecological variation in this system which is also a unique biodiversity hotspot

and a Wetland of International Importance under Ramsar Convention (Barzen et al. 2009, de Leeuw et al. 2010, Finlayson et al. 2010).

Our analysis was intended as the first step in the top-down hierarchical assessment of seasonally variable Poyang Lake surface composition. We explored new approaches to select training data for a basic object-based image classification and to investigate classification uncertainty both in terms of its spatial distribution and quantitative magnitude. We pursued the following specific objectives: 1) to classify major general surface cover types of Poyang Lake using OBIA, 2) to find an approach for selecting training objects for the classes of interest using spectral indices (SIs) derived from the satellite imagery, 3) to propose additional quantitative criteria for assessment of classification uncertainty and 4) to investigate changes in cover type composition and classification uncertainty following dynamics of Poyang Lake water body during the 2007-2008 low water period.

Methods

Study area

This study focuses on the main extent of Poyang Lake in the lower Yangtze River basin of China (28°25'-29°45'N, 115°48'-116°44'E; Figure 1). Surface water coverage here varies from >4000 km^2 during summer monsoon rain season to <1000 km^2 in winter, when the area becomes a system of sub-lakes interspersed with mudflats, sediment beds and vegetation (Shankman et al. 2006, Andreoli et al. 2007, Jiang et al. 2008). Water level fluctuations affect local cover types, soil moisture and inundation gradients producing a mosaic of aquatic and wetland ecosystems (Barzen et al. 2009). The low water period at Poyang Lake lasts approximately from November to late February-early March, although the exact timing may vary across years (Shankman et al. 2006, Andreoli et al. 2007, Wang et al. 2012). Generally, during this period the overall reduction of the water body area is expected to continue until the next rain season; however, winter precipitation events and hydrological variation (Figure 2a, b) may produce more complex dynamics. While water level changes of the low water season are less dramatic than those of the rain season, they influence lake-wetland cover types, vegetation and ecosystem productivity during the 'cool' lower-temperature winter growing season, which, in turn, governs the availability of food and habitat to wildlife (Chen et al. 2007, Wang et al. 2012).

Remote sensing data

We used November 30, 2007 and January 01, February 16 and March 02, 2008 images (hereafter scenes Nov07, Jan08, Feb08 and Mar08, respectively) of Beijing-1 microsatellite sensor (Surrey Satellite Technology Ltd) which has three spectral bands (near-infrared (NIR) 0.77-0.90 μm, red 0.63-0.69 μm, green 0.52-0.60 μm), five-day revisit time and wide 600-km image swath. Given the large size of the Poyang Lake system and common cloudiness which limit frequent acquisition of high-quality scenes, we used Beijing-1 data as the compromise between maximizing revisit time and scene size and reducing spatial resolution. Because this sensor does not have a calibration system on board, we used only Digital Numbers (DNs), and not ground-level reflectance, in the analysis. For image classification and change detection, we conducted relative radiometric calibration of Nov07, Feb08 and Mar08 scenes to Jan08 image using scene-to-scene regression of image DNs from pseudo-invariant targets selected among temporally stable features such as bright sand in dunes and dark water in permanent reservoirs in ENVI 4.7 (ITT Visual Solutions Inc.). To delineate the main lake- wetland area for the analysis, we used Envisat ASAR WSM image for August 16, 2007 when water extent was near its annual

maximum. We also delineated and isolated human residential areas and intensive land uses such as agriculture and man-made reservoirs outside wetland using Microsoft Bing Maps image layer within ArcGIS 10 (ESRI Inc.) and Google Earth (Google Inc. 2010).

General procedure and image segmentation

First, we implemented image segmentation and object classification in eCognition Developer 8 (Definiens 2009) by building rule sets that were applied to each scene (Figure 3). In classification we considered the following major general Poyang Lake cover types: Water, Vegetation, Sand, Mudflat (Table 1). Then we conducted post-classification change detection and accuracy assessment in ArcGIS 10 (ESRI Inc.) and further evaluated spatial distribution and quantitative magnitude of classification uncertainty (Figure 3).

To segment each scene into small prototype objects we used eCognition multiresolution segmentation tool because in a heterogeneous natural landscape "meaningful" spectrally homogeneous objects can occur at different spatial scales (Blaschke et al. 2000, Arbiol 2006). Because varying soil moisture and water depth could emphasize the variation of spectral reflectance in the NIR region, we gave higher weight to NIR band than to others.

To select the most suitable segmentation, we assessed the output sensitivity to multiple combinations of shape, scale and compactness (Benz et al. 2004, eCognition Developer 8 Reference Book, Clinton et al. 2010) and evaluated the following criteria:

1) Mean object homogeneity, as scene-average within-object standard deviation (SD);
2) Mean contrast to neighbors, as scene-average Mean Difference to Neighbors (MDN; eCognition Developer Reference Book);
3) Variation in object shape, as scene-average ratio of object length to width (L/W).

Criterion 1 was the most important (Borsotti et al. 1998, Blaschke et al. 2000, Chabrier et al. 2006) because as classification units, prototype objects need to be homogeneous. Maximizing MDN was also important (Levine and Nazif 1985, Borsotti et al. 1998) but not the highest priority because similar neighbor objects were expected given potential spatial autocorrelation along the wetness gradients in this landscape. Finally, criterion 3 was considered specifically for Poyang Lake low water period when high variation in shapes is expected with objects ranging from more compact (pools of water) to narrower long features (stream channels, belt-shaped near-shoreline areas).

We found that scene-average SD for each band increased with both greater scale and greater shape parameter values. Scene-average MDN generally decreased with greater compactness, and as segmentation shape increased, the difference in MDN between low and high compactness values became greater. Finally, the highest scene variance of L/W occurred at lower shape and lower compactness. Thus, the combination of low shape (0.2), low compactness (0.1) and small scale (5) values represented the suitable compromise providing relatively low within-object variation, relatively high scene-average MDN and variation in object shape and were chosen for the analysis.

Image classification

Pre-processing

Prior to classification of the natural wetland area, we isolated darker-colored areas corresponding to patches of dead reeds (*Miscanthus* and *Phragmites* spp.) that had been harvested and burned by local people. Burned areas (<4% of the total study area) were isolated using scene-specific

rule sets which first detected dark burned patch objects that were best discriminated from other classes. We then applied a region-growing procedure to these objects until the mean absolute difference of Normalized Difference Vegetation Index (NDVI) to neighbors reached a threshold value indicating the end of the burned area and beginning of another cover type. In classification maps and change analysis burned areas were labeled as Vegetation because they were typically located next to similar undisturbed reed stands and contained young regrowth.

Next, we conducted supervised classification of prototype objects in each scene into Water, Vegetation, Sand and Mudflat (Table 1) using supervised nearest neighbor classifier within eCognition. This procedure requires a set of class-specific training objects from which the distributions of object-level variables (features) are obtained to evaluate membership functions of each class; ideally, these features should be selected so as to facilitate the best discrimination of classes based on training data. Resulting membership functions are applied to each non-training object to evaluate its membership to alternative classes and to assign a class based on the maximum membership value.

At this stage of analysis we identified two major challenges which were addressed in later steps. First, it was necessary to select the appropriate training objects adequately representing each class given the lack of "standard" object types in this heterogeneous landscape. Below in section 2.4.1 we present a method for training sample selection using statistical distributions of spectral indices. Second, to identify the locations of potentially heterogeneous Mudflat objects (Table 1), we had to classify Vegetation, Water and Sand classes first and then apply additional spectral and context criteria to find training samples and classify Mudflat (Figure 3), as discussed in section 2.4.2.

Training sample selection

We propose a method to select training samples from the initial segmentation result, which to our knowledge has not been previously used in supervised object-based wetland classifications. This approach is based on the premise that our chosen classes (Table 1) are distinct cover types, appropriate for the given image spatial resolution. Hence one may assume that the most "representative" objects for a class are located close to the extremes of the spectral indexes (SIs) or band transformations which highlight that class most effectively. Specifically, we used NDVI to represent Vegetation, where higher object-level NDVI values indicated a higher probability of a vegetated object. Likewise, Normalized Difference Water Index (NDWI; McFeeters 1996) represented Water, with higher NDWI suggesting higher chance of a water object. For Sand the eCognition feature Brightness was used (eCognition Developer Reference Book) with the highest values corresponding to bright homogeneous sand dunes and beaches.

Importantly, to determine which objects with the highest values of a respective index should be included in the training set, we needed to specify a cutoff threshold value for the index so that training objects could be selected from a pool of objects above that threshold value. The latter should be low enough so that the range of index values above the threshold is representative of the corresponding class, while also high enough to minimize the risk of including "mixed" objects containing other classes. The additional challenge in our study was to make threshold cutoffs consistent among the four radiometrically balanced scenes, so that the classification outputs could be compared in post-classification change detection analysis. Therefore, we used multi-temporal statistical distributions of each spectral index from all four radiometrically balanced images to determine the appropriate cutoff thresholds.

Specifically, from each scene we built the histograms for object-level NDVI, NDWI and Brightness at a small bin size (0.01 for NDVI and NDWI, 0.5 for Brightness) with fixed bin ranges (from -1 to 1 for NDVI and NDWI; from 30 to 140 for Brightness). Then for each index, we added the number of objects per each bin and investigated the resulting "multi-temporal" histogram shape in terms of the pronounced inflection points where the curvature of the histogram function changed (Figure 4). We expected that these inflection points would reflect the natural variation in cover classes. For instance, main area of the Water class is relatively unchanged during the low water season, hence the most representative water segment values in terms of NDWI should add up to a thicker right tail of the cumulative NDWI histogram (Figure 4a). Expansion and development of Vegetation, on the other hand, should have produced a more gradual build-up of the right tail of the distribution, which was also reflected in a corresponding inflection point (Figure 4b). Due to potential confusion of Sand with dry Mudflat, we were only interested in the brightest Sand objects corresponding to predominantly non-vegetated sand features as training objects. These features were expected to occupy a very small fraction of the study area given relatively infrequent occurrence of isolated Sand features (Table 1). Therefore, for Brightness index we selected the high-value inflection point separating thinner part of the right tail from the rest of the multi-temporal histogram (Figure 4c). The pronounced inflection points reflecting these phenomena were chosen as cutoff values.

To avoid redundant training samples and to ensure representative sampling coverage of the whole area, we selected sample objects for Vegetation, Water and Sand as local maxima for NDVI, NDWI and Brightness above the chosen cutoff threshold values within a specified search distance, respectively, for each scene.

Classification and change detection

Next, we performed a two-step classification of the study area (Figure 3). First, using selected training objects for Vegetation, Water and Sand, we classified the area into these three classes. Second, we used all unclassified objects (with minimum membership values less than 0.1 for any class) to determine training segments for Mudflat. We considered scene Nov07 to be the most suitable for locating representative mudflat areas since the main water recession already happened according to local water level observations but the newly exposed mudflats had not yet been fully colonized by vegetation. Therefore, we first determined characteristics of Mudflat training objects from scene Nov07 and then applied these values to other radiometrically balanced images.

Due to potential fine-scale heterogeneity of Mudflat (Table 1), we used smaller objects for its training segment selection than with other classes. We merged and then re-segmented all the candidate objects at smaller segmentation scale of 3 using the same compactness and shape parameters as above. Next, we temporarily isolated objects that were direct neighbors of the already classified Vegetation, Water and Sand because those had greater chance to be "mixed" objects. We then investigated the statistics of NDVI, NDWI, Brightness and other features for the remaining unclassified objects.

Analysis of these unclassified objects along with field notes and photos suggested that the most representative Mudflat object values had NDVI, NDWI and Brightness values concentrated around the unclassified object mean value for each respective index. Of the three indices, NDWI appeared to have the least skewed distribution among the unclassified objects in all scenes. Therefore, to select Mudflat training objects, we applied the search for local maxima of the mean

NDWI difference to neighbors, within one standard deviation from the unclassified object mean November NDWI value. The same range of NDWI values was then applied to scene-specific unclassified object areas for other images to locate their Mudflat samples. Resulting Mudflat training objects were best separated from other classes with NDVI, NDWI, the eCognition Maximum Difference function describing variation in brightness measures within an object (Max. Diff.; eCognition Developer Reference Book) and object-level mean NIR features, which were then used to estimate object membership to Mudflat.

Finally, we repeated classification of the whole study area into four classes for each scene and updated object class membership values (Figure 3). Applying our eCognition rule sets to each scene separately helped to select training samples for different classes in proportion to the class areas. Next, we analyzed the change among the major cover types (Table 1) between successive scenes in ArcGIS 10.0.

Importantly, in this study we intended to test our proposed methods using the 'major' general cover types (Table 1) and a small number of spectral bands of the chosen sensor. We did not introduce any further subcategories for classes in Table 1 to further account for intrinsic variation within each class due to different plant canopy closure, surface wetness etc. However, future steps of top-down analysis of Poyang Lake surface cover should address the intrinsic variation within classes in Table 1 and test these methods on class subcategories as well.

Fuzzy class membership and classification uncertainty

We also examined how classification uncertainty varied during the study period. Object class membership values in eCognition represent the likelihoods of an object belonging to each class according to the membership function derived from training data. Therefore, classification uncertainty may be represented by objects which either 1) have relatively high membership value to more than one class or 2) do not have sufficiently high membership to any class (Gong et al. 1996), which we refer to as "fuzzy objects".

The definition of "fuzziness" depends on the membership function cutoff value, i.e. the objects assigned to a primary class are considered fuzzy if their membership to at least one secondary or alternative class exceeds some cutoff membership value. In the "ideal" scenario, if training data and discriminating features allow perfect separation of classes, such cutoff values should be at or very close to zero. In reality, membership functions may overlap even for well-defined classes especially when the number of spectral bands and discriminating features is limited. This creates a chance that some objects are assigned non-zero memberships to alternative classes when these alternative cover types are absent from these objects in reality. At the same time, objects may also be fuzzy when the boundary between different cover types lies within an object or when two or more cover types are "mixed" at finer spatial scales.

It follows then that classification uncertainty represented by the fuzzy classification outcome may be characterized with the following criteria:

1) the proportion of fuzzy objects in the total area of each class at any given cutoff value;
2) the cutoff value at which the number of fuzzy objects within each class becomes zero;
3) the shape of the curve which relates the proportion of fuzzy objects within a class to the corresponding membership cutoff value.

Criteria 1 and 2 can be used to evaluate the overall uncertainty in a given classification outcome for a given class. The higher are the proportion of fuzzy objects within a class and the cutoff value at which the class has no more fuzzy objects, the more likely this class is to be

confused with others. Criterion 3 can be used to evaluate sensitivity of class "fuzziness" to change in membership cutoff values and to determine at which cutoff value the "fuzziness" starts to decline with further increase in cutoff values thus providing an estimate of the minimum fuzzy membership values in the output. We investigated and compared these criteria both among classes and among image dates (sections 3.3 and 4.2).

Fuzzy accuracy assessment

Field survey and other reference data

For classification accuracy assessment, from each scene we used 130 reference objects, approximately 50-55% of which represented Vegetation as the primary class, ~20% objects - primarily Mudflat, 15-20% objects – primarily Water, and ~10% objects – primarily Sand. These reference objects were assigned for each segmented image using field data and supplementary information as explained below.

In December 2007, 103 geolocated field stops were surveyed along 600-3200 m field transects representing cover types and vegetation of the Poyang Lake natural wetland area. Transects were arranged approximately perpendicular to water boundaries and represented different vegetation types, stages of bottomland exposure by receding water and soil moisture gradients. Transect starting and end points were selected based on access to the wetland area from roads or boat-reachable waterways. Depending on site access, visibility and mobility within the wetland, the size of sampling area surveyed at each field stop varied from 30×30 m to >100×100 m. At each survey location, we recorded presence/absence of vegetation, water, sand and/or mud; percent cover of vegetation, dominant vegetation types and species ID, their average height, spatial extent of coverage and phenology status; spatial extent and depth of flooding; evidence of grazing by livestock and/or waterbirds; evidence of other human activities. In addition, detailed descriptive information and photos were taken for the surrounding areas. Changes in vegetation status and phenology, presence of flooding and/or snow coverage were further noted for some accessible sites during January and early March 2008 revisits conducted without rigorous sampling due to weather and logistical constraints. In April 2008, 177 geolocated field stops were again surveyed within approximately 30×30 m plots along twelve transects of 300-1800 m length in a part of the study area which included some of December 2007 sites as well as new areas that became accessible by the end of the low water season.

Given frequent cloudiness in Poyang Lake area, it was not possible to predict the days of high-quality satellite data acquisition in advance. Therefore, we were not able to match every scene in this analysis with the simultaneously obtained field dataset. Detailed information collected in December 2007 visit allowed us to generate testing data for November 2007 and January 2008 scenes, while additional revisits in winter and early March 2008 were used to guide score assignments for scene Feb08. These data together with vegetation survey in April 2008 were also used for Mar08 classification testing. Importantly, both the beginning and the end of the study period were relatively far in time from the periods of rapid major change in water levels that occur before and after the rain season. Field observations from previous and subsequent years indicated that a number of areas accessible for field visits were consistently free of water during the low water season and had similar grazing agents present (Wang, Dronova, unpublished data from 2006-2007, 2008-2009, 2010-2011 low water seasons). Therefore, in assigning classes to reference locations, we supplemented our expert evaluation of the latter with information from field visits in March 2006, March 2007, early May 2009,

November 2010 and January 2011 during which similar information about vegetation and non-vegetated cover types was collected as in 2007-2008.

Because objects were used as the minimum-size units in image classification, we assigned individual unclassified objects covering field-surveyed locations as reference data "units", instead of using field stops as separate reference points. When multiple field-surveyed locations fell within a single object, we used the information from all covered locations to determine the prevalence of classes of interest within that object. From the field data described above we generated 80-85 reference objects from scenes Nov07, Jan08 and Mar08 and Feb08. To include cover types which were not directly accessible in the field (non-vegetated Mudflat, high sand dunes, open Water and aquatic Vegetation), we further added about 45-50 reference locations for each scene using field observations recorded in areas with high visibility (e.g. at the margins of water bodies) and visual assessment of fine-resolution images from Google Earth, Microsoft Bing and additional data courtesy of State Key Laboratory of Remote Sensing Science, China.

Fuzzy accuracy estimation

In order to account for high spatial heterogeneity of the Poyang Lake wetland, we conducted fuzzy accuracy assessment (Gopal and Woodcock 1994, Townsend and Walsh 2001, Gilmore et al. 2008). Based on the area characteristics known from field surveys and/or fine-resolution reference images, each reference object was assigned a score for each class (Table 1) using 'linguistic scale' from 1 to 5 (1- Absolutely Wrong; 2- Understandable but Wrong; 3 – Reasonable or Acceptable Answer; 4 – Good Answer; 5 – Absolutely Right; Gopal and Woodcock 1994). This step was implemented independently of image classification and without knowing the classification result (Townsend and Walsh 2001). Next, we overlaid reference locations with each classification output and estimated: a) the frequency of matches and mismatches of the MAX function which describes whether the class assigned to a test location has the highest score in that location, and b) the frequency of matches and mismatches for RIGHT function which describes whether the class assigned to a test location has the score equal to or greater than a minimum acceptable score of 3 (Gopal and Woodcock 1994). The MAX criterion resembles the conventional "hard" accuracy assessment since a match counts only when the assigned class has the highest reference score for a location. The RIGHT criterion is less restrictive in that it recognizes any class with acceptable score (even if lower than maximum) as a match. The difference in match frequency between RIGHT and MAX outcomes can be thus interpreted as the score "improvement" with RIGHT function relative to MAX (Gopal and Woodcock 1994).

Results

Seasonal cover types and their change

In all four scenes, Vegetation was consistently the dominant cover type occupying about 49% of the wetland area during Nov07-Jan08 and slightly declining to 41-42% in Feb08-Mar08 (Figure 5). Overall, spatial distribution of Vegetation class was relatively stable, and during the three change periods ~83-90% of this class area was derived from already existing Vegetation (Table 2). The most pronounced shifts from Vegetation (10.5-18.5% of previously assigned Vegetation class; Table 2) in each change period were to Mudflat, with minor losses to Water (0.5-5.9%; Table 2) and Sand (0-0.1 %; Table 2). In turn, new Vegetation areas in each change period emerged also primarily from Mudflat (5.5-17.3%; Table 3), and a small percent – from Water (1.2-3.6%; Table 3) and Sand (0-4.2%; Table 3).

The area of Water, the second largest class, slightly declined from Nov07 to Jan08, but then increased to 33.6% of the area in Feb08 and again declined to 25.8% in Mar08 (Figure 5). This pattern was both interesting and surprising, given that the difference between scenes Feb08 and Mar08 was only two weeks. However, local hydrological measurements confirm a similar pattern of rapid increase in water levels by almost 3 meters from mid-January to mid-February 2008, followed by 2-m reduction by early March (Figure 2a), consistent with our results (Figure 5; Tables 2, 3). Except for these fluctuations, spatial distribution of Water class did not change considerably: 69-98% of new Water area in scenes Jan08, Feb08 and Mar08 was from the previous water body area (Table 3). Most of the losses from Water class at each change period were to Mudflat (3.2-20.4% of previously assigned Water class; Table 2) and then to Vegetation (2-4.4%; Table 2), consistent with the overall water body recession in winter. New Water areas were also primarily derived from flooded Mudflat (91.4-22.3%; Table 3) and Vegetation (0.8-8.5%; Table 3).

Mudflat class increased its area from 13.8% of the wetland in Nov07 to ~22-24% during Jan-Feb08 to 30.7% in Mar08 (Figure 3). Spatial distribution of this class appeared to be more "dynamic" compared to Vegetation and Water: about 71.6%, 51.5% and 69.7% of its area were preserved as Mudflat (Table 2) during Nov07-Jan08, Jan08-Feb08 and Feb08-Mar08 periods, respectively. New Mudflat areas emerged primarily from Vegetation (21.9-39.8% of the new Mudflat area; Table 3) and Water (3.5-22.3%; Table 3) during the study period, and in Nov07-Jan08 also from Sand (21.4%; Table 3).

Sand was a relatively static class from Jan08 to Mar08, occupying 1.6-2.2% of the study area (Figure 5). In Nov07, however, Sand was classified as 8.7% of the study area, and various bright Sand features at the margins of water bodies were particularly visible in scene Nov07. Our results show that about 18% of these Sand areas remained Sand in scene Jan08, while the rest were classified mainly as Mudflat, and some shifted into Vegetation and Water (Table 2). In turn, Mudflat contributed ~22% of the Sand extent during Jan-Feb08 and ~40% of new Sand area during Feb-Mar08.

Change in class membership values

The change in a particular cover type can be manifested not only in the shift from one dominant class to another, but also in the change of class membership value within a particular class. We examined spatial distribution and magnitude of changes in membership values to each class across the wetland area between successive pairs of images (Figure 6). Changes in memberships to Vegetation (Figure 6a-c) and Mudflat (Figure 6g-i) were the most extensive, while change direction also varied among transition periods. High incidence of reduction in Vegetation class memberships in Nov07-Jan08 and Jan08-Feb08 periods was accompanied by a less pronounced increase in Vegetation membership on some exposed mudflats (Figure 6a, b). During Feb-Mar08 period, however, Vegetation membership increased in a number of areas, while the incidence of reductions considerably decreased (Figure 6c). Interestingly, for some areas in northeast portion of the lake mapped as Vegetation in scene Nov07 (Figure 5a) membership to Vegetation decreased in Nov07-Jan08 (Figure 6a), while their membership to Water slightly increased at this time and further intensified during Jan-Feb08 (Figure 6d, e). These locations were most similar to aquatic vegetation beds that were closest to and potentially overlapping with Water class and thus particularly prone to flooding.

Changes in membership to Vegetation among scenes were also consistent with the general atmospheric temperature trend among corresponding dates (Figure 2c) assessed for Nanchang (28°41'N 115°53'E, Jiangxi, China) from National Climatic Data Center (NCDC 2011). Gradual decline in daily mean temperature was observed from November 11, 2007 to January 02, 2008 (Figure 2c). The coldest period of the 2007-2008 low water season with some days below freezing point was from January 13 to February 01, 2008 (Figure 2c). Both periods corresponded to observed decline in Vegetation class membership in many areas (Figure 4a, b). After February 01-12 daily mean temperatures started increasing again (Figure 2c), while for a number of areas Vegetation membership increased between scenes Feb08 and Mar 08 (Figure 6c).

Overall, spatial extent of changes in memberships to Water was much smaller than to Mudflat or Vegetation and was primarily associated with existing water bodies. The highest magnitudes of change in Water class memberships were observed as declines in Nov07-Jan08 period for a number of smaller shallow lakes (Figure 6d) and as increases in Jan-Feb08 and Feb-Mar08 within water bodies, likely reflecting flooding events. Membership to Mudflat increased in a number of locations, often near water bodies, during Nov07-Jan08 and Jan-Feb08 periods (Figure 6a,b), while some declines also occurred, especially around the central water body area. These patterns were consistent with various transitions of other classes to and from Mudflat (Tables 2 and 3). A more pronounced decrease in Mudflat membership values during Jan08-Feb08 (Figure 6h), accompanied by increase in Water membership values (Figure 6e), was consistent with the abovementioned increase in water levels in this period. Interestingly, during Feb-Mar08 reduction in Mudflat membership values outweighed the increases in other locations (Figure 6i), despite the overall increase in Mudflat area at this time (Figure 5c,d). A number of locations decreased their membership value to Sand and shifted to Mudflat and Vegetation between scenes Nov07 and Jan08, consistent with our abovementioned findings (Figure 6j, Table 2). Changes in Sand class among Jan08, Feb08 and Mar08 were small and concentrated around large sand dunes in northeast portion of the study area (Figure 6k, l).

Classification uncertainty

As expected, the proportion of each class area occupied by fuzzy objects was sensitive to the fuzzy membership cutoff value (Figure 7), generally declining as the cutoff threshold value increased. As discussed in section 2.5, three aspects of these curves were of particular interest: the overall magnitude of fuzzy area proportions at each cutoff value, the minimum cutoff values at which classes had no fuzzy objects and the pattern of decline in fuzzy percentages with the increase in cutoff values.

The highest overall proportions of fuzzy objects within each class were found in scene Nov07 (Figure 7a), while the lowest – in Feb08 and Mar08 (Figure 7c, d). Mudflat consistently had the highest proportion of fuzzy objects than other classes, with the exception of scene Feb08 (Figure 7c) where Vegetation class had slightly higher proportion of fuzzy objects at ~0.05-0.12 cutoff value range. Prevalence of fuzzy area within Vegetation compared to other classes was the second highest across the whole range of cutoff values in Jan08 and Feb08 (Figure 7b, c), the third highest in Nov08 (Figure 7a) and the lowest in Mar08 (Figure 7d). Water had generally lower proportion of fuzzy area compared to other classes, and its maximum fuzzy area at zero cutoff value did not exceed 40%. Sand had also relatively low proportion of fuzzy objects during Jan08-Mar08 (Figure 7b-d), however, in scene Nov07 this class appeared considerably fuzzy (Figure 7a).

Notably, Mudflat consistently maintained the highest percentages of fuzzy areas than other classes, i.e. the rate of decline in "fuzziness" with greater cutoff values was the slowest for Mudflat, and cutoff values at which there were no more fuzzy objects – the highest (Figure 7a-d). This finding was consistent with relatively lower accuracy of Mudflat compared to Vegetation and Water except Jan08 (Table 4). At the same time, for most Mudflat objects the cutoff values at which there were no more fuzzy areas did not exceed 0.4-0.45 even in Nov07 as indicated by the curve shapes in Figure 7. Such cutoff values decreased for other classes from Nov07 to Feb-Mar08, but this pattern was most strongly pronounced for Vegetation (Figure 7a-c). Interestingly also, in scene Nov07 the proportion of Mudflat fuzzy objects started declining more rapidly after cutoff value of 0.05-0.07 and not zero (Figure 7a) indicating that the minimum membership values to other classes within Mudflat were within this range.

Classification accuracy

Given problematic field access to most of the seasonal Poyang Lake wetland area and the lack of field data perfectly matching each satellite image in time in this study, we suggest that focusing on the absolute values of the match and mismatch scores would not yield the most meaningful interpretation of accuracy assessment results. Instead, it is useful to investigate the following criteria: 1) the relative differences in accuracy among classes for a given criterion (MAX, RIGHT), 2) the improvement of match frequency with RIGHT criterion compared to MAX criterion for a given class and among classes and 3) the relative differences in both MAX and RIGHT accuracy among the images.

Fuzzy classification accuracy varied among both image scenes and classes (Table 4). The highest accuracy was found for Vegetation class (greater than or equal to 90%; Table 4). In all scenes Vegetation was confused with Water due to presence of either flooded emergent vegetation areas or aquatic vegetation in parts of the study landscape. In scenes Nov07, Jan08 and Feb08 Vegetation was confused with Mudflat which, however, was an acceptable alternative candidate class for these Vegetation locations as indicated by 3-10% score improvement with RIGHT match frequencies. The best MAX accuracy for Vegetation (97%) was found in scene Mar08 (Table 4), suggesting some reduction of confusion among this class and others with progression of the growing season. Importantly, 100% match frequencies between our classification results and reference data do not automatically mean that all areas of the particular class were classified correctly, especially since more than one class could be good or acceptable match for a reference location.

MAX-based accuracy for Water varied from 82-91% among image scenes, with lower scores corresponding to the periods preceding and following the temporary water level increase in Feb08 scene as discussed above. The lowest Water MAX accuracy of 82% was found in Jan08 when water levels were close to the minimum values of the study period. Most of the mismatches for Water class were due to confusion with Mudflat, and in scenes Nov07 and Mar08 – also with Vegetation (Table 4). In all scenes there was an "improvement" of match frequency with the RIGHT criterion suggesting that for most mismatches Water was also suitable, although not the best, candidate class. Mudflat generally had lower MAX-based accuracy values than Water and Vegetation in all scenes except Jan08, being confused with these two classes and also with Sand in Nov07 and Jan08 (Table 4). Both MAX and RIGHT match frequency for Mudflat declined progressively from 86% and 95% respectively in Nov07 to 76% and 86% in Mar08, consistent with gradual colonization of Mudflats by emerging vegetation. However, using RIGHT criterion in each scene improved Mudflat match frequencies by 8-12%

(Table 4), because this class was an acceptable candidate based on the reference data. The accuracy for Sand was relatively high according to reference information, and the confusion occurred primarily with Mudflat in Nov07 and Mar08, and with Water and Vegetation in Jan08 (Table 4).

Discussion

Poyang Lake surface during the low water period

Our findings suggest that spatial distribution of Poyang Lake seasonal cover types in many locations could be closely associated with fluctuations of the water level and spatial extent of flooded surface. Previous studies mentioned that these dynamics are driven primarily by exogenous factors such as precipitation during the monsoon season, seasonal variation in river discharge (especially from Yangtze River) and human water level regulations (Shankman et al. 2006, Jiang et al. 2008, Qi et al. 2009). While research efforts to better understand complex Poyang Lake hydrology are in progress (Andreoli et al. 2007, Hu et al. 2007, Hui et al. 2008), it is evident that seasonal recession and expansion of the water body affect both distribution and extent of other cover types, particularly vegetation and mudflats.

We found that during 2007-2008 low water season Poyang Lake water body did not gradually recede from November to March. In contrast, the interaction among precipitation events throughout winter and flooding in February 2008 likely produced fluctuations in spatial distribution and extent of the flooded areas which, in turn, affected surface properties of the adjacent Mudflat and Vegetation patches. Two important consequences followed from these findings. First, despite the relatively small magnitude of fluctuations in class areas during the study period, various transitions among classes were detected as well as considerable changes in class membership values even with no change in the primary assigned class. Therefore, any future work involving multiple-season of Poyang Lake surface cover properties should incorporate satellite images from more than one stage of the "low water" period to adequately represent this season in the analysis. Second, the lack of consistent water recession could be one of the factors contributing to waterlogged status of wetland soils in many Poyang Lake sites, which significantly limited ground or boat access and collection of *in situ* reference data. It was useful, therefore, to employ the proposed semi-automated methods of selecting training objects using image segmentation and statistical distributions of spectral indices highlighting classes of interest. The suggested approach incorporated *a priori* assumptions about class associations with spectral characteristics of the study area, and allowed us to obtain reasonable training samples for Vegetation, Water, Sand and then Mudflat without ample ancillary and field data. Future enhancement of the proposed methods can explore other spectral indices and transforms which may better highlight subclasses of general cover types considered here, as well as more advanced machine-learning classifiers.

Change in Water class

Decrease in the Water class area in Nov07-Jan08 was consistent with recession of the water body during this period, while variation in spatial extent and location of both Water and Mudflat from Jan08 to Mar08 (Figures 5, 6) closely followed fluctuations in the water levels according to local hydrological observations (Figure 2a). Pronounced changes among Water and Mudflat (Tables 2, 3) occurred due to temporary winter flooding with the peak in mid-February 2008 closely matching the date of scene Feb08 (Figure 2a). While the mechanisms behind hydrological

variation at Poyang Lake are complex and may involve human regulations (Jiang et al. 2008, Qi et al. 2009), there was a correspondence between this February 2008 flooding and precipitation record (Figure 2b) from Nanchang meteorological station (NCDC 2011). Specifically, the period from January 10 to February 6, 2008 was characterized by frequent precipitation events (Figure 2b) which preceded the observed water level rise (Figure 2a). Some of this precipitation was snow which covered substantial portions of the Poyang Lake wetland (Lin Wang, personal observation) and stayed on the ground until atmospheric temperatures began to increase (Figure 2c). Thus, even after precipitation events the ongoing snowmelt could contribute to shallow-water coverage of many wetland areas. Furthermore, winter precipitation and hydrological changes in the basin area and upstream Yangtze River could also contribute to rise of the water levels and to flooding within our study area (Andreoli et al. 2007b, Hu et al. 2007), particularly the central part (Figure 5c). Given presumably strong effect of this hydrological variation on Vegetation and Mudflat class memberships (Figure 6), our results suggest that even short-term inundation events within the low water season may affect composition of the surface cover and discrimination of cover types from satellite images.

Some of the Water class change could be related to Vegetation class, which contributed 7.7-8.5% of the Water extent during Nov07-Jan08 and Jan-Feb08 as well as emerged out of some Water-dominated areas (Table 3). The examples of transitions among these two classes include: 1) spread of inundation-tolerant plant species over flooded surfaces; 2) decrease of the water level and eventually extent via transpiration of dense vegetation stands (Wetzel 2001); 3) senescence of submerged and floating aquatic vegetation within water bodies. These transitions could contribute to the confusion between Water and Vegetation in Nov07 and Mar08 (Table 4), when both aquatic and flooded emergent vegetation were present on a landscape. However, the changes between Water and the areas likely dominated by aquatic vegetation have to be interpreted with caution. Senescence of submerged aquatic plants in clear-water areas may intensify the contribution of water signal in spectral reflectance from aquatic plant bed locations, which could increase the extent of mapped Water class without producing new flooded areas. These findings need to be tested at finer spatial scales but they may suggest the target research areas where the key transitions in prevalent vegetation functional types might occur (Wang et al. 2012) potentially affecting system nutrient and energy fluxes (Ding et al. 2005, Kao-Kniffin et al. 2010).

Vegetation change

Winter growing season at Poyang Lake is characterized by the expansion of emergent wetland vegetation, especially *Carex spp.*, although the magnitude of these dynamics may differ among years (Chen et al. 2007, Wang et al. 2012). While our results show that the overall area of Vegetation class did not change considerably during the study period, numerous non-vegetated locations of Mudflat, Water and Sand shifted to Vegetation. These transitions reflect plant colonization of exposed bottomland, sand features and shallow-water areas (Chen et al. 2007, Wang et al. 2012). Higher frequencies of increases in Vegetation membership coupled with decrease in Mudflat membership values during Feb-Mar08 period (Figure 6c, i) were consistent with intensified vegetation development and growth at the onset of spring and warmer temperatures, even though the total area of Vegetation class did not change dramatically from scene Jan08 to Feb08 and Mar08. However, pronounced reductions in Vegetation class memberships in Nov07-Jan08 and Jan-Feb08 periods (Figure 6a, b) reflected an opposite trend of Vegetation decline in a number of locations. Reduction in Vegetation membership did not

always result in shift to another class and could be attributed to a number of factors, some of which we discuss below.

First, plant phenology affects spectral response and thus membership to Vegetation and fuzzy classes at the object level. Thus, decline in photosynthesis and red light absorption in senescing leaves of species that are less tolerant of lower winter temperatures could reduce the values of NDVI and membership to Vegetation. Our field observations showed that after a series of sporadic winter snowstorms and cold events, top parts of sedge tussocks typically changed from green in November to brown and dry in January. *In situ* collected spectral reflectance (Dronova, unpublished data) indicated that this transition reduced the absorption of the red waveband by *Carex* leaves leading to lower NDVI and thus lower Vegetation class membership consistent with Figure 6a and 6b.

Second, ecological tolerance to prolonged inundation or periodic flooding determine vegetation status in flooded locations (Pezeshki 2001, Liu et al. 2006a) and thus class memberships to Vegetation and Water. Temporary flooding of short emergent vegetation from mid-January to mid-February could inhibit certain species, increase the contribution of non-vegetated background to pixel- and object-level spectral reflectance and thus also reduce class memberships to Vegetation.

Finally, considerable change in Vegetation could be attributed to grazing by livestock and numerous wintering waterbirds from October to March (Markkola et al. 1999, Ji et al. 2007). Livestock grazing occurs in different parts of the study area depending on the seasonal access to wetland by local people and animal herds. Waterbird grazing preferences and intensity vary among avian food guilds and may be more explicitly related to wetland "zones" shaped by vegetation and water depth (Barzen et al. 2009). Either type of grazing is likely to reduce the amount of vegetative cover and strength of plant spectral response at the pixel and object level. Harvesting and burning of reeds by local people (Wang et al. 2012) may have a similar effect. Even though we treated burned areas as Vegetation based on field surveys, the amount of green vegetative cover in burned locations was much smaller than in unburned patches, resulting in lower Vegetation class membership. Importantly, removal of plant biomass inevitably exposes soil (mudflat) background, and thus, areas affected by grazing and harvesting were likely to increase membership to Mudflat. Thus, grazing and harvesting of vegetation during the low water period could contribute to observed shifts from Vegetation to Mudflat, Water and Sand as well as to the overall variation in class membership values.

One of the limitations in our analysis was using a single general class for Vegetation. We acknowledge that differences in canopy closure, density, greenness, moisture status may increase variation of spectral reflectance within this class and contribute to classification uncertainty. Given our purpose of testing the new proposed methods using broadly defined yet distinctive cover types and the small number of satellite image bands, we did not split Vegetation into further subcategories. However, future work should extend this analysis to Vegetation subclasses based on plant appearance and phenology (e.g., green versus senescent), density or canopy closure (e.g., dense versus sparse) or association with water body (emergent, floating, submerged).

Variation in Mudflat and Sand

Mudflat appeared to be a particularly "dynamic" class in our study, both in terms of its spatial distribution and variation in class memberships. Despite the reduction in Mudflat membership

values coupled with Vegetation membership increases during Feb-Mar08, the overall area of Mudflat increased from Nov07 to Mar08 at the expense of both Vegetation and Water (Figure 5, Table 3). However, given typical expansion of Vegetation in winter-spring (Chen et al. 2007), one could expect a gradual reduction in Mudflat area due to plant colonization, which is not shown by our results. One reason for this pattern could be attributed to the abovementioned February 2008 flooding, which could inhibit plant expansions in areas that otherwise would have been colonized by March 2008. Second, waterbird and livestock grazing could considerably increase membership to Mudflat in a number of locations earlier classified as Vegetation. As discussed above, pronounced declines in Vegetation class membership (Figure 6a,b) were consistent with this observation. Progressive decline in Mudflat classification accuracy from Nov07 to Mar08 (Table 4) further indicated that compositional heterogeneity of Mudflats and, thus, the chance of confusion with other classes, increased during the study period. Finally, greater overall classification uncertainty and lower accuracy of Mudflat compared to Water, Vegetation and sometimes Sand (Figure 7, Table 4) suggest that some of the detected Mudflat expansion could be due to classification error and noise in the data.

Additional classification uncertainty for Mudflat results from its similarity to Sand class. While our definition of the latter includes mainly bright sand features (Table 1), various mixtures of sand with finer-textured lake sediment and debris produces an array of gradations between Sand and Mudflat especially at the boundaries between these two classes. Furthermore, elevated water sediment loads and water fluctuations may lead to sand deposition in various locations and on top of already exposed mudflats, thus contributing to classification uncertainty and Mudflat-Sand confusion in these areas. In particular, greater Sand extent in Nov 07 (Figures 5, 6j) resulted from numerous bright features along the shoreline some of which were not found in other scenes. We speculate that some of these features could have been deposited by receding water with high sediment content from sand dredging (Wu 2008). The latter activity had been extensively implemented at Poyang Lake until the temporary ban on sand mining in April 2008 awaiting environmental impact assessment (de Leeuw et al. 2010).

Additional confusion between Mudflat and Sand penalizing the accuracy of each class could arise from drying and thus spectral "brightening" of non-vegetated mudflats, especially in scene Nov07 following earlier drought conditions (Zhang et al. 2008). In our results, the best matches between classified Sand and reference data were locations where isolated, spatially extensive Sand features with little vegetative cover. Flooding by water and colonization by vegetation of both Mudflat and Sand could further exacerbate the confusion between two classes and affect their classification accuracies (Table 4). Future work on resolving the confusion between Mudflat and Sand classes could benefit from collecting their spectral reflectance *in situ* and determining the best discriminating spectral features.

Classification uncertainty and fuzzy accuracy

The important sources of OBIA classification uncertainty include landscape characteristics, object sample reliability and object features as discussed by Yu et al. (2008). In our study these factors are largely represented by a) the initial "fuzziness" of locations containing more than one cover class contributing to spectral signal at a given spatial resolution and b) variation in class-specific spectral, textural and shape object characteristics contributing to confusion between classes in both training and testing data. Atmospheric effects and noise (which were difficult to exclude due to the lack of sensor calibration system and usage of DNs in the analysis) could also

contribute uncertainty to spectral index cutoff thresholds for training objects and class discrimination.

Our study illustrates the utility of fuzzy classification accuracy assessment which takes into account multiple class memberships for a given location (Gopal and Woodcock 1994, Townsend and Walsh 2001, Gilmore et al. 2008) in this heterogeneous, seasonally variable landscape. The improvements of most classification mismatches with RIGHT criterion relative to MAX (Table 4) demonstrated that the assigned classes were acceptable for the vast majority of reference locations even if they were not always the best matching classes. Comparison of the uncertainty curves (Figure 7) among images and classes was generally consistent with accuracy assessment results; both illustrated potential sensitivity of classification accuracy and uncertainty to Poyang Lake water body fluctuations. For instance, higher proportions of fuzzy areas for all classes in scene Nov07 reflected transitional state of the landscape between earlier water level decline and subsequent spread of emergent vegetation over exposed mudflats. The lowest MAX-based match frequencies for Water class in scene Jan08 when water levels were relatively low (Table 4; Figure 2a) may also reflect greater confusion between shallow water and mudflat surfaces. The improvement of Water and Mudflat accuracies by 18% and 8%, respectively, with the RIGHT criterion (Table 4) in scene Jan08 also supports this argument since shallow flooded areas often represent a fine-scale mosaic of both water and exposed mud.

Vegetation had the highest classification accuracy and generally was the easiest class to access in the field. As cool growing season progressed from Nov07 to Mar08, Vegetation MAX accuracy increased further, possibly due to increases in plant biomass and coverage in already vegetated locations reducing the effect of mud and sand background on spectral reflectance. Some local Vegetation membership declines during Nov07-Jan08 and Jan-Feb08 (Figure 6a, b) could be attributed to the uncertainty of submerged aquatic vegetation (SAV) detection due to mixing of water column and vegetation signals in SAV bed locations. Our analysis revealed a Nov07-Jan08 "hotspot" of SAV as a large patch of Vegetation in northeast portion of the lake which changed into Water by Feb-Mar08 (Figure 5). Because at Poyang Lake most SAV species were expected to be dormant in winter (Wu 2008), this area was not included in previous field surveys and should be addressed in future work.

Greatest proportions of fuzzy areas within Mudflat compared to other classes in all images agree with frequently lower MAX-based Mudflat accuracies (Table 4) and its inherent compositional heterogeneity (Table 1). Such heterogeneity is driven primarily by temporal variation in spectral reflectance of mudflats due to changing soil wetness following water body recession on the one hand, and on the other hand – gradual colonization of exposed sites by wetland vegetation. Our results show that even in scene Mar08 with low proportions of fuzzy area within other classes, Mudflat maintained relatively high proportions of fuzzy area at the lower range of cutoff values (Figure 7d) and had the lowest classification accuracy (Table 4). Importantly also, whenever confusion existed between Mudflat and alternative classes, Mudflat was more often "penalized" in terms of lower MAX classification accuracy than were other classes (Table 4). However, 8-12% improvements of Mudflat accuracy with RIGHT criterion suggest that in a number of reference locations this class was an important secondary cover type and a contributor to background reflectance. Spatial and compositional heterogeneity make Mudflat a unique and special seasonal landscape feature which provides growth substrate for emergent wetland vegetation during the growing season and a critical feeding ground for a number of wintering waterbird species (Chen et al. 2007, Barzen et al. 2009). Strong sensitivity

of this class to changes in neighbor cover types potentially make associated habitats more prone to risks of flooding or drought conditions due to climatic variation and human regulations of the wetland water levels. This vulnerability coupled with classification uncertainty, dynamic composition and difficult field accessibility of Mudflat make this class an important research target for future analysis at finer spatial scales.

Our proposed approach to examine classification uncertainty by analyzing spatial variation and magnitude of change in class membership values (Figure 6) and sensitivity of class uncertainty to fuzzy cutoffs (Figure 7) revealed important aspects of landscape change during the study period. In a number of instances class membership values changed without changing the primary assigned class, which could reflect dynamic within-class processes such as growth or senescence of plants, change in soil wetness and water table height. Due to spatial resolution and data quality constraints at pixel and object level, it may not be always possible to interpret these changes directly from the satellite images. However, the analysis of fuzzy class membership values provided the indication of these processes and highlighted their spatial hotspots such as Vegetation-Mudflat interfaces which can be investigated in future work.

Relevance to other Poyang Lake research

Our analysis of the dominant Poyang Lake cover types can be applied to various future research projects in this system. The mapped cover types represent useful categories to stratify subsequent finer-scale analyses, and, given the access difficulties, to guide selection of priority target research sites and field sampling efforts. The four mapped classes provide important contextual information on vegetation patch locations and neighborhoods, which can assist the studies of the key plant functional types (Wang et al. 2012) and inference of system productivity and nutrient fluxes, including greenhouse gas emissions (e.g., Wang et al. 2012, Kao-Kniffin et al. 2010).

Major food guilds of Poyang Lake waterbirds (including many endangered species) are also associated with specific cover types (Burnham 2007, Barzen et al. 2009, Kwaiser 2009) whose spatial distribution and dynamics are coupled with seasonal water and wetland surface characteristics (Wu 2008, Wang et al. 2012). Since low water season at Poyang Lake hosts the largest abundances of wintering waterbirds (Ji et al. 2007), some of the transitions between cover types such as change from Vegetation to Mudflat by late winter may highlight important habitat features and the uses of vegetation resource by birds. Even locations with higher classification uncertainty may represent important ecological boundaries (ecotones) at the margins of cover types and indicate potential "hotspots" for finer-scale studies (Walker et al. 2003). Thus, mapping and analyzing major general cover types is an important first step in top-down investigation of Poyang Lake ecosystem mosaic and its spatio-temporal variation.

Summary

This study presents an object-based classification of Poyang Lake natural wetland surface and change analysis of its general cover types during the 2007-2008 low water season. Our mapped classes represent spatially dominant components of the study landscape which may nest various categories for subsequent hierarchical analyses such as plant functional types, water depth zones, belts of different soil moisture and thus can be used to guide future finer-scale studies and *in situ* sampling efforts.

Our study has demonstrated the use of spectral indices for generating training objects for a supervised object-based classification when available reference data are limited. Future work should explore more advanced classification approaches to discriminate cover types and the possibility to develop custom SIs for various cover types. Given high seasonal and year-to-year variability in Poyang Lake flood extents and surface composition (Shankman 2006, Wu 2008), developing more automated approaches for extracting basic cover type information and its uncertainty should facilitate monitoring the ecological conditions of Poyang Lake.

Our results suggest that changes in spatial distribution of major cover types largely followed the dynamics of the Poyang Lake water body, which decreased through Nov 07-Jan 08 and expanded again during Jan-Mar 08. Vegetation was the most extensive class followed by Water, Mudflat and Sand. Local decreases in the strength of vegetation membership function could be attributed to flooding and potentially grazing which remains to be tested in future work. The increases in Vegetation membership values in various locations throughout the study period increases highlighted progression of the cool growing season. Mudflat class posed high challenge for classification accuracy due to its compositional heterogeneity and problematic ground access. Given the ecological importance of this class for both vegetation and wildlife habitat, future work should explore alternative strategies to enhance discrimination of this cover type from others and monitor its compositional variation.

Our analysis revealed that in a number of locations classification membership values changed without changing the dominant class, which in a hard classification would be equivalent to "no change". We were able to detect these locations and interpret their dynamics by addressing the dynamic landscape change both in terms of primary assigned classes and fuzzy membership values to all classes. Substantial spatial and temporal variations in class memberships were consistent with both flooding events and changes in atmospheric temperature. Our change detection and uncertainty analyses confirm that low water season at Poyang Lake is characterized by considerable dynamics of surface cover type composition, despite much lower magnitude of water body change compared to the onset of rain season in later spring-early summer and rapid recession in early fall. Therefore, future studies focusing on the whole-year wetland dynamics should choose more than one satellite image to represent the low water winter season.

Acknowledgements

This research is partially supported by the NASA student Earth and Space Science Fellowship 2009-2012 (NNX09AO27H) and a grant from the National High Technology Programme of China (2009AA12200101). We are also grateful to the State Key Laboratory of Remote Sensing Science (Beijing, China), Poyang Lake Ecological Station for Environment and Health, (Duchang, China) and professor Shuhua Qi (Jiangxi Normal University, China). This study also benefited from discussions with James Burnham and Jeb Barzen (The International Crane Foundation) and from the support and services of UC Berkeley Geospatial Innovation Facility (GIF), gif.berkeley.edu. Finally, we thank two anonymous reviewers for their time and useful feedback that helped to improve this paper.

Tables

Table 1. The major general surface cover types of the Poyang Lake natural lake-wetland area.

Class name	Description	Typical occurrence in Poyang Lake area
Vegetation	Predominantly vegetated areas containing wetland and aquatic plants, including emergent, floating and submerged vegetation.	Mostly natural wetland and aquatic vegetation constrained to lake periphery over the rain season and colonizing exposed bottomland during the low water period, and also dense stands of submerged aquatic plants 'visible' to sensor through the water column
Water	Areas covered by the aboveground water layer	Rivers, sub-lakes, water pools and stream channels
Mudflat	Seasonal cover type composed of soft waterlogged sediment beds exposed by the receding water body or the inundated wetland soil and therefore difficult to access *in situ*. Sparse vegetative cover and/or a thin water layer may be present occasionally producing fuzzy areas with Vegetation and/or Water classes.	Flat beds of the exposed lake bottomland often located at the edges of the water bodies or in places of small pools or sub-lakes that lost aboveground water following water level decline.
Sand	Spectrally bright deposits of predominantly sand material formed by water action or bank erosion; total area expected to be smaller than for other classes.	Dunes, beaches, river sand bars, occasional sandy hills, typically located immediately next to the water features.

Table 2. Change in the major cover types shown as percent of the From class area. (Example: in case of 'Nov 2007 - Jan 2008', the first row indicates that of the area classified as 'Vegetation' in scene Nov 2007, 85.1% was still 'Vegetation' in scene Jan 2008, while 4.3% changed to 'Water', 10.5% to 'Mudflat' and 0.1% to 'Sand').

Nov 2007 - Jan 2008

	To class:			
From class:	**Vegetation**	**Water**	**Mudflat**	**Sand**
Vegetation	85.1	4.3	10.5	0.1
Water	2.0	85.4	12.4	0.2
Mudflat	18.9	9.2	71.6	0.3
Sand	22.4	2.0	57.8	17.8

Jan 2008 - Feb 2008

	To class:			
From class:	**Vegetation**	**Water**	**Mudflat**	**Sand**
Vegetation	75.7	5.9	18.3	0.1
Water	2.1	94.5	3.2	0.2
Mudflat	15.5	31.4	51.5	1.6
Sand	1.1	7.5	23.3	68.1

Feb 2008 - Mar 2008

	To class:			
From class:	**Vegetation**	**Water**	**Mudflat**	**Sand**
Vegetation	80.9	0.5	18.5	0.0
Water	4.4	75.0	20.4	0.2
Mudflat	24.8	1.6	69.7	3.9
Sand	2.6	3.2	15.0	79.2

Table 3. Change in the major cover types shown as percent of the To class area. (Example: in case of 'Nov 2007 - Jan 2008', the second column 'Vegetation' indicates that of the area classified as 'Vegetation' in scene Jan 2008, 89.2% was 'Vegetation' in scene Nov 2007, while 1.2% was 'Water', 5.5% was 'Mudflat' and 4.2% was 'Sand' in Nov 2007 classification).

Nov 2007 - Jan 2008

	To class:			
From class:	**Vegetation**	**Water**	**Mudflat**	**Sand**
Vegetation	89.2	7.7	21.9	2.8
Water	1.2	87.1	14.9	3.4
Mudflat	5.5	4.6	41.8	2.7
Sand	4.2	0.6	21.4	91.1

Jan 2008 - Feb 2008

	To class:			
From class:	**Vegetation**	**Water**	**Mudflat**	**Sand**
Vegetation	89.7	8.5	39.8	2.4
Water	1.3	68.8	3.5	2.3
Mudflat	9.0	22.3	54.9	22.7
Sand	0.0	0.4	1.8	72.6

Feb 2008 - Mar 2008

	To class:			
From class:	**Vegetation**	**Water**	**Mudflat**	**Sand**
Vegetation	82.6	0.8	25.3	0.6
Water	3.6	97.6	22.3	2.5
Mudflat	13.7	1.4	51.6	39.7
Sand	0.1	0.2	0.8	57.2

Table 4. Fuzzy accuracy for the major general Poyang Lake cover types.

Class name	#Sites classified as	MAX(M)		Right(R)		R-M	Confusion classes
		%Match	%Mismatch	%Match	%Mismatch		
November 2007							
Vegetation	71	90	10	100	0	10	Water, Mudflat
Water	21	90	10	100	0	10	Vegetation, Mudflat
Mudflat	22	86	14	95	5	9	Vegetation, Water, Sand
Sand	16	75	25	94	6	19	Mudflat
January 2008							
Vegetation	61	93	7	100	0	7	Mudflat, Water, Sand
Water	17	82	18	100	0	18	Mudflat
Mudflat	39	87	13	95	5	8	Vegetation, Water, Sand
Sand	13	77	23	85	15	8	Vegetation, Water
February 2008							
Vegetation	60	93	7	100	0	7	Water, Mudflat
Water	23	91	9	100	0	9	Mudflat
Mudflat	33	82	18	94	6	12	Vegetation, Water
Sand	14	100	0	100	0	0	
March 2008							
Vegetation	59	97	3	100	0	3	Water, Sand
Water	15	87	13	100	0	13	Vegetation
Mudflat	38	76	24	87	13	11	Vegetation, Water
Sand	18	83	17	89	11	6	Mudflat

Figures

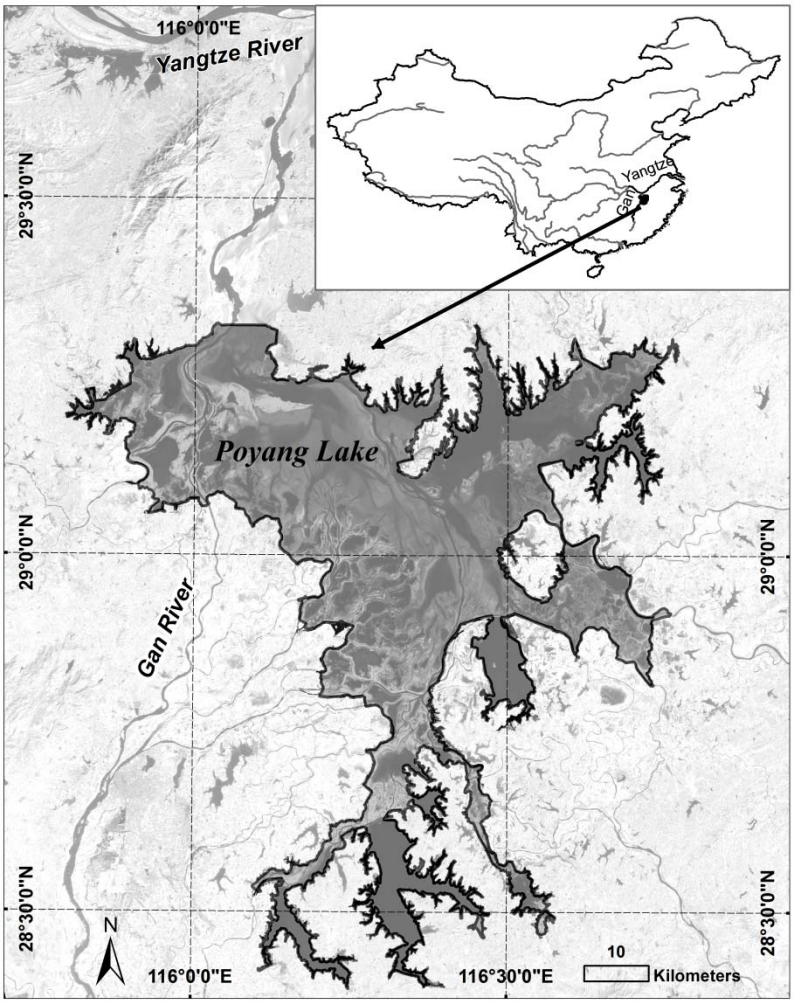

Figure 1. Spatial location and extent of the study area of Poyang Lake, Jiangxi Province, People's Republic of China.

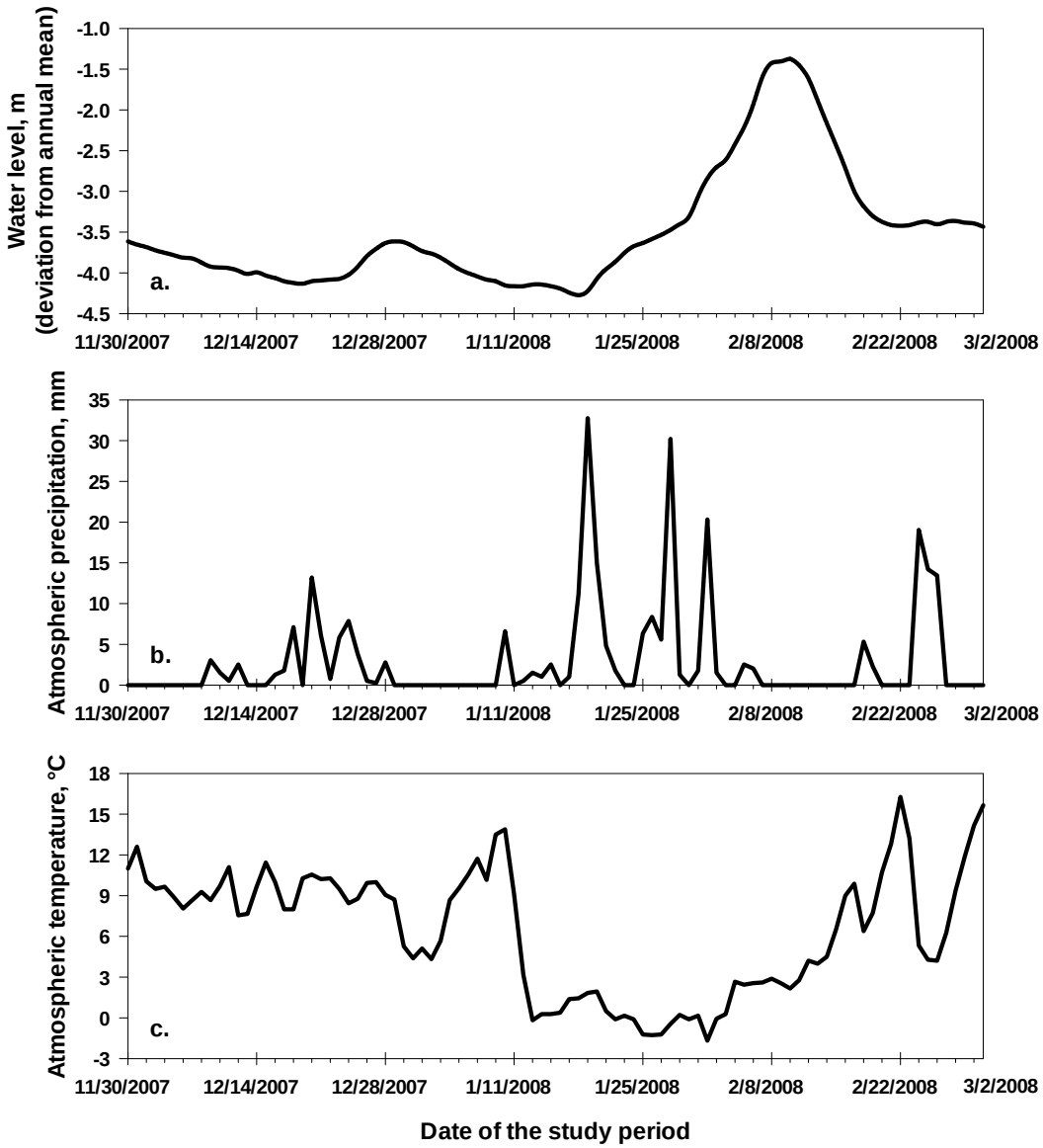

Figure 2. Hydrological and climatic variation during the study period of November 30, 2007-March 2, 2008: a) water level at Duchang hydrological station (Duchang, Jiangxi, China) shown as deviation from the annual mean water level (data of State Key Laboratory of Remote Sensing Science, China); b) daily precipitation at Nanchang meteorological station (Nanchang, Jiangxi, China), in millimeters; c) daily atmospheric temperature at Nanchang meteorological station (Nanchang, Jiangxi, China), in degrees Celsius (data for (b) and (c) from NOAA/National Climatic Data Center, http://www.ncdc.noaa.gov/oa/ncdc.html).

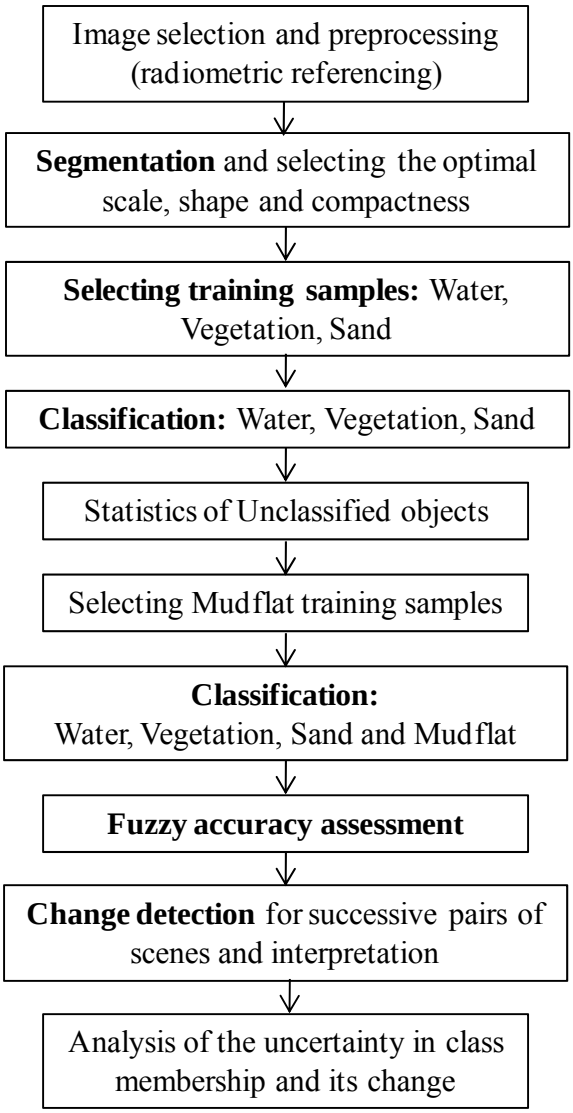

Figure 3. The outline of study procedures.

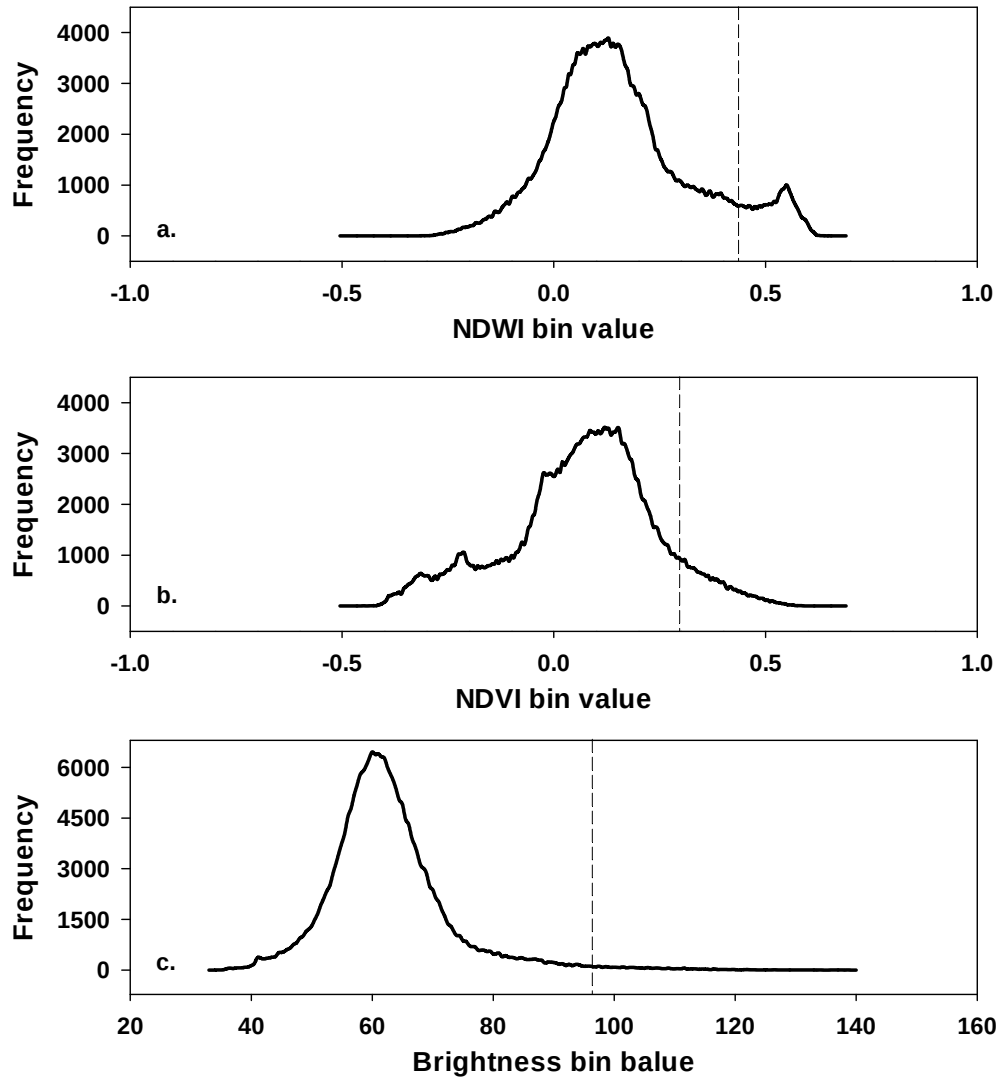

Figure 4. Histograms of a) Normalized Difference Water Index (NDWI), b) Normalized Difference Vegetation Index (NDVI), and c) eCognition Developer Brightness feature, summed per-bin among four Beijing-1 scenes representing 2007-2008 Poyang Lake low water period. Bin sizes were 0.01, 0.01 and 0.5 for NDVI, NDWI and Brightness, respectively. Dashed lines are placed at inflection points representing index cutoff thresholds for selecting training samples for a) Vegetation, b) Water and c) Sand from objects with respective index value above the corresponding threshold value.

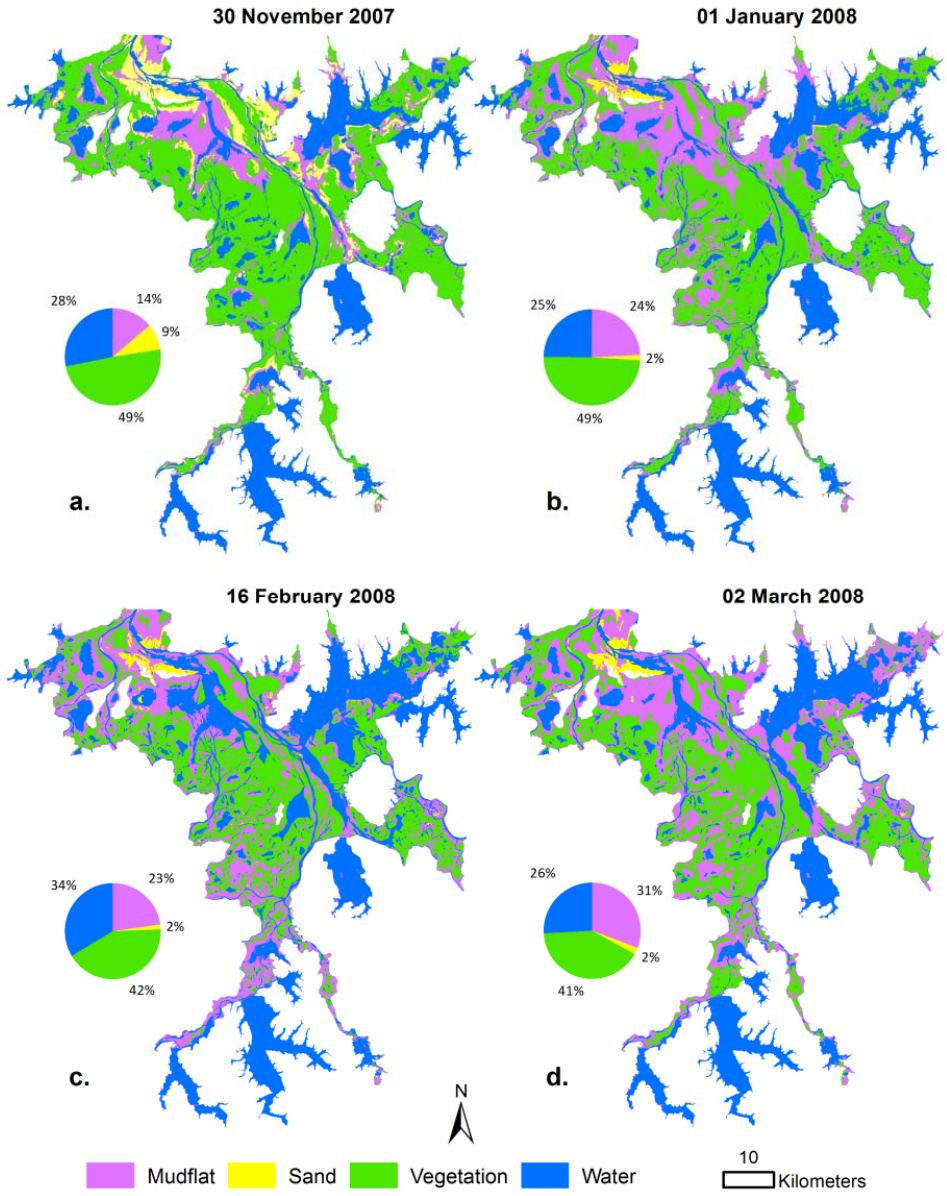

Figure 5. Classification of the four Beijing-1 scenes representing 2007-2008 Poyang Lake low water period and relative proportions of the major wetland cover types: a) November 30, 2007; b) January 01, 2008; c) February 16, 2008 and d) March 02, 2008. Empty white areas inside the study area correspond to major residential and other active human land use areas not included in wetland classification.

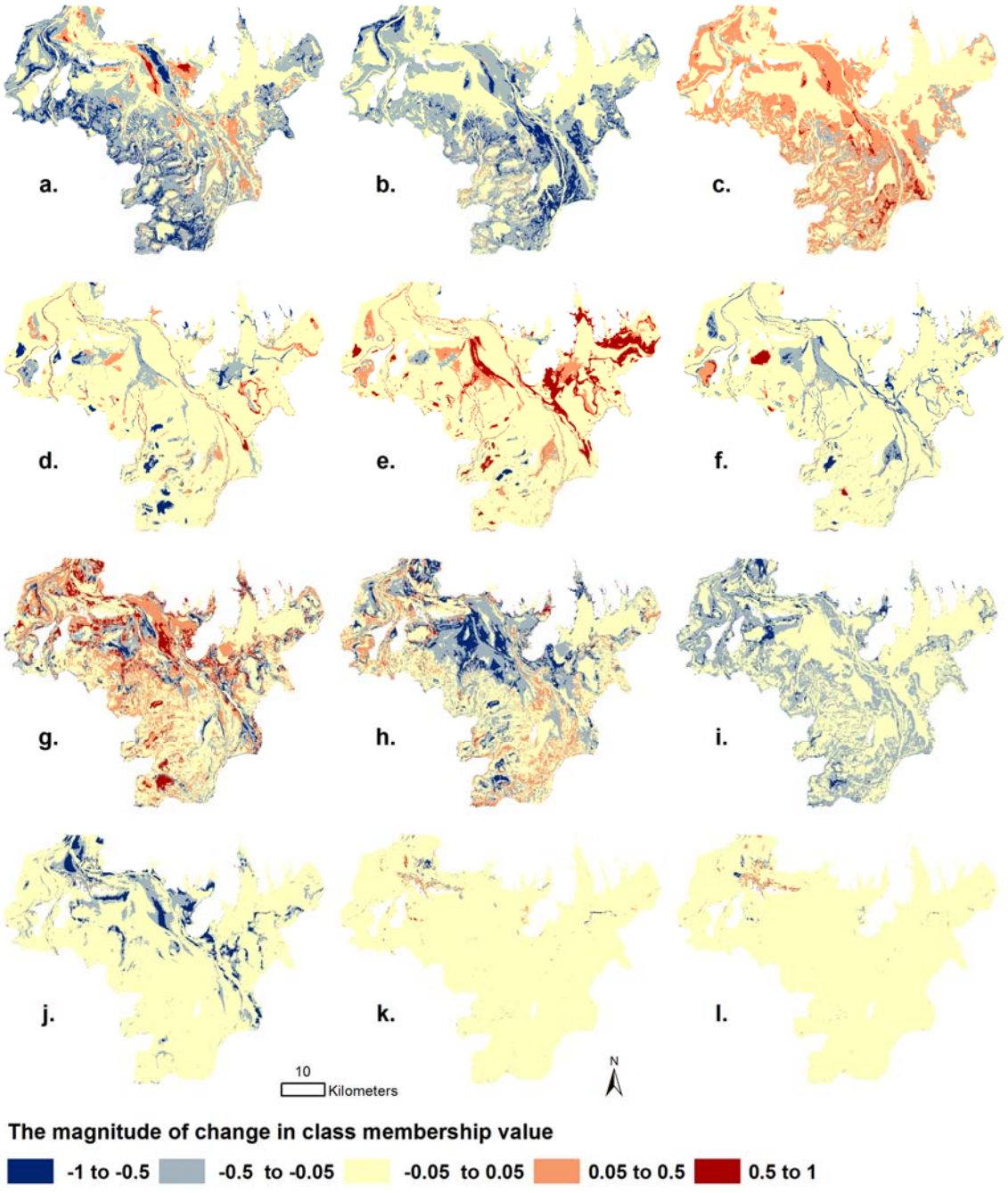

Figure 6. Spatial distribution and value of change in fuzzy membership to Water, Vegetation, Mudflat and Sand among successive pairs of Beijing-1 scenes for 2007-2008 Poyang Lake low water period, for the main subset of the study area. The maps are arranged horizontally by class: Vegetation (a,b,c), Water (d,e,f), Mudflat (g,h,i) and Sand (j,k, l) and vertically by change periods: Nov07-Jan08 (a,d,g,j); Jan-Feb08 (b,e,h,k) and Feb-Mar08 (c,f,i,l).

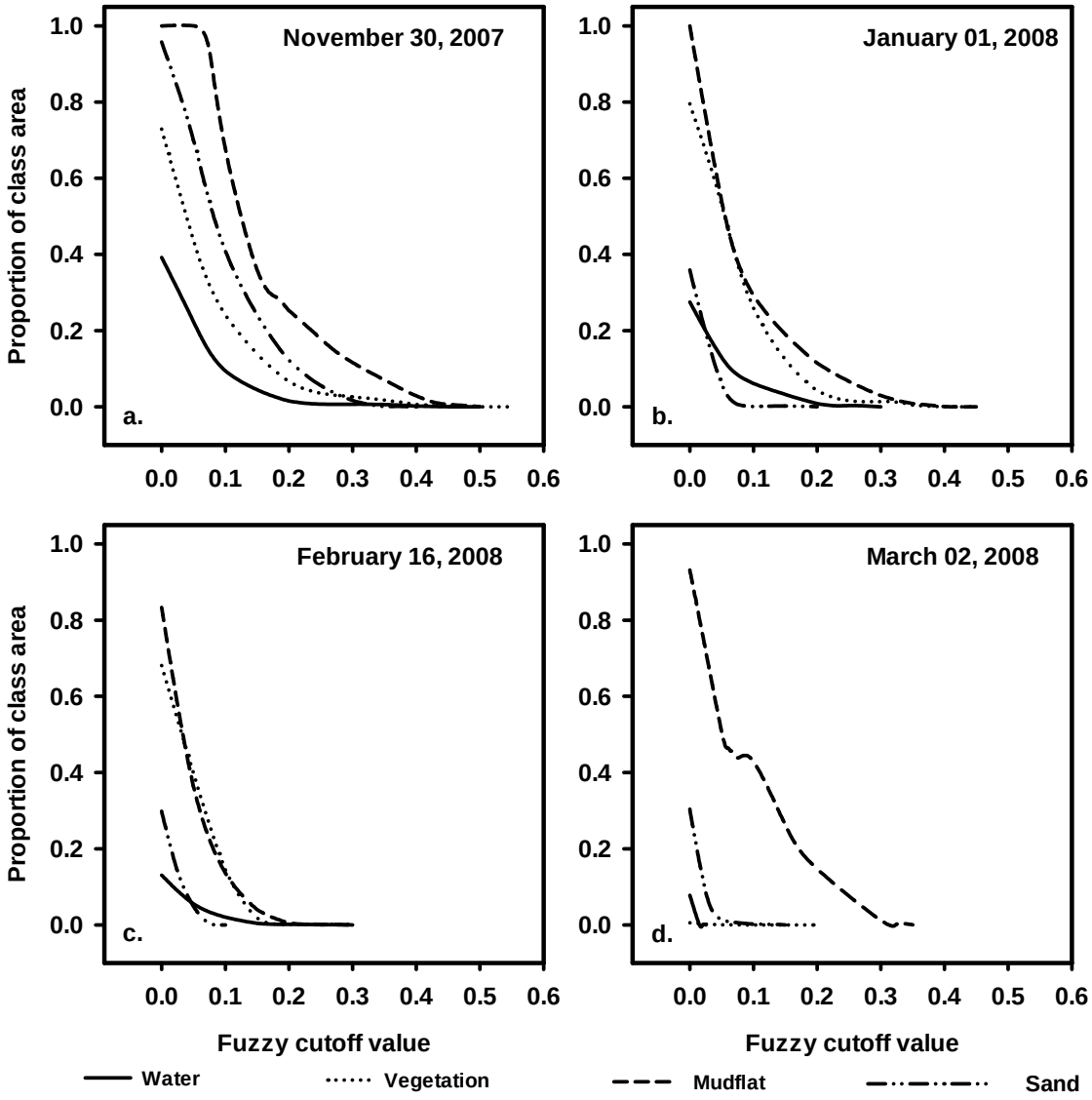

Figure 7. Proportions of fuzzy objects within the area of each class and their change with increasing fuzzy class membership cutoff value in scenes a) November 30, 2007; b) January 01, 2008; c) February 16, 2008 and d) March 02, 2008. Here class membership cutoff value for an object assigned to a primary class (based on the maximum membership to candidate classes) indicates the minimum membership value of secondary classes at which the object is considered "fuzzy".

CHAPTER 2. Landscape analysis of wetland plant functional types: the effects of image segmentation scale, vegetation classes and classification methods

This article has been published previously and is reproduced here with permission from the publisher, Elsevier

Dronova I, Gong P, Clinton N, Wang L, Fu W, Qi S, Liu Y. 2012. Landscape analysis of wetland plant functional types: the effects of image segmentation scale, vegetation classes and classification methods. *Remote Sensing of Environment 127:*357-369.

Abstract

Remote sensing-based analyses of vegetation function such as photosynthesis and productivity are challenging in wetlands with complex cover and difficult field access. Recent advances in object-based image analysis (OBIA) and machine-learning algorithms offer new image classification tools; however, few comparisons of different approaches have been discussed to date. We applied OBIA to delineate wetland plant functional types (PFTs) for Poyang Lake, the largest freshwater lake in China and Ramsar wetland conservation site, from a spring 2008 Landsat TM image. We targeted major PFTs that represent dominant vegetation groups along wetland inundation gradients and affect ecosystem biogeochemical cycles and ecological habitats. Classification results were compared among: a) several "small" object segmentation scales (with average object sizes 1350-9000 m^2); b) algorithms from six families of statistical machine-learning classifiers (Bayesian, Logistic, Neural Network, Decision Trees, K-Nearest Neighbors and Support Vector Machines) and c) two hierarchical levels of vegetation classification, a generalized 3-class set and a more specific 6-class set. We also examined the response of classification accuracy to four basic object-level texture metrics. The highest accuracies (>85-90%) and best agreement among algorithms occurred at coarser object scales rather than close-to-pixel scales. No single machine-learning algorithm was consistently superior at all scales, although support vector machine, k-nearest neighbor and artificial neural network most frequently provided the highest overall and PFT-specific accuracies. Including texture metrics had both positive and negative low-magnitude effects on classification accuracy that were not consistent among scale values, algorithms or PFT classes. Individual PFTs differed in scales at which they were best discriminated from others, reflecting their unique landscape positions, ecology of dominant species and disturbance agents. There was a 29-35% disagreement between mapped areas of generalized PFTs and their respective subclasses, suggesting potential mismatches between the ecological classification scheme and PFT landscape patch structure, and raising concern on error propagation in multi-scale classifications. We conclude that OBIA with machine-learning classifiers is useful for landscape vegetation analyses, however, considerations of spatial scale and image segmentation outcomes are critical in mapping PFTs and should be more thoroughly investigated in future work.

Introduction

Remote sensing is useful for ecosystem analyses at landscape scales due to radiometric sensitivity of instruments to biophysical properties of the surface, instantaneous coverage of large areas and possibilities of consistent revisit by sensors (Xiao et al. 2008, Hilker et al. 2008, Ustin and Gamon 2010). Because vegetation plays a critical role in nutrient cycles and productivity of many terrestrial and aquatic systems, accurate classifications of plant cover from

remote sensing data are essential for broad-scale assessments of ecosystem structure and dynamics. However, the inference of vegetation properties from the images is challenging in heterogeneous continuous-cover landscapes with high species diversity and cover type complexity (Yu et al. 2006, Dobrowski et al. 2008). Particular difficulties arise in wetlands where plant mosaics are driven by fine-scale variation in topography, hydrology and disturbance (Johnston and Barson 1993, Ozesmi and Bauer 2002, Hestir et al. 2008), while ground-truthing may be limited by field access (McCarthy et al. 2005, Davranche et al. 2010, Dronova et al. 2011), infectious disease agents (Chen and Lin 2004) or the risk of disrupting fragile habitats (Tuxen and Kelly 2008). At the same time, dramatic worldwide losses of wetlands in recent decades, ongoing human-induced pressures and alien species invasions in remaining sites (Gibbs 2000, Dudgeon et al. 2006, Hestir et al. 2008, Gong et al. 2010) create an urgent need to improve both the scientific understanding of wetland ecosystems and methods for their assessment and monitoring.

Despite increasing availability of high-resolution (<10m) imagery, moderate-resolution (15-30 m) data remain popular for studying large wetland systems due to vast area coverage, affordable cost, consistent revisit and historical data records (McCarthy et al. 2005, Baker et al. 2006, Wright and Gallant 2007, Conchedda et al. 2008, Liira et al. 2010, Michishita et al. 2012). Extraction of vegetation characteristics from such images may be enhanced by several strategies. First, classification schemes may benefit from integrating floristic and taxonomic information with structural, physiological or phenological features that contribute to spectral contrasts among classes. Previous studies proposed the plant functional type (PFT) framework, where species are grouped based on common traits (e.g., life form, photosynthetic pathway, leaf longevity) that determine functions of interest such as biomass or the rates of photosynthesis and primary productivity (DeFries et al. 1995, Gitay and Noble 1997, Duckworth et al. 2000, Ustin and Gamon 2010). Although exact definitions may vary, PFTs are meant to reflect similarity in species' resource utilization and response to environmental controls, but not necessarily phylogenetic or synecological relationships within communities (Duckworth et al. 2000). In the broader landscape context, PFTs incorporate both ecophysiological and spectral (optical) characteristics of the locally dominant vegetation (Ustin and Gamon 2010, Khanna et al. 2011) that facilitate their classification from remote sensing imagery and provide the basis for spatial extrapolation of the ecological function(s) (Bonan et al. 2002). However, to date PFT classifications have been conducted predominantly in terrestrial systems and less often in wetland or aquatic environments (Hestir et al. 2008, Khanna et al. 2011, Wang et al. 2012).

Second, discrimination of plant types in complex wetland landscapes may benefit from using object-based image analysis (OBIA) instead of traditional pixel-based methods (e.g., Tuxen and Kelly 2008, Tian et al. 2008, Gilmore et al. 2008, Ouyang et al. 2011, Dronova et al. 2011). Within OBIA, the images are first segmented into groups of pixels, i.e. objects, which are further assigned to classes via statistical and/or rule-based classification (Blaschke et al. 2000, Benz et al. 2004). Important OBIA advantages relative to the pixel-based framework include 1) lower likelihood of "salt-and-pepper" speckle among different class assignments that is common in pixel-based classifications of heterogeneous landscapes and 2) the possibility of using texture, shape and contextual object attributes as additional discriminating features (e.g., Blaschke et al. 2000, Yu et al. 2006, Kim et al. 2011). For landscapes where patches of the same cover type vary greatly in size, shape and structure, previous studies have proposed using small primitive objects as minimum classification units (Tian et al. 2008, Kim et al. 2011, Dronova et al. 2011). The maximum allowed object-level spectral heterogeneity and object size are controlled by the

segmentation "scale"[1] parameter (eCognition Developer Reference Book) which has been shown to affect both the quality of segmentation and image classification accuracy (Dorren et al. 2003, Addink et al. 2007, Liu and Xia 2010). Manipulating scale also allows constructing layers of nested objects for hierarchical classifications (Burnett and Blaschke 2003, Tuxen and Kelly 2008, Kim et al. 2011, Ouyang et al. 2011). Overall, OBIA has been useful for wetland detection within heterogeneous landscapes (Grenier et al. 2007, Richmond 2011) and for classifications of wetland cover types (Kim et al. 2011, Dronova et al. 2011), plant communities (Wang et al. 2004, Gilmore et al. 2008, Tuxen and Kelly 2008, Laba et al. 2010) and ecological habitats (Tian et al. 2008, Rokitnicki-Wojcik et al. 2011). However, OBIA has not been yet extensively applied for plant functional classifications in wetlands (Ouyang et al. 2011).

Finally, separability of vegetation classes may be enhanced with recently proposed supervised machine-learning algorithms (Clinton et al. 2010b, Khanna et al. 2011, Richmond 2011, Wang et al. 2012). For wetlands, improvements in classification accuracy relative to the maximum likelihood method have been reported with, e.g., classification trees (Na et al. 2009, Davranche et al. 2010), support vector machines (SVM; Sanchez-Hernandez et al. 2007, Fung et al. 2009, Wang et al. 2012), and artificial neural networks (Han et al. 2003, Berberoglu et al. 2004, Zeng et al. 2007, Fung et al. 2009). However, little is still known on relative performance of various supervised approaches, and very few comprehensive method comparisons have been reported so far (Clinton et al. 2010b, Richmond 2011). Furthermore, possibilities of high user customization of both OBIA and machine-learning processes in modern software may introduce superfluous subjectivity to classifications and limit applicability of the algorithms to other images for repeated analysis and monitoring (Khanna et al. 2011, Rokitnicki-Wojcik et al. 2011, Zhao et al. 2011).

This study explored the utility of OBIA and several machine-learning classifiers to delineate PFTs for Poyang Lake, the largest freshwater lake in China and an important Ramsar waterbird conservation site (Figure 1). Climate change together with human-driven pressures, including pending dam projects (Barzen et al. 2009), create an urgent need to improve the scientific understanding of this wetland environment. However, comprehensive analyses of its composition and dynamics have been historically limited by the large lake size and constrained field access (Dronova et al. 2011, Wang et al. 2012). Previous vegetation classifications of Poyang Lake used mainly floristic and taxonomic groups (Chen et al. 2007, Zeng et al. 2007, Michishita et al. 2008), while the assessments of plant functional diversity have started only recently (Wang et al. 2012).

Our primary objective was to classify Poyang Lake wetland PFTs using OBIA and to determine which image segmentation scales and machine-learning algorithms optimize class discrimination. We also examined the consistency of segmentation scale and classifier performance among two levels of PFT hierarchy suggested by vegetation ecology: a generalized 3-class set and a more specific 6-class set, and evaluated the agreement in class allocation between the highest-accuracy maps of these class levels. Finally, we tested the effects of including basic first- and second-order texture metrics on classification accuracy.

[1] Since popular image segmentation software algorithms call the parameter controlling maximum allowed spectral heterogeneity and average object size the "scale" parameter, hereafter we will use the term "scale" and "object scale" to denote the scale of image segmentation.

Methods

Study area and general vegetation characteristics

Poyang Lake is located in the basin of the lower Yangtze River (28°25'-29°45'N, 115°48'-116°44'E; Figure 1). Spatial extent of its water body varies between >4000 km^2 in summer and <1000 km^2 in winter following an annual flood cycle driven by monsoonal climate and river hydrology (Shankman et al. 2006, Andreoli et al. 2007). The annual dynamics of local vegetation have distinct "warm" and "cool" seasons that overlap with monsoonal "wet" and "dry" seasons, respectively (Chen et al. 2007, Wang et al. 2012). During the warm "wet" season from late April-May until September, large portions of the area are flooded and support aquatic vegetation. With flood recession in October, parts of the lake bottomland are exposed as seasonal mudflats and then colonized by emergent plants of the "cool" growing season, primarily sedges (*Carex* spp.) with C3-photosynthesis (Pearcy and Ehleringer 1984) and various forbs (*Artemisia, Potentilla, Lapsana, Polygonum* spp. and others). Higher-elevation lake peripheries may also sustain less flood-tolerant grasses with C4 photosynthesis: reeds (*Miscanthus, Arundinella* spp.) and "short" C4 grasses (*Cynodon, Paspalum* spp.) near roads and residential areas (Zeng et al. 2007). Unlike C3 grasses and forbs, C4 vegetation grows mainly during the warm season, similar to other mixed-grassland biomes (Davidson and Csillag 2003), and may often be senescent in winter (Dronova, field observation), which facilitates its detection with multi-date remote sensing data.

This study focused on the 22,400 ha Poyang Lake National Nature Reserve (PLNNR) located in the northwestern part of the lake (Figure 1). Established in 1983 as a nature protection area, PLNNR hosts >150 vascular plant species and >300 bird species, including endangered migratory waterbirds (Wu and Ji 2002, Burnham 2007, Barzen et al. 2009). Due to its protected status, this area has been less subject to intensive land uses and has been studied in more detail than other parts of Poyang Lake (Wu and Ji 2002, Zhao et al. 2011), making it a suitable target for our analysis.

Remote sensing image data

This study used a terrain-geocorrected (Level 1T) Landsat 5 TM scene for May 16, 2008 at near-peak biomass stage of the spring 2008 growing season before the new monsoonal flooding, when multiple vegetation types were present and soil background effects were minor due to high plant density. The image was geo-referenced and corrected to surface reflectance with the 6S algorithm (http://modis-sr.ltdri.org/code.html). Because similar phenology states of green vegetation at this time of year could increase spectral confusion among classes, we included supplementary phenological information as a Normalized Difference Vegetation Index (NDVI) from January 01, 2008 scene of Beijing-1 microsatellite (32-m), georeferenced and resampled to 30-m Landsat resolution. The latter scene represented the winter stage of the same growing season when phenology-driven spectral differences between C3 and C4 grasses were more prominent.

Field vegetation surveys

The start of flooding in April 2008 restricted access to many wetland areas at the time when the May 2008 Landsat scene was acquired. For this reason, we utilized field data collected in two surveys earlier that season: late December 2007 (perennial vegetation locations, 103 geolocated field stops) and late April 2008 (177 geolocated field stops). We also referred to the field data

from March 2006, March 2007, May 2009 and late March 2011 from locations of either perennial vegetation, consistently observed from year to year, or permanent small water bodies which supported aquatic vegetation every year. At different visits, field data were collected in similar ways along transects representing natural wetland vegetation and stages of bottomland exposure, including parts of Poyang Lake wetland outside PLNNR (Figure 1). These transects of 300-3200 m in length, depending on location and access, were set up approximately perpendicular to water edges. At each stop we surveyed an area between 30×30 m and more than 100×100 m in size and recorded percent cover of vegetation, dominant plant types and species names, their average height, phenology status, spatial extent and depth of flooding (if any), evidence of grazing or human activities such as reed harvesting. In addition, dominant vegetation, other cover types and human activities along with field photos were recorded for the areas surrounding survey stops.

PFT selection based on the dominant species

Candidate PFTs were determined by cluster analysis of the key structural, physiological and phenological traits of 51 common Poyang Lake wetland species detected as dominants or co-dominants in springtime surveys in different years (examples are given in Table 1). Trait information was obtained from field observations and relevant publications (e.g., Cook 1996; Wu et al. 1994-). Life form, habit and height traits were chosen because they influence the architecture of individual plants (thus canopy-light interactions) and may also reflect plant differences in tolerance to inundation (Lenssen et al. 1999). Photosynthetic pathway was used as a physiological trait linked with plant photosynthetic rates, potential productivity, light and water use efficiency, leaf nutrient content and competitive performance (Pearcy and Ehleringer 1984). Finally, phenology was considered because it could affect plant density at the time of satellite image acquisition and thus class-specific effects of soil or water background on vegetation reflectance (Hestir et al. 2008). Cluster analysis was conducted using the single linkage method with Euclidean distance as a similarity measure in Stata 11 (StataCorp LP 2011).

Based on the results of cluster analysis, in subsequent classifications we used two hierarchically related PFT sets (Table 1): the generalized 3-class set (C3 grasses and forbs; mixed C4-dominated grasses; Aquatic macrophytes) and the specific 6-class set (C3 grasses; C3 forbs; C4 and C3 reeds; C4 short grasses; emergent aquatic macrophytes; floating and submerged aquatic macrophytes). While these PFTs largely reflect species' differences in photosynthesis, phenology and tolerance to flooding, they are also related to Poyang Lake ecological habitats, ecosystem dynamics and disturbance. For instance, large numbers of wintering waterbirds at Poyang Lake are known to utilize food resources from tuber-producing submerged aquatic plants or young C3 grasses (Burnham 2007, Barzen et al. 2009). C3 grass and forb-dominated areas are often used for livestock grazing in accessible areas, while C4 and C3 reeds are harvested by local people for domestic purposes and sometimes burned (Wang et al. 2012). Short C4 grass species (Table 1) include fast-growing weeds with global distribution (Guglielmini and Satorre 2004), but the potential effects of their expansion on wetland vegetation at Poyang Lake are not well known.

Object-based image analysis

Image segmentation and training object selection

To implement the object-based PFT classification, we first carried out image segmentation (Figure 2) in eCognition Developer 8.0 software (Trimble Inc.). We used the multiresolution

segmentation tool which allows construction of primitive objects of different sizes and enhances the response of object generation to landscape patch structure compared to other approaches (Baatz and Shäpe 2000). Based on the field observations, we expected that representation of wetland patches in this heterogeneous landscape would vary with object size even at small segmentation scales. Therefore, we generated nine small-object segmentations with scale values from 2 to 10 resulting in average object sizes of 1350-9000 m^2 (see examples in Figure 3) and ran separate classifications of 3- and 6-class PFT sets with each of these segmentation outputs. We did not implement segmentations beyond scale 10 because for a number of PFTs it was no longer possible to find representative homogeneous objects within field-surveyed locations, and the chance of class mixture inside the objects increased with object size (Yu et al. 2008, Liu and Xia 2010). The other segmentation parameters required by eCognition 8.0, shape and compactness, were kept at constant values of 0.9 and 0.1, respectively. These values were chosen through pilot investigation to enhance spectral contrast among primitive objects and increase the diversity of their shapes (Dronova et al. 2011). The input Landsat bands 1-5 and 7 were given equal weights.

Following segmentation, objects corresponding to water and bright non-vegetated sand were isolated using histograms of spectral indices, Normalized Difference Water Index (NDWI; McFeeters 1996) and Brightness index calculated by eCognition from spectral values of input image layers (eCognition Reference Book; Dronova et al. 2011). Human residential and active land use areas were also isolated using fine-resolution images from Microsoft Bing in ArcGIS 10 (ESRI Inc.) and Google Earth (Google Inc. 2010). The remaining objects representing vegetated wetland areas were then used in PFT classification.

Next, for each segmentation scale we selected training and test objects for classifications from field-surveyed areas that were likely to contain 75% or more cover of a given class. Whenever possible, objects from smaller-scale segmentations were "nested" within coarser-scale objects per same location. As a result, for each scale we generated 124-140 training/test objects with 12-25 objects per class (depending on the observed class prevalence in the study landscape) for the 6-class PFT set and 40-50 objects for the 3-class set. Unfortunately, problematic field access and lack of fine-resolution imagery at the time of study constrained our capability to allocate more objects while minimizing the chance of including mixed objects within a training/test set.

In PFT classifications we used spectral object attributes, specifically, Landsat TM bands 3,4,5,7, NDWI and a version of NDVI calculated with the shortwave-infrared TM band 5 instead of near-infrared. We tested the response of classification accuracy to four basic object-level texture metrics (Johansen et al. 2007, Laliberte and Rango 2009, Kim et al. 2011) for Landsat bands 3,4 and 5, specifically: standard deviation, coefficient of variation (the ratio of the object-level band value standard deviation to its mean) and grey level co-occurrence matrix (GLCM)-based entropy and homogeneity (Haralick et al. 1973). These texture metrics were added to the feature space with object-level spectral band means and indices, and changes in classification accuracy with added texture were compared among classes, methods and scales.

Machine-learning classifiers

Finally, we selected six machine-learning algorithms from the rich library of the open-source data mining software Weka 3.6.5 (http://www.cs.waikato.ac.nz/ml/weka/; Hall et al. 2009). Selected classifiers represented different machine-learning principles: a probabilistic Bayes method (NaïveBayesSimple in Weka notation), a logistic regression method (SimpleLogistic in

Weka), an artificial neural network algorithm (MultilayerPerceptron (MLP)), a support vector machine tool with polynomial kernel and complexity parameter value of 10 (SMO in Weka), a K-Nearest Neighbors (IBk in Weka) and a tree-based classifier (RandomForest). Detailed description of these classifiers can be found in Weka documentation and relevant literature (e.g., Witten and Frank 2005, Hall et al. 2009). Our objectives were to compare relative performance of these algorithms across different scales and to use the consistently top-performing methods for mapping the PFTs of interest. Therefore, we avoided extensive fine-tuning of the algorithms to training data and discuss the possibility of more rigorous parameterization in Discussion.

Classification accuracy assessment and uncertainty analysis

Due to the limited number of representative objects for training and validation, classification accuracy was assessed as 10-fold cross-validation (Witten and Frank 2005), repeated with ten different random seeds. From the error matrices of these 10 cross-validation results for each classifier and scale combination, we estimated mean values of the overall classification accuracy as well as class-specific user's and producer's accuracies and their averages. Although such averages should be used with caution due to different types of error represented by user's and producer's accuracies, they were appropriate in our study because a) all PFTs were of equal importance, thus, both omission and commission errors had to be minimized for each class; and b) the PFT classification procedure was applied to only vegetated areas without using any non-PFT classes. The calculations of accuracy metrics were based on the number of segments per class only, without considering object size. Classification method performance and pairwise class confusions were compared among nine image segmentation scales for 6-class and 3-class PFT sets and also for spectral feature sets with and without texture metrics.

Finally, we converted classification outputs into PFT maps for the PLNNR area. Based on classification results, generalized PFTs were mapped at a single segmentation scale using predictions from the highest-accuracy method, while the specific PFT map was compiled from predictions by the highest-accuracy scale-classifier combinations for each class (section 3.1 below). Using PFT-specific user's and producer's accuracies and the number of object samples, we estimated the overall accuracy of the composite map. We then quantified the uncertain areas corresponding to either overlaps among specific PFTs or locations where no specific classes were assigned with their respective highest-accuracy scale and method. Finally, we compared spatial extents and locations of the mapped generalized PFTs with their respective subclasses and evaluated the agreement between the assignments of these two hierarchical levels.

Results

Responses of classification accuracy to segmentation scale

The overall classification accuracy was sensitive to changes in image segmentation scale for both PFT sets (Figure 4a,b), and several features of this response were notable. First, for all six methods overall accuracy increased from scales 2 and 3 to coarser levels, with the peak around scale 8. Second, beyond scale 8 the overall accuracy did not continue to increase and even declined for some methods (Figure 4). Finally, the magnitudes of the overall accuracy values and change were relatively similar among different classifiers. The maximum accuracy for the 3-class set was 90% with the artificial neural network MLP and for the 6-class set – 88% with the support vector machine SMO, but performance of other methods was in most cases comparable.

Similar patterns of increasing accuracy from finer to coarser segmentation scales occurred for individual classes (Figure 5). For each generalized PFT, the highest average user's and producer's accuracy was found at scale 8 with the MLP method (Figure 5 a-c), while variation in accuracy across scales was the highest for mixed C4 grasses (Figure 5b). Among specific PFTs, however, both scales and methods of the highest accuracy varied. For C3 grasses, the maximum accuracy occurred at scale 8 with SMO (88%; Figure 5d), for C3-C4 tall reeds – at scales 3 (79.7%) and 8 (75.7%) both with IBk (Figure 5e); for emergent aquatic – at scale 6 with IBk (85%, Figure 5f) and for C4 short grasses – at scale 8 with SMO (91%, Figure 5h). Finally, C3 forbs (Figure 5g) and submerged and floating aquatic macrophytes (Figure 5i) had the highest class-specific accuracies (up to 98%) that were less sensitive to scale and method changes than for other PFTs.

The most common confusions among pairs of PFTs within both 3- and 6-class sets were also sensitive to changes in scale (Figure 6). For the 3-class set, misclassification of mixed C4 grasses with C3 grasses and forbs was consistently the largest component of error at all scales, but as the average of six methods it declined from scales 2-3 to scale 8 and then increased again at scales 9-10 (Figure 6a). The lower-magnitude confusion between aquatic macrophytes and mixed C4 grasses followed a similar pattern, also with the minimum value at scale 8. The average confusion between aquatic macrophytes and C3 grasses and forbs varied little with scale and involved less than 2% of all test objects (Figure 6a). For the 6-class PFT set, the confusions of C3 grasses and forbs with reeds, and of emergent aquatic macrophytes with submerged and floating involved the largest proportion of test objects at all scales (Figure 6b), with the minima at scales 6 and 8.

The effect of texture metrics on classification accuracy

Adding object-level texture metrics did not substantially improve overall accuracy for different method-scale combinations relative to the results without texture (examples for the highest-accuracy scale 8 are given in Figure 7). None of the detected improvements with added texture were sufficient to exceed maximum accuracy based on "spectral-only" inputs for either class hierarchy level. Most of the changes were within 3% of the "spectral-only" scenarios, and their magnitude and sign were inconsistent among scale values, methods and class sets. Notably, both MLP and IBK classifiers, which often delivered high accuracy with spectral-only inputs, performed consistently worse with each of the texture metrics included (Figure 7). In both PFT sets, none of the individual classes clearly benefited from adding texture, while occasional increases in accuracy for some of the classes were always accompanied with losses in accuracy for other classes (data not shown). Changes in class-specific accuracy with added texture inputs were predominantly within 0-3% of the "spectral only" values and not consistent among scales, algorithms or PFT hierarchy levels.

Final PFT maps and classification uncertainty

Both the generalized and specific PFT maps reflected belt-shaped zonation of wetland vegetation types around water features (Figure 8a,b), and spatial distributions of PFTs were consistent with previous maps of PLNNR vegetation (Zeng et al. 2007, Wang et al. 2012) and wetland annual submersion times (Andreoli et al. 2007, Zhao et al. 2011). The highest-accuracy scale values for most specific PFTs (Figure 5) were proportional to spatial extents and general degree of fragmentation of class patches within the study landscape (Figure 8b). For the specific 6-class PFT set, the overall accuracy of the composite map was 91.1%, indicating ~3% improvement

relative to the best single-method result (SMO at scale 8). However, the compositing approach resulted in two types of uncertainty (Figure 8c): areas where assignments of two or more specific PFTs overlapped (~13% study area) and areas where no class was assigned based on its highest-accuracy scale and method (~7% study area and 6-13% of generalized PFT areas, Figure 8d). Comparison of the 3- and 6-class maps also revealed that ~22% area of each generalized PFT overlapped with specific PFT subclasses from the other generalized category (Figure 8c,d), indicating potential mismatches between class levels. At the same time, 65-72% of each generalized PFT were filled with their respective subclasses exclusively (Figure 8d).

Discussion

The utility of OBIA for PFT classification in the study area

Our results demonstrate utility of the object-based approaches for mapping wetland plant functional types and confirm the importance of object scale in such analyses (Liu and Xia 2010, Kim et al. 2011). The highest overall and class-specific accuracies in most cases occurred not at the finest scales close to pixel level, but at coarser scales with 5-8 Landsat 30-m pixels per average object. Integration of spectral signal across a larger number of pixels apparently accentuated the contrasts among PFTs in both 3- and 6-class sets, leading to higher classification accuracy with most methods. These outcomes were consistent with previously discussed reduction in within-class spectral variation at coarser segmentation scales which may remove the "salt-and-pepper" speckle (Yu et al. 2006, Liu and Xia 2010, Kim et al. 2011, Ouyang et al. 2011) and enhance the relationships between image object parameters and ground-assessed vegetation variables (Addink et al. 2007). At the same time, accuracy metrics did not continue to increase with scale, because class mixtures were more likely to occur in larger objects making the latter less representative of their primary classes (Wang et al. 2004, Yu et al. 2008).

Our results suggest that averaging of spectral signal across larger number of pixels could smooth the local variation and enhance class representation by objects, provided that the latter match class' patch primitives (Clinton et al. 2010a). However, to fulfill the latter condition, it is important that segmentation outputs approximate patch structure of classes of interest prior to classification (Liu and Xia 2010, Clinton et al. 2010a). In our study, generalized PFTs were reasonably well represented by a single segmentation scale 8; however, for specific PFTs no single scale value could be declared as optimal for all classes. Hence, in the future work, it would be essential to rigorously evaluate the correspondence between segmentation outcome and landscape patch structure for classes of interest. Given problematic field access at Poyang Lake, such a priori patch information may be obtained from the high-resolution imagery.

The lack of accuracy improvement with texture

The lack of improvement in classification accuracy with added texture metrics in our study could be attributed to 30-m input image resolution, the small number of pixels per object at the considered range of scale values and the lack of pronounced textural differences among grass-dominated classes (Ouyang et al. 2011). It is possible that class-specific heterogeneity in canopy structure and composition was smoothed within 30-m pixels, thus contributing more strongly to spectral than to textural contrasts among PFTs. Several object-based studies that benefited from using texture in vegetated landscapes used high ($\leq$ 4m) resolution images and class sets with more pronounced differences in surface type and structure (e.g., Johansen et al. 2007, Hájek 2008, Laliberte and Rango 2009, Laba et al. 2010, Kim et al. 2011). In such analyses, textural patterns enhancing class contrasts were particularly important at scales where the number of

pixels per object and levels of allowed spectral heterogeneity were large (e.g. scales 55-70 in Laliberte and Rango 2009, scales 20-25 in Kim et al. 2011), and spectral contributions of the edge pixels were small (Laliberte and Rango 2009).

In contrast, Ouyang et al. (2011) did not find texture metrics particularly useful even with high-resolution QuickBird data for Yangtze River estuarine wetlands with predominantly herbaceous vegetation and high spatial variability among primitive objects, similar to our study area. Furthermore, in our results texture only occasionally enhanced contrast for specific class pairs, but not within the whole 3- or 6-class PFT sets. Thus, to further test potential benefits of texture for Poyang Lake PFT analysis, future work may use higher-resolution images to examine class-specific spatial patterns, add digital texture layers as inputs to segmentation (Johansen et al. 2007), or apply texture only at specific decision steps in customized rule-based classifications.

Effects of machine-learning classifiers

No single algorithm of the six considered approaches was consistently superior across different scales and PFT sets. Frequently high performance of the SMO method for most classes and scales suggests that non-linear decision boundaries among PFTs in our feature space were successfully learned with support vector machines, despite relatively small training sample sizes. However, K-Nearest Neighbors IBk, artificial neural network MLP and logistic regression SimpleLogistic were also sufficiently flexible to discern the patterns in the data and deliver comparably high classification accuracy. While these four methods were often superior to RandomForest and NaiveBayesSimple, our results do not distinguish any single "best" algorithm among them.

To date, only few studies have compared multiple machine-learning approaches in wetland or vegetated object-based landscape studies. Clinton et al. (2010b) modeled presence/absence and infestation levels of an invasive grass in western USA and achieved the best results with SVM methods and boosted J48 regression trees, which performed better than MLP and RandomForest. Richmond (2011) investigated the effect of topographic features on wetland classification by applying Weka classifiers to IKONOS imagery and found that IBk and two decision tree methods, including RandomForest, were generally superior to logistic regression, NaïveBayes and SMO. These findings together with our results suggest that suitable machine learning methods need to be experimentally matched to the problem at hand (Caruana and Niculescu-Mizil 2006). Obtaining larger training samples, more thorough evaluation of the algorithm parameters and testing larger attribute sets would be the important future steps to test and improve classifiers' capacity for mapping Poyang Lake wetland PFTs.

Classification success among specific PFT groups

Observed differences in the scale and magnitude of maximum classification accuracy for individual PFTs likely arose from class-specific ecology of dominant species, unique phenology and disturbance that affected their radiometric characteristics. For instance, the highest individual accuracies of submerged and floating macrophytes and their low sensitivity to segmentation scale (Figure 5i) could be related to unique permanently flooded status of this type and contribution of water in plant tissues and canopy gaps to spectral reflectance. Portions of submerged plant beds, however, could be missed due to water turbidity and early growth stage. Similarly, relatively high classification accuracy of C3 forbs (Figure 5g) could be attributed to distinctively rougher canopy surface and lower albedo compared to grasses, while their small highest-accuracy scale value reflected small size and fragmented distribution of the forb patches

within the grass matrix (Figure 8b).

The other four specific classes were all dominated by emergent grasses (Table 1), and more frequent confusion among them could result from similarities in canopy structure (Ouyang et al. 2011), plant and soil moisture status and disturbance agents. The most extensive Poyang Lake PFT, C3 grasses, often occurred in vast belts where dominant *Carex* species contributed to >90% cover (Chen et al. 2007; Dronova, field observation; Figure 8a). However, livestock and waterbird grazing, uneven flooding due to variable topography and presence of C3 forbs may cause localized heterogeneity and increase similarity to other grassland PFTs. Notably, the pronounced confusion of C3 grasses with C4 and C3 reeds at all scales and classification methods (Figure 6) was most likely affected by human disturbance. Recurrent reed harvesting by local people (Wang et al. 2012) opens the canopy and leads to colonization of harvested areas by shorter C3 grasses and forbs. Subsequent reed regrowth from stubble produces gradients of plant vigor and patchy areas where dry biomass and live plants are mixed at fine spatial scales. As a result, relatively higher accuracy for reeds was observed at either fine segmentation scales 2-3 where object sizes approximated smaller reed clumps of similar phenology state or at coarser scales 5-8 where some of the reed patch heterogeneity was smoothed over larger numbers of object pixels (Figure 5e). However, including object-level texture did not substantially enhance the contrast among reeds and other PFTs, likely due to large compositional variation within these mixed areas and smoothing of their structural heterogeneity within 30-m Landsat pixels.

In contrast, C4 short grasses were relatively well distinguished from both reeds and C3 grasses. This result was consistent with ecological capacity of the dominant C4 short grasses to form dense monospecific swards (Horowitz 1972, Guglielmini and Satorre 2004), as well as with their distinct seasonality from C3 grasses captured in the supplementary winter NDVI input layer. At the same time, emergent aquatic macrophytes were frequently confused with both C4 short grasses and other PFTs by all machine-learning methods. We explain this confusion by the landscape position of emergent aquatics between higher-elevation PFTs with shorter annual submersion times and floating/submerged vegetation in the adjacent water bodies (Figure 8a,b). Overlaps in spatial distributions of emergent aquatic and more upland species likely increased the chance of mixed pixels and objects along the edges of class patches (Lenssen et al. 1999, Wang et al. 2004). Resolving this confusion in the future work would require higher-resolution images and accurate digital elevation models.

Disagreement between PFT classification levels

The observed confusions among PFT classes and differences in their individual highest-accuracy scale values contributed to spatial variation of the uncertainty in PFT maps and to the mismatches between generalized PFTs and their respective subclasses. Most of the uncertainty areas were concentrated along class boundaries (Figure 8c), where sub-object class mixtures could lead to different predictions among methods, and even small changes in scale could strongly affect object-level class memberships. This type of uncertainty may be addressed in the future work by combining object- and pixel-based classification approaches (Wang et al. 2004).

Our results highlight two principal caveats that need to be considered in landscape classifications with OBIA at multiple object scales. First, the relationships among spectral object attributes at different spatial scales may not necessarily match the proposed hierarchy of PFTs based on exclusively ecological information (i.e. plant traits). This issue can be addressed in the future by explicitly incorporating intrinsic spatial patterns of PFTs (inferred via high-resolution

imagery) and optical variability (Ustin and Gamon 2010) into design of classification schemes. Second, hierarchical top-down and bottom-up mapping approaches that use different nested scales to represent PFT class levels would likely suffer from error propagation among scale levels, which has not been extensively discussed in previous studies. Because the possibility of multi-scale object-level analyses is one of the key OBIA strengths (Tuxen and Kelly 2008, Kim et al. 2011), developing a methodology for monitoring classification uncertainty across multiple object scales would be a powerful enhancement to this research framework.

Summary and future work

This study represents the first application of object-based image analysis to classify and map wetland plant functional types in the large heterogeneous wetland of Poyang Lake, PR China. We focused on major PFTs suggested by ecophysiological, phenological and structural characteristics of the dominant wetland plant species. Our objective was to determine which image segmentation scales from a range of small values [2-10] and which machine-learning classifiers from six popular families could facilitate PFT classification in this area. We found that the highest overall and PFT-specific classification accuracies occurred at object scales that were markedly coarser than pixel level, although specific PFTs differed in their scales of maximum accuracy.

Results suggest that OBIA may facilitate discrimination of heterogeneous wetland vegetation types by smoothing the local variability at the object level, which is important for studying complex Poyang Lake landscape with problematic field access. By treating localities as patches, the OBIA framework can address at least some of the uncertainty in vegetative cover and improve classification accuracy relative to pixel-equivalent scales even with spectral features alone. Including basic object-level texture metrics did not enhance the accuracy, likely due to smoothing of the class patterns within the 30-m Landsat pixels and small values of the object scale for which training and test data could be obtained. Future research should test image segmentation outcomes against landscape patches derived from localized high-resolution data and couple these analyses with wide-swath medium-resolution imagery for broad-scale PFT mapping.

Comparison of results at two PFT hierarchy levels revealed a 29-35% disagreement between the area of each generalized PFT and its respective subclasses, suggesting that future multi-scale analyses should more closely match classification schemes with spatial and spectral hierarchy among class landscape patches. Results indicate that the effects of grazing and harvesting and class mixtures along the inundation and topographic gradients could affect classification error in addition to spectral similarity among PFTs. Furthermore, none of the six machine-learning classification methods was consistently superior at discriminating among classes and reducing major components of error. Future work should conduct a more rigorous pre-classification selection of algorithm parameters as well as object attributes that define feature space for machine-learning tools (Yu et al. 2008, Clinton et al. 2010a,b, Richmond 2011).

Our results illuminate spatial characteristics of Poyang Lake wetlands that may be relevant to multiple research efforts, including analyses of plant function and biogeochemical fluxes (Wang et al. 2012), environmental drivers of habitat for waterbirds (Barzen et al. 2009), infectious disease agents (Chen and Lin 2004) and flooding hazards (Jiang et al. 2008, Qi et al. 2009). The mapped spatial distributions of PFTs may provide useful inputs to models of climate and land use change impacts on Poyang Lake wetland dynamics and habitats. For instance, fringe-like

distribution of the C4 short grasses (some of which are distributed globally as opportunistic weeds) may reflect the importance of the annual food cycle in controlling their intrusion into wet C3 grasslands. The uncertainty of climate change and new local dam structure effects on future Poyang Lake hydrological regimes suggests the need to investigate more thoroughly the feedbacks among C4 grass spread, flooding and climate variables. Similarly, changes in Poyang Lake water levels following closure of the Three Gorges Dam project upstream Yangtze River (Guo et al. 2012) may also alter broad-scale hydrological controls on vegetation composition and function across this landscape, which should be investigated through landscape-level ecosystem models. Extending our research framework to other seasons, years and remote sensing data sources will facilitate cost-effective monitoring of Poyang Lake plant functional diversity and studies of its response to climatic, hydrological and human-induced change drivers.

Acknowledgements

This research was supported by the PR China 863 High Technology Program (2009AA12200101) and the National Aeronautics and Space Administration (NASA) Earth and Space Science student Fellowship (NNX09AO27H). We thank the Key Lab of Poyang Lake Ecological Environment and Resource Development (Jiangxi Normal University, PR China), Dr. Lingguang Huang (Center for Remote Sensing/GIS Application of Jiangxi Province, Nanchang, PR China), Dr. Wan Wenhao (Nanchang University, PR China), Qiming Zheng, Xuelin Zhou, Xiaoli Liu, Zhan Li and Shaoqing Shen for the assistance with Poyang Lake field surveys. The study benefited from the support and services of the University of California, Berkeley's Geospatial Innovation Facility (gif.berkeley.edu). We are also grateful to the two anonymous reviewers for their comments and suggestions that have greatly helped to enhance this paper.

Tables

Table 1. Summary of Plant Functional Types (PFTs) determined from cluster analysis of dominant wetland macrophytes.

Generalized Plant Functional Type	Specific Plant Functional Type	Examples of dominant species (>70% cover)	Common life form	Habit	Photosynthetic pathway	Main growing season at Poyang Lake	Typical height above the soil, m
C3 grasses and forbs	C3 grasses	*Carex cinerascens, C. unisexualis, C. scabrifolia Phalaris arundinacea, Alopecurus japonicus*	Graminoid/grass	Erect	C3	October-May	0.1-1.5
	C3 forbs	*Artemisia selengensis, Artemisia lavandulaefolia, Potentilla limprichtii, Rumex crispus , Lapsana apogonoides, Polygonum hydropiper, P. minus, P. japonicum, Mazus japonicus, Gnaphalium affine, Cardamine hirsuta*	Forb/herb	Erect or prostrate	C3	October-May	0.03 - 1.5
Mixed C4 tall and short grasses (also incl. C3 reeds)	C4 and C3 reeds	*Miscanthus sacchariflorus (C4), M. floridulus (C4), M. sinensis (C4), Arundinella hirta (C4) , Phagmites communis (C3)*	Graminoid/reed	Erect	C4 or C3	April - October	0.8 – 5
	C4 short grasses	*Cynodon dactylon, Paspalum distichum, Digitaria spp.*	Graminoid/grass	Creeping	C4	March-October	0.05-0.5
Aquatic macrophytes	Emergent aquatic macrophytes	*Zizania latifolia, Scirpus marqueter, Carex doniana, Eleocharis valleculosa, Eleocharis tuberosa*	Graminoid/grass	Erect	C3, C4-C3	March-October	0.5 – 3
	Floating and submerged aquatic macrophytes	*Nymphoides peltata, Trapa natans, Potamogeton franchetii , P. malaianus, Hydrilla verticillata, Vallisneria spiralis, Ceratophyllum demersum*	Forb/herb	Floating/mat and/or submerged	C3, C3-C4, C3-CAM*	April - October	0.5– 2.5 including underwater

*Crassulacean Acid Metabolism (CAM), a type of photosynthetic pathway which may occur also in aquatic plants (Sculthorpe 1967)

Figures

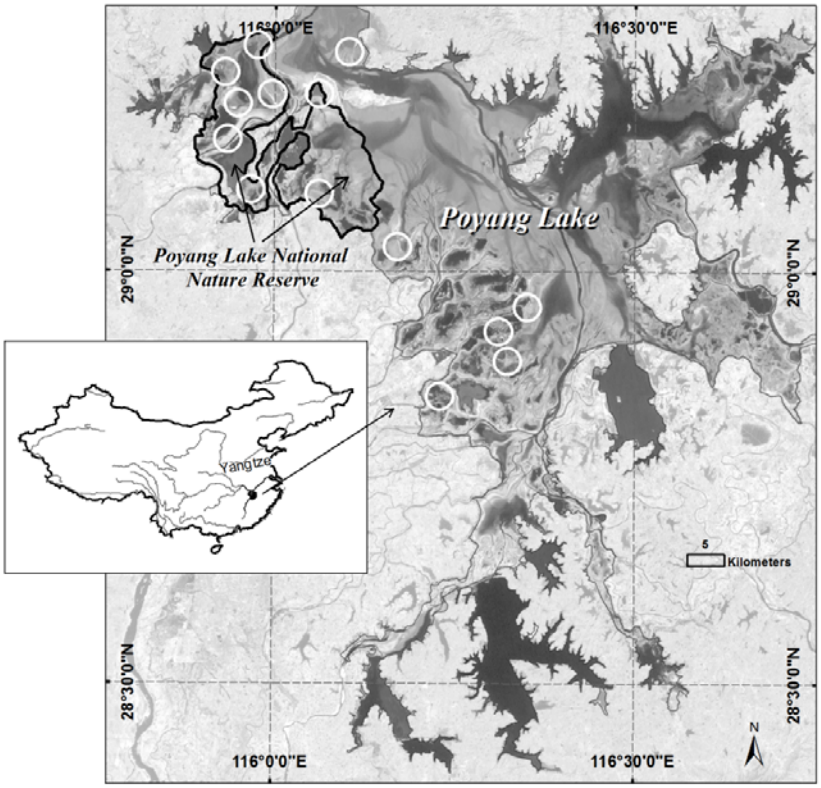

Figure 1. Study area of Poyang Lake, Jiangxi Province, People's Republic of China and Poyang Lake National Nature Reserve. White circles indicate locations of field-surveyed sites.

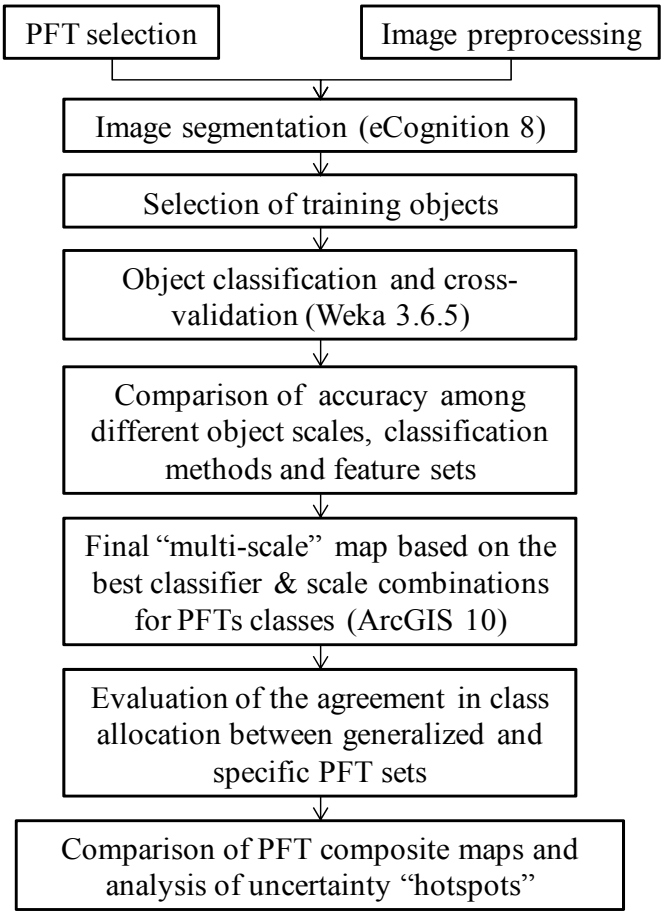

Figure 2. Outline of the study procedures.

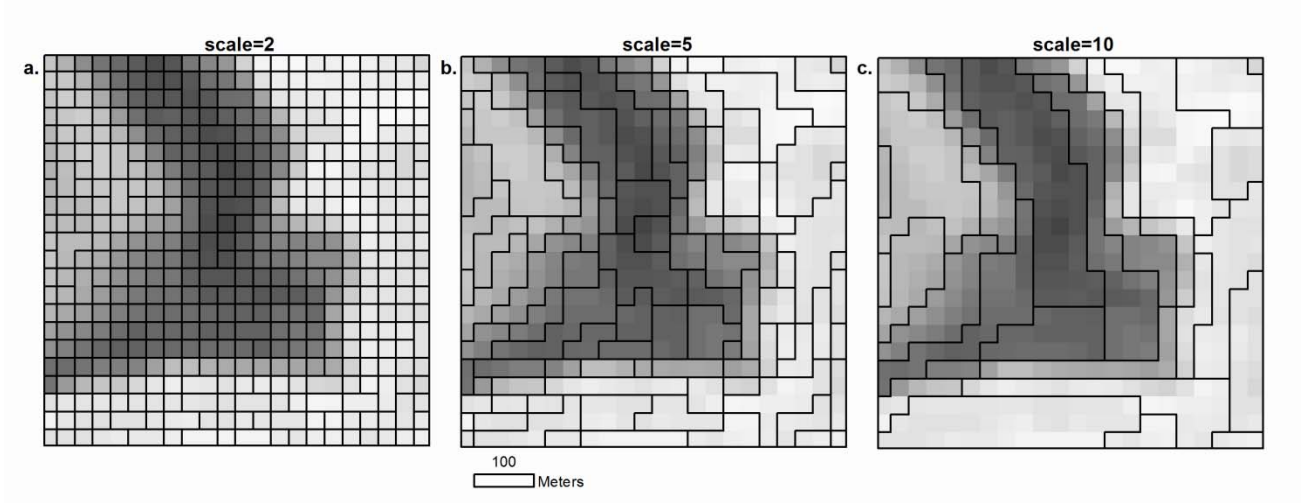

Figure 3. Examples of the multiresolution segmentation output for the Landsat image at scale values a) 2; b) 5 and c) 10.

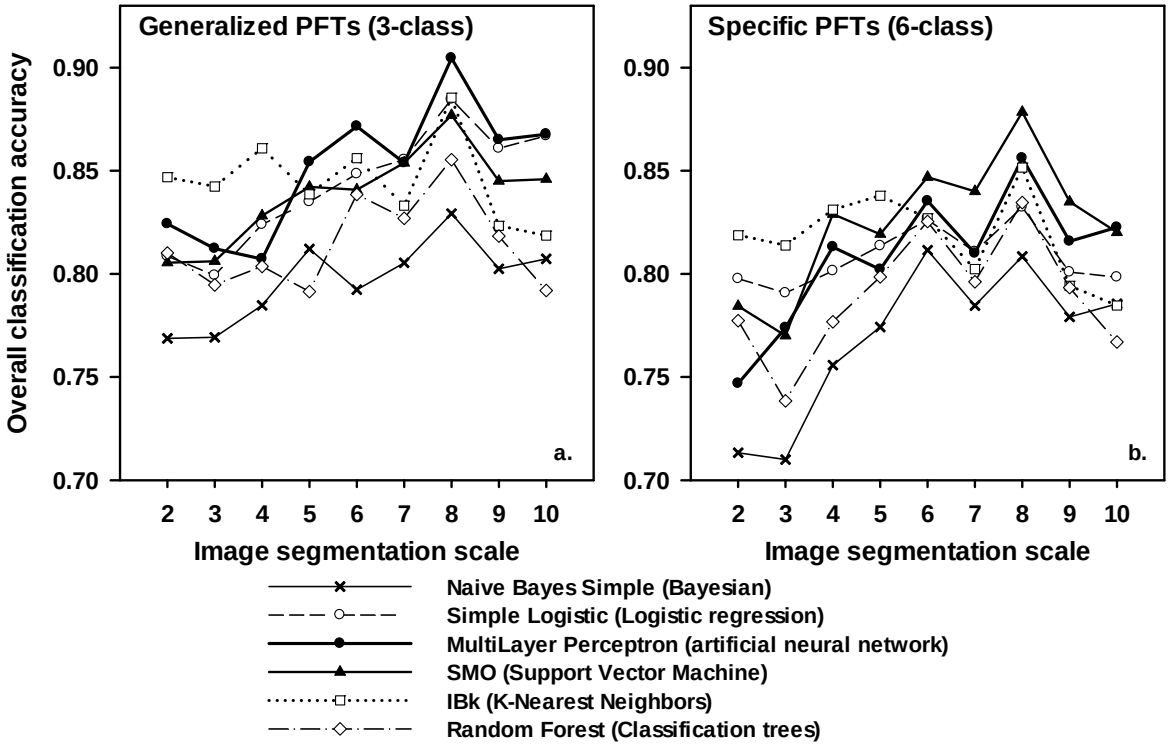

Figure 4. Variation in overall classification accuracy for a) 3-class generalized and b) 6-class specific Poyang Lake wetland plant functional type sets with image segmentation scale.

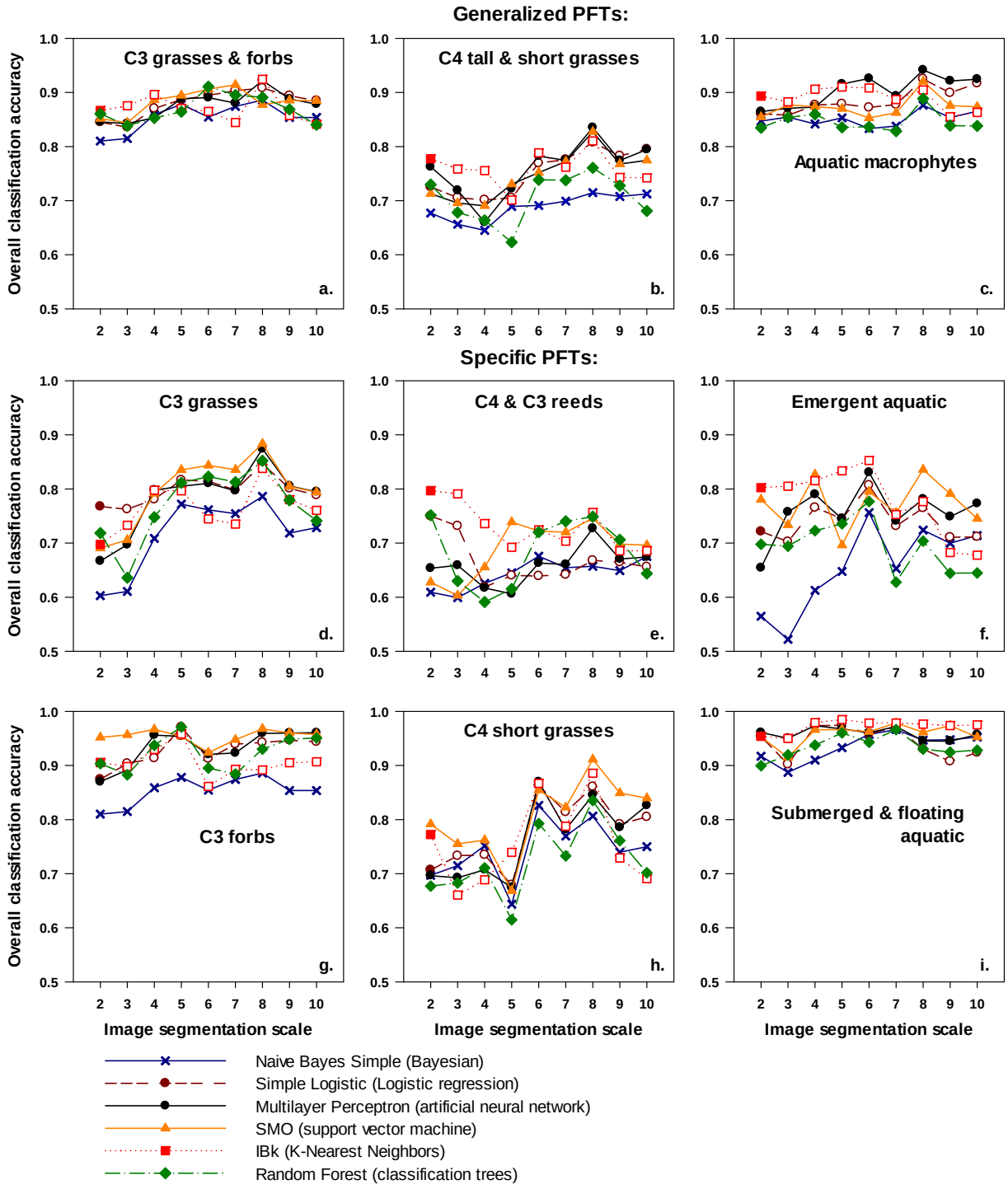

Figure 5. The average of user's and producer's accuracies for the 3-class (a-c) and 6-class (d-i) sets of Poyang Lake wetland plant functional types shown for six machine-learning classifiers.

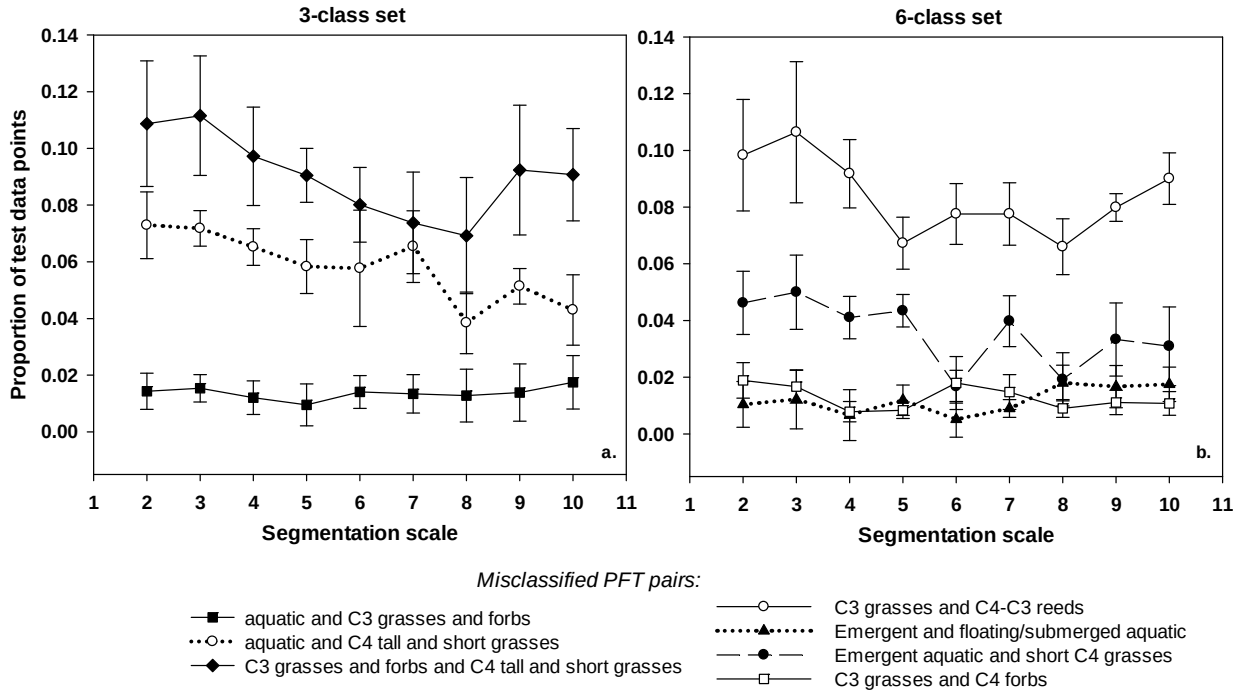

Figure 6. The most common pairwise confusions among a) generalized and b) specific plant functional types that consistently contributed to image classification uncertainty, shown as proportion of the total number of testing objects averaged among six highest-accuracy classification methods (error bars indicate standard deviations of confusion estimates).

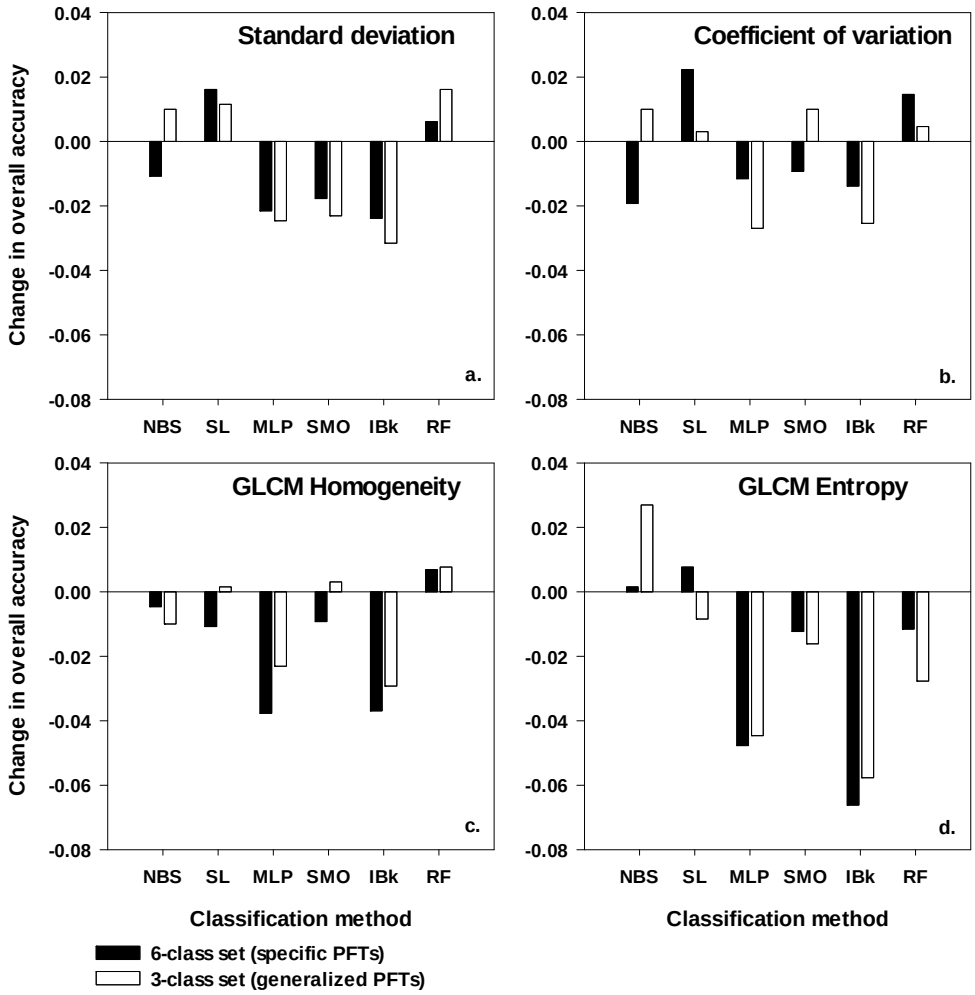

Figure 7. Change in the overall classification accuracy following addition of the object-level texture metrics based on Landsat bands 3,4 and 5: a) standard deviation; b) coefficient of variation, c) GLCM homogeneity and d) GLCM Entropy; shown for the highest-accuracy segmentation scale 8 and six machine-learning classifiers in Weka (NaïveBayesSimple (NBS), SimpleLogistic (SL), Multilayer Perceptron (MLP), support vector machine (SMO), K-Nearest Neighbors (IBk) and RandomForest (RF)) .

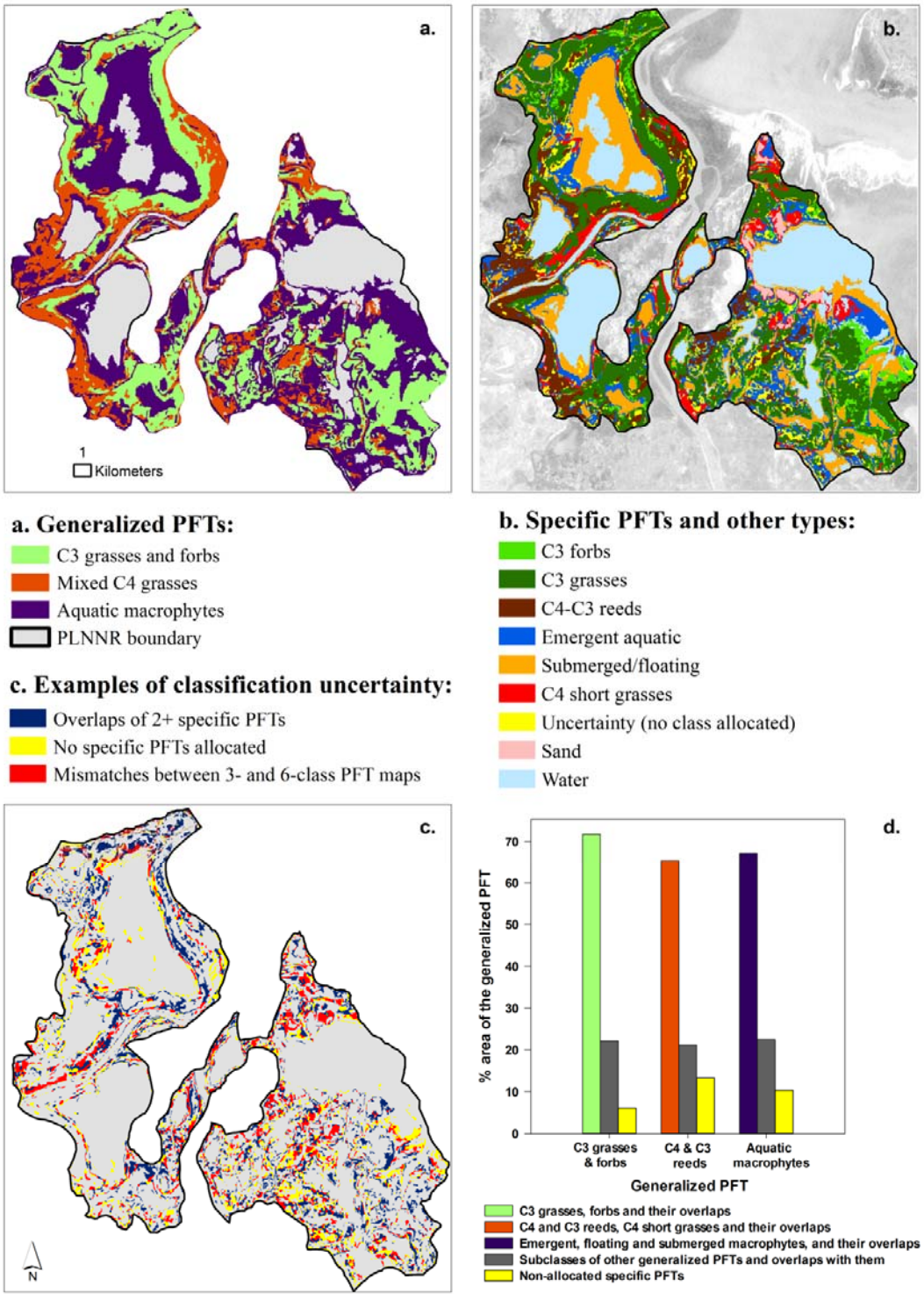

Figure 8. Poyang Lake plant functional types and classification uncertainty: a) generalized PFTs mapped with the highest-accuracy Multilayer Perceptron method at segmentation scale 8; b) specific PFTs mapped with their highest-accuracy classifier and scale combinations; c) locations of different types of classification uncertainty and d) proportions of assigned and misallocated specific PFTs per each generalized PFT.

CHAPTER 3. Object-based "dynamic cover types" – a new framework for monitoring landscape-level ecosystem change

Abstract

Traditional approaches of monitoring ecosystem change with remote sensing data often focus on 'static' cover types and assess their change per spatial units of interest. However, in dynamic landscapes with frequent disturbance long-term surface changes may be obscured by high-magnitude short-term dynamics. Availability of cloud-free remote sensing data is often inconsistent among change periods, which contributes to the uncertainty in change detection among 'static' classes. Alternatively, I propose Dynamic Cover Types (DCTs) to characterize highly variable areas based on their nested change regimes shaped by climate, phenology and disturbance. I define DCTs as sequences of surface transformations that have distinct temporal trajectories observable across landscapes within a given change period. I combined multispectral and microwave satellite imagery to classify DCTs for a large seasonally inundated freshwater wetland in China in 2007-2008. Instead of using pixels, I mapped DCTs using object-based image analysis and used principal components transformation to enhance their spectral contrast. Resulting spatial distributions and extents of mapped DCTs simultaneously reflected several key drivers of wetland change, including broad-scale changes in submersion times, vegetation phenology and prevalence of plant cover and localized fine-scale disturbance. I further examined DCT response to a hypothetical scenario of a warmer wetter early spring by substituting spring 2008 images with 2007 ones. In this comparison, the strongest response was detected from DCTs that were closely associated with the water body which expanded their extents and changed spatial position (permanent water and ephemeral inundated mudflats). Even classes with small change in total extent exhibited substantial re-distribution expressed in shifts to higher-elevation areas in opposite direction from permanent water bodies and localized expansion of change classes with green emergent vegetation state. Overall, results indicate that object-based dynamic class boundaries may provide useful spatial units to highlight characteristic types of landscape change for environmental research, ecosystem monitoring and management and to enhance spatially explicit modeling of terrestrial and wetland biospheric processes.

Introduction

Landscape ecosystems are never truly "stable"; they constantly vary due to physical processes, biological interactions, phenology and disturbance. The assumption of "change" versus "no change" for a given ecosystem property depends on the research subject and on temporal frequency, spatial resolution and extent of the landscape data (Crews 2008, Coops et al. 2009b, Assendorp 2010, Liu and Cai 2011). In the face of changing climate and growing human population, rapid and accurate assessments of environmental change are of critical importance for ecological conservation, adaptive management, land use planning and forecasting landscape response to scenarios of the future (Foley 2005, Parmesan 2006, Friend et al. 2007, Thuiller et al. 2008, Grimm et al. 2008, Randerson et al. 2009, Liu and Cai 2011). Remote sensing platforms are particularly useful in these tasks by providing cost-effective opportunities for repeated monitoring of change over large areas and locations with difficult ground access (Chambers et al. 2007, McCleary et al. 2008, Xiao et al. 2008, Rebelo et al. 2009, Gong et al. 2010).

Traditional landscape analyses from remote sensing data often use "static" classes which correspond to single states (cover types) observable for extended periods of time. The "change" occurs if a location changes states, i.e. its highest-probability cover types differ among

successive points in time. A variety of digital change detection techniques have been developed to compare classes among different image dates or to infer cover type transitions from processed multi-temporal image stacks (Singh 1989, Mas 1999, Lu et al. 2004, Coppin et al. 2004). However, most of their applications have focused on the contrast between change and no change in landscapes (often bi-temporal) where classes persist in time and shift only as a result of disturbance, succession or land use conversion (Liu and Cai 2011). Change detection may be less straightforward in rapidly varying areas such as periodically inundated wetlands, where long-term trends in surface composition may be obscured by shorter-term dynamics of the local ecosystems (Crews 2008, McCleary et al. 2008). High-quality remote sensing data are discrete in time and may not always match the stages of change periods (e.g. flood stages) or phenology precisely, which contributes to error in classification and change detection (Lunetta et al. 2002, Hess et al. 2003, McCleary et al. 2008). At the same time, due to their spatial and temporal heterogeneity, such "dynamic" landscapes often host high biological diversity and play important roles in local and regional climate and biogeochemical fluxes (Gibbs 2000, Dudgeon et al. 2006, Ordoyne and Friedl 2008). Thus, alternative approaches are needed to characterize and monitor such areas in order to detect their response to climate change and human activities (Ordoyne and Friedl 2008, Wang et al. 2012).

I propose a framework of "dynamic cover types" (DCTs) defined here as sequences of states with distinct temporal trajectories observable across the landscape within a given change cycle period. This idea is based on the premise that in dynamic landscapes, temporal signature of a given location is a product of multiple simultaneous drivers including physical environment, climatic variation, vegetation phenology and ecological adaptations as well as natural and human-induced disturbance such as flooding, fire, grazing etc. Periodic processes may produce "regimes" of change which shape unique ecosystem types and functions, sometimes along the gradients of change-inducing factors (e.g., inundation). Thus, any "snapshot" landscape composition observed on a single-date remote sensing image is actually a manifestation of multiple change "regimes" at that point in time. Spatial extents and distributions of these change units (approximated by DCTs with multi-temporal imagery) may highlight different types of ecosystem dynamics for a given change period (e.g. growing season or flood cycle) as well as longer-term landscape trends if compared among multiple years.

The DCT concept builds on multiple previous studies that characterized landscapes in terms of transitions rather than static states. For instance, Hess et al. (2003) used "cover-state classes" based on physically possible "bi-temporal" transitions among cover states between low and high flood stages for inundated wetlands in the central Amazon. A number of studies used "change classes" along with static cover types and mapped those from either multi-date composites of the original images (e.g., Weismiller et al. 1977, Soares and Hoffer 1994)or ecologically meaningful data-reducing transformations such as principal component analysis (PCA), Kauth-Thomas algorithm and other methods (e.g., Ribed and Lopez 1995, Collins and Woodcock 1996, Coppin et al. 2001, Seto et al. 2002a). In recognition of the complex landscape processes underlying snapshot patterns in temporally discrete data, several studies have analyzed transitions as land-cover change curves or trajectories extracted from multi-temporal imagery (Lawrence and Ripple 1999, Mertens and Lambin 2000, Vagen 2006, Liu and Cai 2011). Finally, panel analysis approach proposed by Crews (2008) infers continuous change trajectories per pixel location from discrete multi-temporal images. Applications of this method demonstrated the importance of both inter-annual and intra-annual dynamics in shaping the overall land cover and land use change in different landscapes (Crews 2008, McCleary et al. 2008).

My framework further extends these ideas in several directions. I define DCTs specifically as the types of continuous transitions among cover types that apply to one cycle of change, e.g. the interval between two annual inundation events or one growing season of vegetation. In turn, the transitions among DCTs between successive change periods should be analyzed as longer-term trends in land cover, which could be further compared with trends in change-inducing geomorphological, climatic and other factors. Dynamic classes may differ in the number of state changes within their spectral-temporal trajectories extracted from discrete multi-date images. Furthermore, state-to-state transitions within a class trajectory do not have to be unique to each DCT - only their sequences are unique. Finally, I propose mapping and analyzing DCTs per spatial units representing small landscape patches rather than individual pixels, to reduce the effect of localized heterogeneity on the confusion among different change trajectories. This paper presents a pilot illustration of the DCT concept for a large periodically inundated wetland, but I also discuss the strategies for generalizing this framework to other dynamic landscapes.

My study performed the DCT analysis for one flood cycle at Poyang Lake, the largest freshwater lake-wetland complex in China (Figure 1). This >4000 km^2 landscape undergoes continuous surface dynamics due to annual monsoon-driven flooding and inter-annual climatic and hydrological fluctuations in the Yangtze River basin (Shankman et al. 2006). During the low water winter season this area hosts large numbers of migratory waterbirds from the East Asian Flyway including critically endangered species (Barzen et al. 2009). Available winter habitat and food resources are shaped by the year-round change in hydrology and vegetation productivity (Barzen et al. 2009). Response of wetland surface to flooding also controls the habitat for snail species *Oncomelania hupensis*, the intermediate host to the parasite *Schistosoma japonica* causing a severe human disease in the region and globally (Seto et al. 2002b, Chen and Lin 2004). Hence, it is important to improve the understanding of spatio-temporal linkages between ecological habitats and wetland change regimes for management, conservation and hazard risk assessments. However, current Poyang Lake dynamics might change in the near future due to reported declines in winter water storage, parallel to closure of the Three Gorges Dam upstream Yangtze River (Liu 2009, Guo et al. 2012), and new proposed local water control structures with uncertain but potentially adverse ecological effects (Barzen et al. 2009, Finlayson et al. 2010). Given multiple anthropogenic pressures and high spatio-temporal heterogeneity of these wetlands, it is difficult to attribute their landscape trends exclusively to any single factor. Furthermore, comprehensive field studies are problematic to implement here due to large size of the lake and limited field access to seasonal marshland. Hence I expected that DCTs may provide useful spatio-temporal units to categorize Poyang Lake dynamics in a single change period, and ultimately to develop more comprehensive approaches to study its long-term change.

I characterized Poyang Lake DCTs as major sequences of local wetland state changes per flood cycle extracted from the combination of passive-sensor multi-spectral and microwave radar satellite images. The DCTs were first mapped for the summer 2007-spring 2008 flood cycle and then compared with a hypothetical "quasi-experimental" scenario of a warmer wetter spring by substituting same-sensor spring 2008 images with those from spring 2007 (Figure 2). To enhance class contrasts and to avoid "salt-and-pepper" speckle from local heterogeneity and spectral noise, I 1) performed the classification using object-based image analysis (OBIA; Blaschke et al. 2000, Benz et al. 2004, Blaschke 2010) rather than pixel-based methods and 2) applied PCA transformation to the object-level means of input bands prior to the object classification. I further discussed the strategies to enhance the DCT framework and adapt it for long-term ecosystem monitoring and landscape environmental modeling in the future work.

Methods

Study area

I focused on the main Poyang Lake water body south from the channel with the Yangtze River (28°25′–29°20′N, 115°48′–116°44′E; Figure 1). During the April-September rain season water coverage may exceed 4000 km^2; this period is also a "warm" growing season for aquatic vegetation and grasses in higher-elevation areas with short submersion times (Wang et al. 2012). The "low water" season from October to April is characterized by flood recession with the lowest water levels and <1000 km^2 water extent in January; at this time the landscape becomes a mosaic of smaller permanent water bodies and exposed mudflats that are gradually colonized by emergent plants of the "cool" growing season (Chen et al. 2007, Dronova et al. 2011, Wang et al. 2012). These dynamics govern local ecological processes, however, specific patterns of change are still not fully understood (Dronova et al. 2011, Wang et al. 2012), while the field surveys are often constrained by vast areas of soft inaccessible mudflat and the risk of infectious disease (Dronova et al. 2011, Feng et al. 2012). Hence I expected that analyses of this wetland's composition at any point in space and time would benefit from the broader spatio-temporal context (Liu and Cai 2011) provided by the DCTs and multi-temporal remote sensing data.

Remote sensing data

I used remote sensing data from April 2007 to May 2008 (Table 1) covering pre-flood conditions of spring 2007, summer flood of 2007 and its recession, and the low water season until the new spring 2008 flooding. I used nine scenes of Beijing-1 microsatellite with 32-m spatial resolution, three multispectral bands (near-infrared (NIR), red and green), 600-km swath and 5-day revisit time (Table 1), and eight scenes of the ENVISAT Advanced synthetic Aperture Radar (ASAR) with C-band (5.3 GHz) in wide swath mode (WSM, 400-km swath) with single polarization (either HH or VV, Table 1), 150-m spatial resolution and 16-43^0 view angle range. Beijing-1 sensor was selected due to its frequent revisit time and spectral sensitivity to both hydrological and flood-free features on the landscape as well as differences in composition and phenology among herbaceous vegetation types (Wang et al. 2012). However, water turbidity at Poyang Lake may increase the confusion between water and newly exposed mudflats in multispectral data (Dronova et al. 2011). Given the lack of reliable high-or medium-resolution digital elevation and bathymetric data, I thus included the microwave sensor due to its sensitivity to changes in water extent that are controlled by both the flooding and the local elevation gradients (Figure 3).

Because Beijing-1 sensor does not have the calibration onboard, I used raw digital numbers (DNs) in the image analysis, and not surface reflectance. Beijing-1 images were radiometrically calibrated to Jan 01, 2008 scene using empirical linear relationships derived from pseudo-invariant targets of bright permanent sand on high-elevation dunes and dark permanent water reservoirs near cities. The ASAR data were preprocessed by the State Key Laboratory of Remote Sensing Science, Beijing, PR China. Raw images were converted to backscatter coefficient σ^0 with the Basic ENVISAT SAR Toolbox software (the European Space Agency) and corrected for systematic variation using permanent-scatter urban features for HH and VV polarizations (Kwoun and Lu 2009, Wang et al. 2012). Backscattering coefficients at different dates were then radiometrically calibrated using a simple linear model and response from pseudo-invariant urban areas and water bodies (Wang et al. 2012). For the primary DCT classification I combined geo-referenced Beijing-1 and ASAR backscattering coefficient images from near-maximum water extent in July-August 2007 to April-May 2008 at the onset of new flooding (I refer to this set as

summer 2007-spring 2008 flood period). In this image stack, radar bands were resampled to Beijing-1 32-m resolution with their original values preserved. I also performed a second classification of DCTs for a hypothetical scenario of warmer wetter spring, where February-May 2008 Beijing-1 and April 2008 ASAR scenes were replaced with April-June 2007 Beijing-1 and ASAR data; I will refer to this image set as a hypothetical "quasi-experimental" scenario as discussed in 2.6 below.

Poyang Lake DCTs

Poyang Lake DCTs were defined as common types of wetland change among its major "static" cover types that can be broadly assigned to vegetation, water, sand and seasonal mudflat (Dronova et al. 2011). Physically plausible transitions among these types form location-specific change sequences which may vary by topographic features, distance to the flood source, time of the year, grazing, plant seed or propagule banks and other factors. These sequences can be characterized by spectral-temporal trajectories derived from multi-date remote sensing images (Wang et al. 2012; Figure 4). Previous studies of Poyang Lake annual inundation patterns (Andreoli et al. 2007, Hui et al. 2008, Zhao et al. 2011, Feng et al. 2012) suggested that, despite the incremental nature of water expansion and recession, flood-related transitions may form relatively extensive "zones" of similar annual submersion times. My DCTs (Table 1) combined hydrological transitions with change patterns from vegetation phenology known from previous field observations and remote sensing analyses of Poyang Lake cover at different seasons (de Leeuw et al. 2006, Zeng et al. 2007, Guan et al. 2008, Chen et al. 2007, Liu 2009, Wang et al. 2012, Dronova et al. 2011, Dronova et al. 2012).

I defined seven DCTs for this study (Table 2, Figure 4), five of which were associated with complete or partial inundation and presence or absence of vegetation in their schedules. Two classes represented seasonally flooded grassland: areas exposed by water in early fall and colonized by C3 plants, mainly *Carex* spp. with the highest biomass in late spring (C3G), and mixed C4-C3 grasslands (C4C3G) in higher-elevation lake periphery with *Miscanthus, Cynodon, Arundinella* spp. that are green in the fall and spring but senescent in winter (Zeng et al. 2007, Guan et al. 2008, Wang et al. 2012). Two DCTs represented ephemeral mudflats exposed later in the fall or winter and flooded again in early spring (EMN and EMV, Table 2, Figure 4). Of those, the EMV class included the change from mudflat to ephemeral vegetation before the new flood; however, specific plant community composition was not well known due to the isolated location and lack of ground or boat access (Liu 2009). Their spectral signatures on remote sensing imagery were close to those of C3 grassland in accessible areas (Dronova, personal observation). The EMN type represented exposed mudflats that do not have enough time to develop dense plant cover due to shorter intervals between flood exposures. Due to spectral confusion between mudflat and wet sand (Dronova et al. 2011), I did not separate transitions involving flooded sand beds and those on finer-textured mudflats. Of the remaining classes, one DCT represented permanent sand features, and two classes – permanent water with different schedules of aquatic vegetation (Table 2). The latter included permanently flooded areas that could support aquatic vegetation only from late spring to mid-fall (PW; Table 2) and those with aquatic macrophytes also from mid-fall to spring (WAM).

Image segmentation and PCA transformation

To classify Poyang Lake DCTs, I used OBIA to avoid the salt-and-pepper speckle common in pixel classifications of wetlands (Blaschke et al. 2000, Hess et al. 2003) and to enhance class

contrast due to smoothing of local noise within objects (Kim et al. 2011, Dronova et al. 2012). The first step in the object-based analysis was segmentation of each multi-date two-sensor image stack into primitive objects used as minimum mapping units (Dronova et al. 2011). Segmentation was carried out in eCognition Developer 8.0 software (Trimble Inc) using multi-resolution segmentation tool which allows for diversity of object sizes in the output (Baatz and Schäpe 2000, Benz et al. 2004). This process requires the parameters of scale (affects object size based on maximum allowed heterogeneity), shape (controls the relative importance of shape versus spectral-only information in object generation) and compactness (affects the degree of compactness of the final objects). Because characteristic shapes of DCT classes were not known a priori, I kept both shape and compactness at a low value of 0.1 to allow spectral values to have the strongest contribution in object generation. For segmentation scale, it was important to capture the boundaries of the minimum-sized patches representing DCTs of interest, which were most likely to be observed during the low water stages. Therefore, I used the scale value of 7, which with 32-m Beijing-1 resolution was close to the highest-accuracy scale in my study of Poyang Lake vegetation from a spring 2008 Landsat TM image (Dronova et al. 2012). Prior to classification I isolated several residential and actively managed human land use areas that were not expected to follow "natural" wetland dynamics using Microsoft Bing image in ArcGIS 10 (ESRI Inc.).

Image classification

Next, I assigned training and test objects, separately for the 2007-2008 flood period and hypothetical scenarios, based on several data sources. Multiple field surveys of wetland cover and vegetation were carried out in March-April and December 2007, January and April 2008 (Dronova et al. 2011, Wang et al. 2012) and later years. Although no continuous observations were implemented *in situ*, these field data allowed me to make an expert judgment on which objects overlapping with field-surveyed areas could serve as examples of proposed DCTs. Surveyed areas included C3 and mixed C4-C3 grasslands, mudflats, permanent water and sand features. For DCTs associated with inaccessible ephemeral mudflats and winter aquatic vegetation, representative objects were assigned using visual comparison of multi-date images with high-resolution data from DigitalGlobe Worldview-1 and QuickBird sensors for May, September, November and December 2007 and January 2008, provided by the National Aeronautics and Space Administration (NASA) and The National Geospatial-Intelligence Agency (NGA) NextView program (http://cad4nasa.gsfc.nasa.gov). I selected 386 total objects with 24-100 objects for each class depending on the expected class dominance; these objects were randomly divided in half into training and test samples. I further examined spectral-temporal signatures of DCTs from training samples with the raw image data (Figure 4) to better understand their key aspects of phenology and inundation cycle.

Prior to classification I performed three principal component transformations on covariance matrices of the object-level spectral means from the original input bands: 1) using only ASAR WSM bands; 2) using only Beijing-1 NIR bands and 3) using only Beijing-1 red and green bands together. This step was taken to account for redundancy in object attributes from large number of input bands and to enhance DCT contrasts. From these transforms, three first PCs and two second PCs (from ASAR and Beijing-1 NIR only) were used as inputs for the object-based image classification instead of the image bands. Note that because training and test objects were assigned separately for each scenario, I did not use standardized principal components (Eastman and Fulk 1993). However, application of this method to longer-term DCT comparison without

reference data for all change periods would require standardization of PCs or other types of transformations in addition to relative radiometric image calibration.

For DCT classification I compared three supervised machine-learning algorithms in Weka 3.6.5 software (Witten and Frank 2005, Hall et al. 2009): Multilayer Perceptron artificial neural network (MLP), a multinomial logistic regression classifier (SimpleLogistic in Weka) and a simple k-nearest neighbors (kNN) classifier. These methods from were chosen because they did not require extensive parameterization and delivered relatively high accuracy in the previous object-based vegetation study at Poyang Lake (Dronova et al. 2012). For Multilayer Perceptron, I used an automatic (driven by Weka algorithms) network building option with Weka parameters learning rate equal to 0.3 and momentum equal to 0.2 (for more detail on the algorithms see Witten and Frank 2005). For kNN I used the number of nearest neighbors equal to 1 and a simple linear "brute force" algorithm for nearest neighbor search in the data space with Euclidean distance similarity function (Witten and Frank 2005). I compared relative performance of these methods and consistency of their errors to better understand the sources of confusion among DCTs. The overall and class specific accuracy were estimated with contingency tables.

Comparison of DCT map with a hypothetical change scenario

Using the highest-accuracy classification algorithm from the previous step, I further compared spatial distribution and extent of DCTs for the summer 2007-spring 2008 period with a hypothetical scenario where spring 2008 image data were replaced with spring 2007 scenes (Figure 2), while fall 2007-winter 2008 images were preserved. Importantly, spring 2007 conditions represent the pre-flood stage shaped by the previous 2006-2007 flood cycle, for which no other data were available at the time of my study. Therefore, comparison of two scenarios was intended only as a hypothetical "experiment" to investigate how the spatial extents and locations of DCTs would change if, following January 2008, spring conditions were those of spring 2007 instead of the actual spring 2008.

While this exercise could not provide a "true" response of DCTs to a change in atmospheric and hydrological conditions, it was used to test the potential sensitivity of classes to landscape differences captured in the images. Specifically, the January-March period in 2007 was characterized by more warm days and higher amount of precipitation in 2007 than in 2008 (Figure 5a,b). Furthermore, mean water levels recorded at a local Duchang hydrological station (data of the State Key Remote Sensing Lab, Beijing, China; Qi et al. 2009) were by 1-2 m lower in December, January, March and April 2008 compared to the same months in 2007, and only the February mean water levels were very close due to a short-term flood event in 2008. Thus, in comparing two scenarios, I expected the response from DCTs with the strongest sensitivity to flooding, such as non-vegetated mudflats, and from emergent C3 grassland which may be sensitive to both temperature and precipitation patterns in late winter-early spring (Dronova et al. 2011). To classify DCTs for the hypothetical scenario, I followed the same procedures as for the summer 2007-spring 2008 period (Figure 2): segmentation of the April 2007-Jan 2008 bi-sensor image stack, PC transformation of the object-level band means and classification with the highest-accuracy method from period 1 classification. At the latter step, however, I used different sets of training and test objects for DCTs which were selected using field and high-resolution image data from spring 2007, not spring 2008. Differences between the hypothetical scenario and summer 2007-spring 2008 period were estimated via simple geospatial overlay of two maps in ArcGIS 10 software.

Results

Spectral trajectories and principal component transformation

Mean DCT-specific spectral values from training sample objects formed unique spectral-temporal trajectories in the raw image data (Figure 4). Each date emphasized contrast between at least three DCTs, but the specific timing of the highest contrast differed among class pairs. Hence the overall spectral differences among classes became evident only when multiple image dates were considered together, regardless of the sensor. Both microwave and near-infrared trajectories (Figure 4) highlighted the contrasts between types that were predominantly "wet" over the course of a flood season (PW, WAM, EMN) versus DCTs that were only partially inundated in short-term intervals (permanent sand and mixed C4-C3 grassland). Two classes with a green emergent C3 vegetation state, EMV and C3G, were similar in the onset of greening in mid-late fall but remarkably diverged in May 2008 due to flooding of EMV and near-peak green plant biomass state of C3G at that time (Figure 4b).

These differences in class spectral-temporal trajectories (Figure 4) translated into DCT contrasts with the most meaningful principal components (Figure 6). In three separate PCA transformations of the object-level means for the near-infrared, microwave and combined red and green image band stacks, the first principal components (PC) explained the largest amount of variance (60%, 66% and 46%, respectively) and highlighted different aspects of class contrasts (Figure 6). The first PC of the NIR contrasted "wetter" types with long submersion times (PW, WAM and EMN) and partially flooded DCTs with higher prevalence of emergent green vegetation within their trajectories (Figure 6a), particularly C3 grasses of the cool growing season with peak biomass in late spring. The first PC of transformed ASAR backscatter coefficients represented differences in annual submersion times and the contrasts among permanently inundated areas, low-elevation features and high-elevation features (Figure 6b). The first PC of the red and green band transformation represented two important contrasts: 1) gradients of wetland inundation and green vegetation density relative to the central water body area and 2) varying levels of water turbidity and sediment on wetland surface (Figure 6c).

The second PCs in each transformation explained 17-26% variance in the data; however, those from ASAR and Beijing-1 NIR band transformations provided most of the new unique change information. Specifically, they highlighted particularly dynamic areas surrounding the central water body that exhibit more frequent fine-scale inundation disturbances and support ephemeral vegetation in winter. The second PC in ASAR band transformation reflected the gradients of flood exposure and submersion time of these areas (Figure 6d), while the second PC in the NIR transformation accentuated spatial variation in persistence of green ephemeral emergent vegetation (Figure 6e).

Classification accuracy and DCT map for summer 2007-spring 2008 period

Among three supervised machine-learning algorithms used to classify DCTs for summer 2007-spring 2008 period, kNN had the highest overall accuracy (93.3%) followed by logistic regression (90.7%) and Multilayer Perceptron (89.6%; Table 3). Major sources of errors were consistent among three methods, with the largest being the confusion of permanent water spatially adjacent non-vegetated mudflats and winter aquatic vegetation (Table 3). Additional confusions occurred between emergent flooded C3 grassland and mixed C4-C3 grassland and between ephemeral vegetated mudflats and non-vegetated mudflats or emergent C3 grassland (Table 3).

The mapped DCT distributions for the summer 2007-spring 2008 change period (Figure 7a) were consistent with both hydrological (Andreoli et al. 2007, Hui et al. 2008) and vegetation-based wetland analyses of Poyang Lake from previous studies (de Leeuw et al. 2006, Zeng et al. 2007, Wang et al. 2012, Dronova et al. 2012). Dynamic classes exhibited broad-scale zonation around permanent water bodies, ranging from partially flooded higher-elevation mixed C4-C3 grassland to flooded emergent C3 grassland to low-lying mudflats. These patterns closely followed known gradients of submersion time (Andreoli et al. 2007, Hui et al. 2008, Zhao et al. 2011) and at the same time reflected prevalence of green vegetation within the change period, which is governed by local disturbance and plant functional type (Wang et al. 2012, Dronova et al. 2012). The most extensive classes were permanent water and emergent flooded C3 grasslands, followed by vegetated and non-vegetated ephemeral mudflats and mixed C4-C3 grassland (Figure 7c). Non-vegetated ephemeral mudflats were predicted by the classifier both in the central water body area and around some of the small winter sub-lakes (Figure 7a).

Comparison of the DCT classification with the hypothetical change scenario

Spatial extent and distribution of DCTs responded to the hypothetical scenario of change with two different spring conditions (Figure 7b,d). With spring 2007 data substituted for spring 2008 images, the estimated total area of permanent water, vegetated ephemeral mudflats, non-vegetated ephemeral mudflats and mixed partially flooded C3-C4 grassland increased by 12.8%, 3.0%, 0.9% and 4.1%, respectively (Figure 7d). In contrast, C3 grasses, winter aquatic macrophytes and permanent sand extents decreased by 5.5%, 55.2% and 18%, respectively. However, even the small-magnitude changes in class extent were accompanied by substantial spatial re-distributions. Two mudflat and two grassland classes with belt-shaped zones around permanent water bodies (Figure 7) shifted in the hypothetical scenario, losing 9-18% their area to lower-elevation neighbors closer to water bodies and taking 8-21% from their higher-elevation neighbors. Most of the change, however, occurred for classes associated with the water boundary – WAM and EMN, which preserved only 36% and 64% area, respectively, in the hypothetical scenario relative to the actual flood season (compared to 74-92% for other DCTs). However, decline in the WAM area in the hypothetical scenario could be attributed to the lower actual extent of this class in 2006-2007 compared to 2007-2008, which I could not validate due to the lack of field data on this class.

Again, I stress that the differences between the actual and the hypothetical change periods should be interpreted only as "potential" shifts in DCTs because it was not possible to verify physical plausibility for all detected transitions. The most useful contribution of this exercise to my study is not in the absolute values, but in the relative magnitude and spatial pattern of the "experimental" responses. Future work should refine this analysis as a multi-year comparison of DCTs among actual discrete change periods.

Discussion

Poyang Lake wetland characteristics in 2007-2008 DCT classification

Landscapes that undergo considerable short-term surface dynamics require special approaches for assessing their composition and longer-term change. It has been long recognized that multi-temporal remotely sensed information can facilitate classifications of land cover and vegetation both in relatively "stable" landscapes (Lunetta et al. 2002, Seto et al. 2002a) and in rapidly changing systems such as inundated wetlands (Hess et al. 2003, Evans et al. 2010). My proposed framework of "dynamic cover types" complements existing approaches by explicitly considering

spatial units of change shaped by topography, phenology, ecological interactions and disturbance together. In locations such as Poyang Lake, where process-based understanding of landscape dynamics is limited by surface complexity and the lack of field and geospatial data, DCTs may serve as a first step in "top-down" analyses towards building more complete and spatially explicit knowledge of the short- and long-term ecosystem processes.

My results demonstrate that DCTs may accentuate different "schedules" for compositionally similar classes with different phenology and roles in ecosystem processes. For example, post-flood expansion of C3 grasses at Poyang Lake may occur both within peripheral wetlands (C3G class) and near the central water body (EMN class). Both types may be spectrally similar on single-date images in winter due to growth of C3 grasses in EMN and grazing pressure on the established plants in C3G (Chen et al. 2007, Wang et al. 2012; Figure 4b). However, at the seasonal and annual time scales, these DCTs would contribute differently to ecosystem biogeochemical fluxes and habitats because of unique schedules of vegetation emergence, peak density, suppression by the new flooding and the overall flood-free time. Similarly, contrasting phenology of winter aquatic macrophytes and permanent water also suggest their different ecological roles in wetland cycles. Permanent water DCT included warm-season aquatic plants which proliferate from spring to fall and then senesce, exposing mudflat or open water (Wu 2008, Wang et al. 2012). Some of their dominant species may overwinter as buried tubers which provide critical food for wintering migratory waterbirds (Barzen et al. 2009). In contrast, photosynthetically active aquatic macrophytes of the cool growing season (WAM) contribute to net primary productivity and canopy-water-atmosphere carbon exchange at this time in addition to emergent grasses.

C3 sedges of the cool growing season also supply food for wintering waterbirds, particularly grass-eating foraging guild (de Leeuw et al. 2006, Barzen et al. 2009). Among the DCTs with this state, by the time of bird arrival to Poyang Lake in late fall only C3G areas are flood-free long enough for emergent C3 grasses to establish. In contrast, EMV develop C3 vegetation later in the winter and represent more distant and isolated locations with lower livestock grazing pressure compared to C3G. This contrast raises two important questions: 1) do EMV areas provide an important secondary bird habitat later in the winter period? and 2) would shrinkage of this DCT following higher water levels in winter (e.g. due to dams) considerably affect migratory waterbird populations? Some of the aerial bird surveys from late winter already noted concentrations of waterbirds in areas that are closer to Poyang Lake center (Figure 1) and further from commonly visited peripheral sub-lakes (Qian et al. 2009). It is not well known whether these patterns represent the "normal" within-season habitat switching or a more specific response to reductions in water levels (Qian et al. 2009, Guo et al. 2012) and human disturbance at wetland periphery. In any case, evidence of bird utilization of the EMV and EMN areas in late winter calls for particular attention to these habitats as targets for more thorough analysis and ecological monitoring, particularly under planned hydrological interventions (Barzen et al. 2009, Finlayson et al. 2010).

Classification of Poyang Lake DCTs likely benefited from the object-based image analysis method which allows for smoothing of the local spectral heterogeneity and incorporation of the spatial context at the object level (Blaschke et al. 2000, Gilmore et al. 2008, Blaschke 2009). While this paper did not explicitly compare OBIA with pixel-based methods, my parallel study discussed the case of salt-and-pepper speckle in a multi-temporal pixel-based classification of Poyang Lake (Dronova et al. to be submitted). Such speckle may increase variation in class

spectral trajectories and obscure ecologically meaningful flood- and phenology-driven transitions. In contrast, objects may provide primitive spatial "units of change" which include pixel neighbors that are likely to exhibit correlated change patterns based on their multi-temporal signatures. This benefit may be especially important with high and very high resolution data with greater levels of within-class spectral heterogeneity (Johansen et al. 2007, Kim et al. 2011).

Comparison of DCT maps between change scenarios and implications for landscape models

Differences in spatial extent and position of DCTs between the 2007-2008 flood period and the hypothetical scenario highlighted two primary aspects of change that were in agreement with "warmer, wetter" experimental conditions. Reallocation of belt-shaped EMN, EMV and C3G towards their higher-elevation neighbors and further away from the water bodies could represent a "directional" response to the expansion of permanent water. This result is consistent with previously raised concerns about potential spatial shifts and ultimate shrinkage of suitable wetland habitats under higher water levels under new hydrological control structures (Barzen et al. 2009). In turn, more localized multi-directional expansions of "vegetated" DCTs suggest potentially strong response of wetland grasses to warmer temperatures and higher precipitation. Given high biological diversity of wetland vegetation and buried seed and propagule banks in the region (Liu et al. 2006a), these responses are likely to be complex and dependent on site-specific plant community composition and disturbance, such as expansion of the mixed C4-C3 grasses into emergent C3 grasslands in my hypothetical scenario. During the low water season, the C4C3G class at Poyang Lake would be largely dominated by reeds and short grasses with C4-photosynthesis which are less tolerant of flooding than C3 sedges (Zeng et al. 2007, Guan et al. 2008, Zheng et al. 2009). Theoretically, based on the eco-physiological differences among C4 and C3 grasses (Pearcy and Ehleringer 1984), one could expect higher competitive performance of C4 species relative to C3 under warmer and more humid growth conditions (Collatz et al. 1998), consistent with my results. At the same time, higher early spring water levels might also constrain livestock grazing to higher-elevation areas thus additionally increasing pressure on C3 grasses. The response of spatio-temporal interaction among C4- and C3-grass dominated vegetation types to climatic and hydrological variability at Poyang Lake should be further investigated with multi-year DCT analysis and field studies.

Although the hypothetical scenario could not be validated, this exercise suggests that DCTs may be sensitive to simultaneous change in multiple drivers of surface cover composition and ecosystem processes. Thus, DCT framework should be further extended to inform landscape modeling of climate change and land use or management effects on ecosystem properties and habitats. Projections of broad-scale changes in biogeochemistry and ecosystem function under future climate change and land use often require coupling process-based models with geospatial land cover and land use information (Melillo et al. 1993, Cao and Woodward 1998, Turner et al. 2004). A recognized limitation of current terrestrial biosphere models is underrepresentation of the intrinsic change events within growing seasons and their year-to-year variation (Keenan et al. 2012). By using input land cover categories defined by their characteristic dynamics, rather than static states, new generations of models may be able to address this challenge and account for differences among ecological regimes nested within a landscape in order to reduce the uncertainty in model outputs. A useful first step towards this may be coupling DCT classifications with existing models that operate at time steps comparable to change periods for which DCTs are defined (e.g., growing seasons). For Poyang Lake specifically, combining DCT classifications with models of hydrological change due to both upstream Three Gorges Dam and

proposed local water control structures (Barzen et al. 2009, Finlayson et al. 2010) would help to assess wetland ecosystem vulnerability under new water regulations.

Insights for the future work: data and methods for DCT analysis

A particularly important issue in the future extension of DCTs to longer time frames is separating 'reference' class dynamics from directional longer-term trends such as succession. Ecosystem processes may be continuous in time and asynchronous, and thus may not be easily "discretized" (Vierling et al. 2011). Hence, dynamic classes may be best informed by the periodic processes which shape discrete recognizable transition cycles within rapidly changing landscapes such as flood cycles at Poyang Lake or plant growing seasons in terrestrial landscapes. Because the timing of common transitions (e.g., leaf flushing, mudflat exposure) may vary from year to year, multi-year DCT comparisons would require assessments of 'reference' class variation with historical data, continuous field observations or biometeorological covariates. Zhong et al. (2011) demonstrated how similar agricultural crops could be correctly classified even with different planting dates, using class-specific spectral metrics extracted from inter-seasonal and inter-annual time series images. Extending the latter approach to natural vegetation and surface types would be a promising strategy to generalize DCT framework and facilitate dynamic type comparisons in the long-term change monitoring.

Future work should also accommodate ways to detect "novel" change types which may occur due to short-term disturbance, unprecedented shifts in climate and hydrology, human management and restoration activities, or alien species invasions. As a first step, unsupervised methods of image classifications may be applied to identify previously unknown transitions as unique spatiotemporal clusters (Ribed and Lopez 1995, Hame et al. 1998), while ground-based knowledge could be further used to verify and incorporate them into existing DCT sets.

These considerations raise an important question of how much data are *enough* to reliably characterize change processes and DCTs for a given landscape. My images represented the key stages of Poyang Lake's flood cycle, although class definitions did not incorporate specific time of state changes between image dates. On the one hand, this made my approach flexible to accommodate some degree of the unknown "reference" within-class variation due to, e.g., plant phenology. On the other hand, given 1-2 month difference between scenes, some DCTs could be misclassified because part(s) of their temporal trajectory had been missing from spectral signatures that determined their principal component values. Precise timing of transitions may be very important in the studies of climate change effects on ecosystem processes and phenology. However, too frequent data may increase within-class heterogeneity and hence the chance of confusion (Zhong et al. 2011). Therefore, future work should investigate the effect of data frequency on DCT classification outcomes, as well as their sensitivity to mismatches in the availability of cloud-free data for transition stages between discrete change periods.

Temporal frequency of available data is coupled with other important characteristics of sensors. Instruments that acquire data daily (e.g., AVHRR, MODIS Aqua and Terra) have medium to coarse spatial resolution which may not be suitable for detecting fine-scale incremental changes. Depending on the spatial scale of interest, DCT analysis from these data may require subpixel inference such as temporal unmixing or independent component analysis (Lobell and Asner 2004, Ozdogan 2010). Novel microsatellites with wide swath and frequent revisit (e.g., 5 days for Beijing-1 in my study) can provide more detailed time series at medium resolution. However, these instruments have relatively short data collection history, small

number of bands and may still be limited by common cloudiness in humid regions such as my study area. Thus, future work should also explore combinations of data by similar sensors collected on complementary dates. My analysis also benefited from combining visible and near-infrared data sensitive to vegetation phenology with microwave imagery sensitive to inundation extents, similar to previous studies (Grenier et al. 2007). However, radar data may be time-consuming to pre-process and costly to acquire at high spatial and temporal resolution. Alternatively, passive-sensor optical imagery could be complemented with digital elevation models and bathymetric data, which were not available for my study area.

Finally, it is important to develop a framework for the appropriate validation of remote sensing-based DCTs. This task is challenging in general (Liu and Cai 2011) because collecting sufficient test data through frequent and comprehensive field surveys of dynamic landscapes may be costly and impractical. Alternatively, future research should consider cost-effective continuous observation approaches such as wireless sensor networks (Gong 2007, Burgess et al. 2010) and digital cameras to capture phenology (Richardson et al. 2009, Sonnentag et al. 2012). These methods could provide reliable information on the change *in situ* and illuminate year-to-year "reference" variation in the timing of within-class transitions.

Summary

The proposed classification framework of "dynamic cover types" allowed me to highlight important changes in wetland cover driven by seasonal flood dynamics and plant phenology in the large and spatially heterogeneous Poyang Lake area. By combining multi-spectral and microwave remote sensing images of the critical flood cycle stages, I were able to differentiate major wetland DCTs despite constrained field access and the lack of continuous in situ observations. Comparison of DCTs from the summer 2007-spring 2008 change period with a hypothetical scenario of warmer, wetter spring conditions detected both a directional hydrological response as re-distribution of belt-shaped wetland DCTs to higher elevation areas, and a more complex localized phenological response from change types with green emergent vegetation. Results suggest DCTs defined per Poyang Lake flood cycle could facilitate the analyses of wetland ecosystem function and wildlife habitats and provide useful inputs to hydrological models in this complex landscape.

My ongoing and future work will extend this framework to multi-year analyses of Poyang Lake ecosystem change to address the possibilities of 1) comparing DCTs across multiple change periods and assessing their "reference" variation with temporally frequent data and 2) detecting short-term changes induced by ecologically important but localized disturbance such as reed harvesting, grazing and aquaculture. Assessment of historical change types in Poyang Lake area would facilitate modeling of "dynamic" habitats for wildlife and infectious disease agents (Seto et al. 2002b), and their potential response to hydrological alterations following the closure of Three Gorges Dam upstream or construction of local water control structures (Barzen et al. 2009). Assessing the future of Poyang Lake ecological regimes that currently support its unique and biologically rich environment must be a critical step in planning of any hydrological structures and flood level management decision-making for this area. DCTs may facilitate such assessments with a cost-effective framework that is easy to adapt for specific change types and ecological and conservation zones of interest. Finally, future work could extend and test this approach in other inundated wetlands globally (e.g., the Pantanal wetlands, Florida Everglades, Okavango Delta) and non-wetland dynamic systems such as sand dunes (Assendorp 2010), transitioning forests and areas with cover type shifts due to climate change.

Acknowledgements

This research was partially supported by the NASA student Earth and Space Science Fellowship 2009 (NNX09AO27H) and a grant from the National High Technology Programme of China (2009AA12200101). I am grateful to the State Key Laboratory of Remote Sensing Science (Beijing, China), the Center of the Earth Systems Science, Tsinghua University (Beijing, China), Poyang Lake Ecological Station for Environment and Health, (Duchang, China) and professor Shuhua Qi at the Jiangxi Normal University (Nanchang, China). Analysis of remote sensing data benefited from the support and services of the Geospatial Innovation Facility at the University of California, Berkeley (gif.berkeley.edu). I also thank National Aeronautics and Space Administration (NASA) and The National Geospatial-Intelligence Agency (NGA) NextView program (http://cad4nasa.gsfc.nasa.gov) for the access to selected high-resolution imagery which facilitated training and testing of the wetland classification algorithms.

Tables

Table 1. Satellite remote sensing images used in DCT classification.

Satellite	Date	Flood stage
Beijing-1 (32 m; NIR, Red, Green)	Apr 19, 2007	Onset of the rain season, emergent vegetation approaching peak biomass
	May 6, 2007	Early stage of the rain season, emergent vegetation near peak biomass
	Aug 16, 2007	Water coverage near annual maximum, only high-elevation ridges and permanent sand features are exposed
	Oct 17, 2007	Flood recession, C4 grasses at high biomass, C3 grasses rapidly emerge on newly exposed mudflats
	Nov 30, 2007	Progression of the cool growing season with C3 grasses as dominant green vegetation
	Jan 1, 2008	Progression of the cool growing season with abundant C3 grasses, C4 grasses mostly senescent and water levels near annual minimum with exposed adjacent mudflats
	Feb 16, 2008	Progression of the cool growing season with a short-term flooding event due to winter precipitation and snowmelt
	Mar 2, 2008	Emergent vegetation development is boosted by warmer temperatures. Water levels very slowly begin to rise.
	May 12, 2008	Early stage of the rain season, emergent vegetation near peak biomass
ASAR WSM (150m, C-band), polarization is given in parentheses for each image date	May 25, 2007 (HV)	Rain season is progressing, vast portions of the area are covered with water, flood-free areas have high green vegetation biomass
	June 29, 2007 (HV)	Water coverage increases towards the annual maximum
	July 31, 2007 (VV)	Water coverage near annual maximum, only high-elevation ridges and permanent sand features are exposed
	Sep 4, 2007 (HV)	Early stage of water table recession,
	Oct 28, 2007 (VV)	Flood recession, C4 grasses at high biomass, C3 grasses rapidly emerge on newly exposed mudflats
	Dec 18, 2007 (HV)	Progression of the cool growing season with C3 grasses as dominant green vegetation
	Jan 3, 2008 (HV)	Progression of the cool growing season with abundant C3 grasses, C4 grasses mostly senescent and water levels near annual minimum with exposed adjacent mudflats
	Apr 4, 2008 (HV)	Water levels begin to rise slowly, emergent vegetation approaching peak biomass

Table 2. Proposed Dynamic Cover Types (DCTs) for Poyang Lake area for summer 2007-spring 2008 flooding period.

Dynamic cover type class	Sequence of states per flood cycle	Description
EMN – ephemeral mudflats, non-vegetated	Water→mudflat/ sand →water	Portions of lake bottomland that are flood-free for a brief period near the minimum water levels in mid-winter; in the spring again become water or aquatic vegetation
EMV – ephemeral mudflats, vegetated	Water→mudflat/sand →green emergent vegetation→water	Portions of lake bottomland that are exposed from flooding in late fall, become colonized by vegetation but then are flooded again in early-mid spring due to close proximity to flood source
C3G – emergent C3 grassland, flooded	Water→mudflat/sand→green emergent vegetation→water	Portions of lake bottomland in higher-elevation areas surrounding smaller sub-lakes that are exposed from flood early enough for green C3 vegetation develop and persist till the next flooding. Their main difference from EMV is in earlier exposure in the fall and later inundation in spring which leads to higher density and longer persistence of green vegetation
C4C3G – mixed C-C3 grassland, partially flooded	Green vegetation →senescent or harvested vegetation→green emergent vegetation→[water]	Perennial vegetation on high-elevation lake periphery and ridges with short annual submersion times. Depending on location, plant composition may include C4 and C3 reeds or short C4 grasses that are often senescent in winter but green from early spring till late fall. May be disturbed by reed harvesting and burning of the stubble
WAM – winter aquatic macrophytes	Water →aquatic vegetation→water	Permanent water with extensive aquatic vegetation beds primarily during the cool winter growing season
PW – permanent water	Water all year round, occasionally with aquatic vegetation from late spring to mid-fall	Areas permanently covered with water within a given flood season. Water color and optical properties may change due to varying sediment content, and aquatic vegetation may influence its reflectance from late spring to early fall
PS – permanent sand	Non-inundated sand features	High elevation sand hills and dunes in north-central part of the study area that are flood-free even at maximum flood stage

Table 3. Contingency matrices for assessment of accuracy for DCT classification in summer 2007-spring 2008 flooding period with three supervised machine-learning algorithms.

Assigned class:	Reference class							User's accuracy
	11	12	15	22	131	141	211	
Method: K-Nearest Neighbors, overall accuracy 93.3%%								
11	45	2	1					0.94
12	4	18	1					0.78
15	1		18					0.95
22				12				1
131					30	1		0.97
141		2				28		0.93
211						1	29	0.97
Producer's accuracy	0.9	0.82	0.9	1	1	0.93	1	
Method: Simple logistic regression, overall accuracy 90.7%								
11	46	6						0.88
12	2	14			1			0.82
15	2	1	20					0.87
22				11				1
131					28			1
141					1	27		0.96
211						3	29	0.85
Producer's accuracy	0.92	0.64	1	0.92	0.93	0.9	1	
Method: artificial neural network Multilayer Perceptron, overall accuracy 89.6%								
11	42	5						0.89
12	3	13			2			0.72
15	3	3	20					0.77
22				12				1
131					27			1
141					1	29		0.97
211	2					1	29	0.91
Producer's accuracy	0.84	0.62	1	1	0.9	0.97	1	

Figures

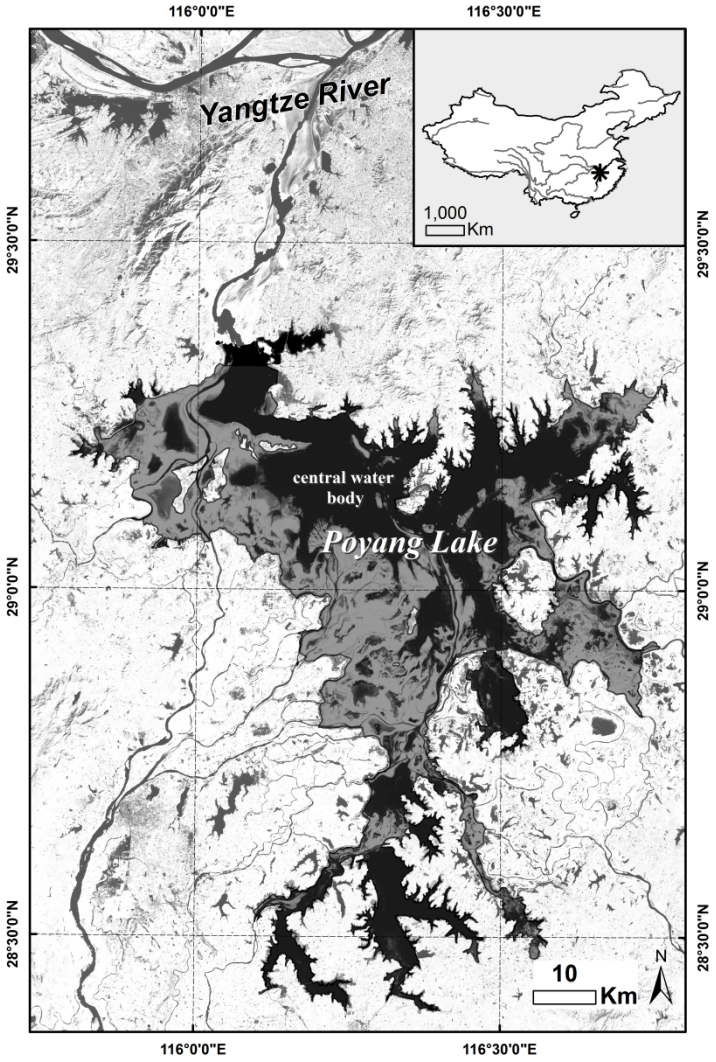

Figure 1. Map of the study area in south-central portion of Poyang Lake, Jiangxi Province, People's Republic of China.

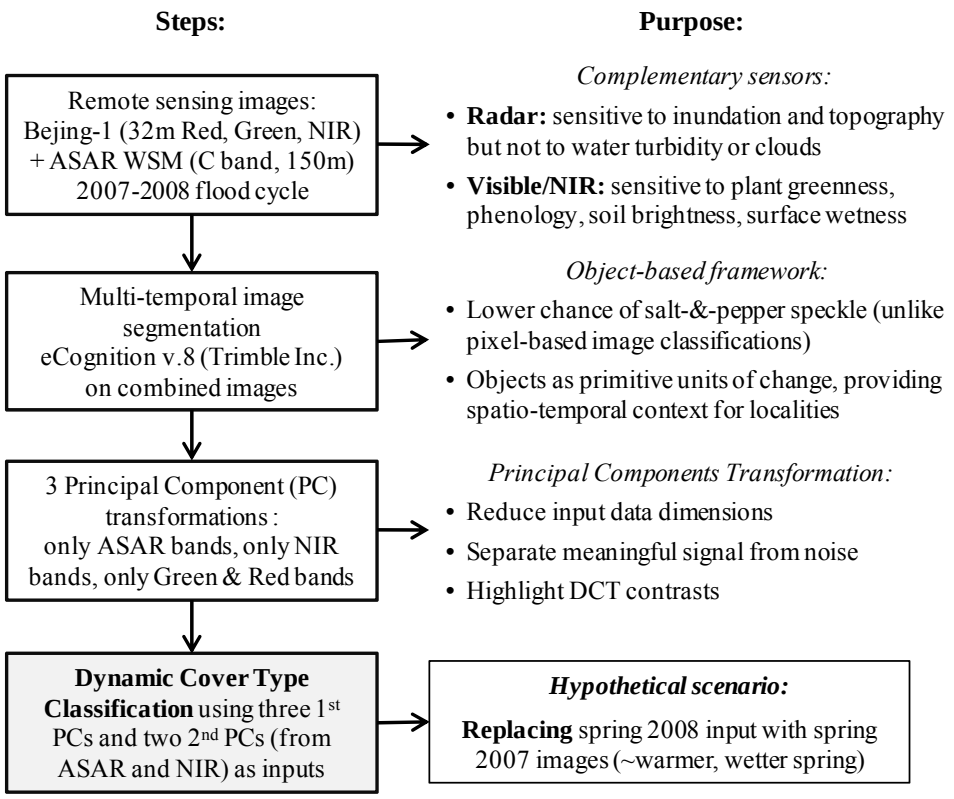

Figure 2. Conceptual diagram of the major steps in dynamic cover type classification and analysis.

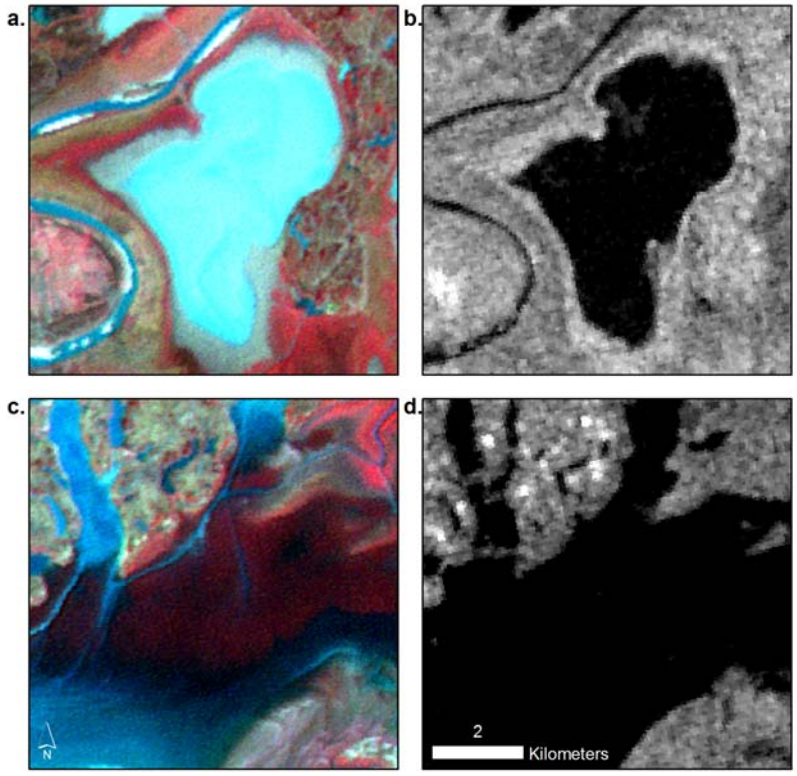

Figure 3. Complementary benefits of Beijing-1 optical (a,c) and multi-spectral and ENVISAT ASAR WSM microwave radar (b,d) imagery, illustrated for two cases of confusing cover types at Poyang Lake, China: a-b) highly turbid lake water is spectrally similar to adjacent light-colored mudflat, but the radar sensor clearly highlights the water-mud boundary; c-d) optical image highlights beds of aquatic vegetation, however, its submerged status is not clear, while the radar image shows spatial extent of submersion at this location.

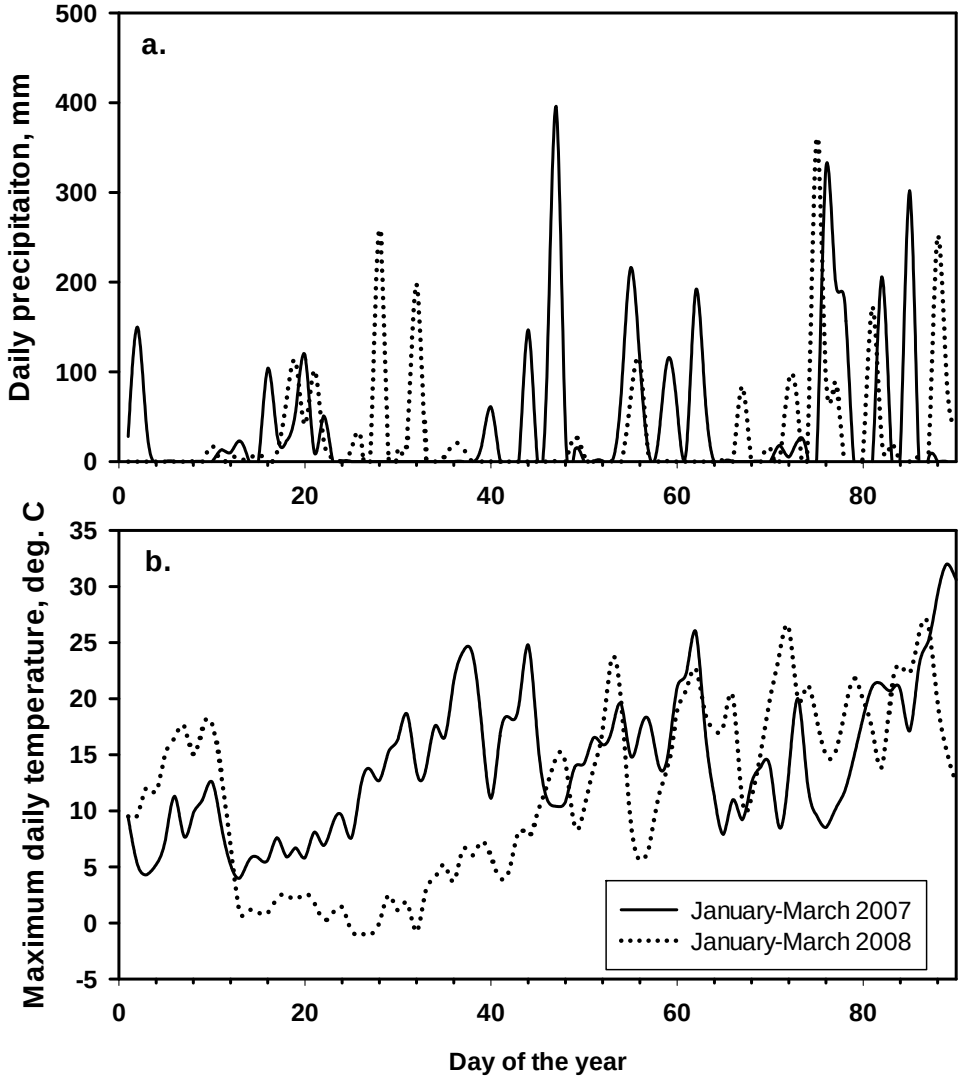

Figure 4. Examples of "spectral-temporal" signatures for DCTs calculated as mean training object values of the non-transformed input layers from a) ASAR WSM backscatter coefficient and b) Digital Numbers of the near-infrared band in Beijing-1 microsatellite images.

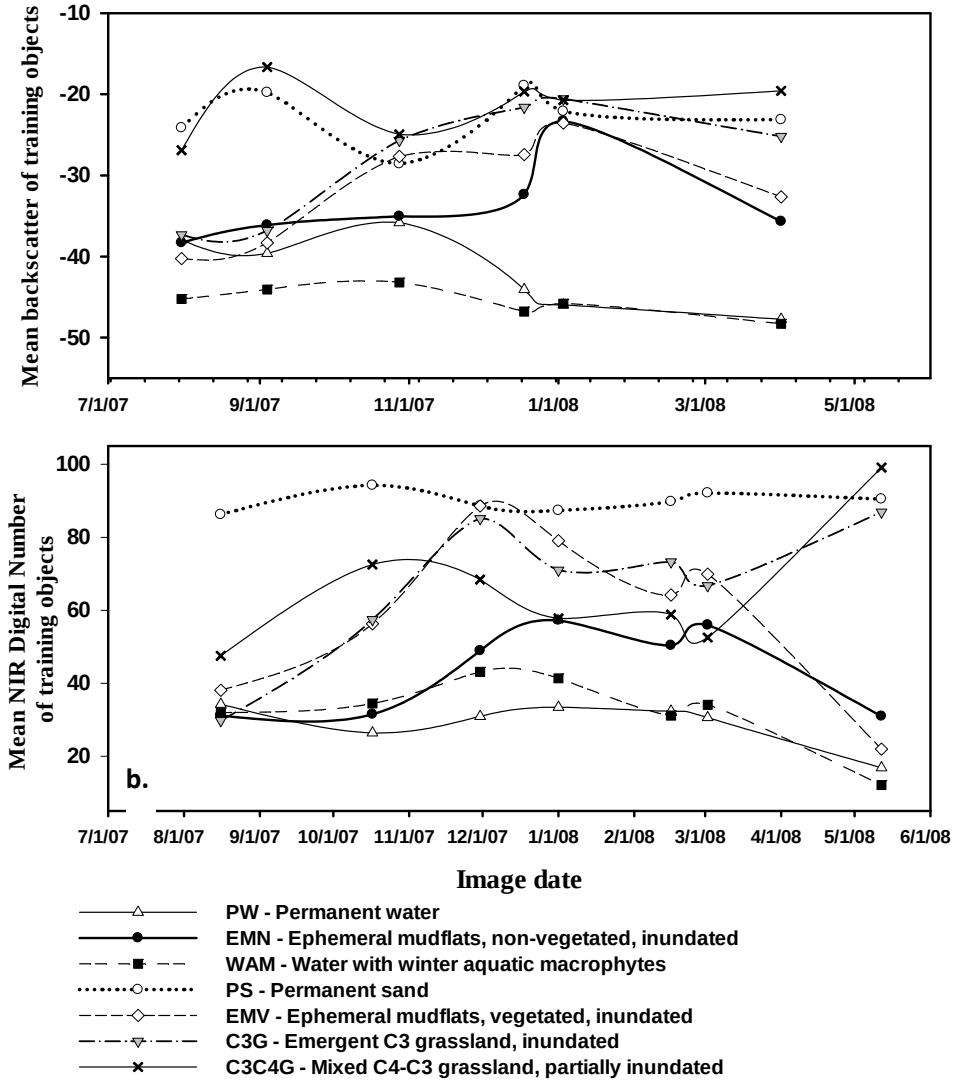

Figure 5. Atmospheric temperature and precipitation at the Nanchang meteorological station for January1-March 31, 2007 and January 1-March 31, 2008 (NOAA/National Climatic Data Center, http://www.ncdc.noaa.gov/oa/ncdc.html): a) daily precipitation at Nanchang meteorological station (Nanchang, Jiangxi, China), in millimeters; b) maximum daily atmospheric temperature at Nanchang meteorological station (Nanchang, Jiangxi, China), in degrees Celsius.

a.

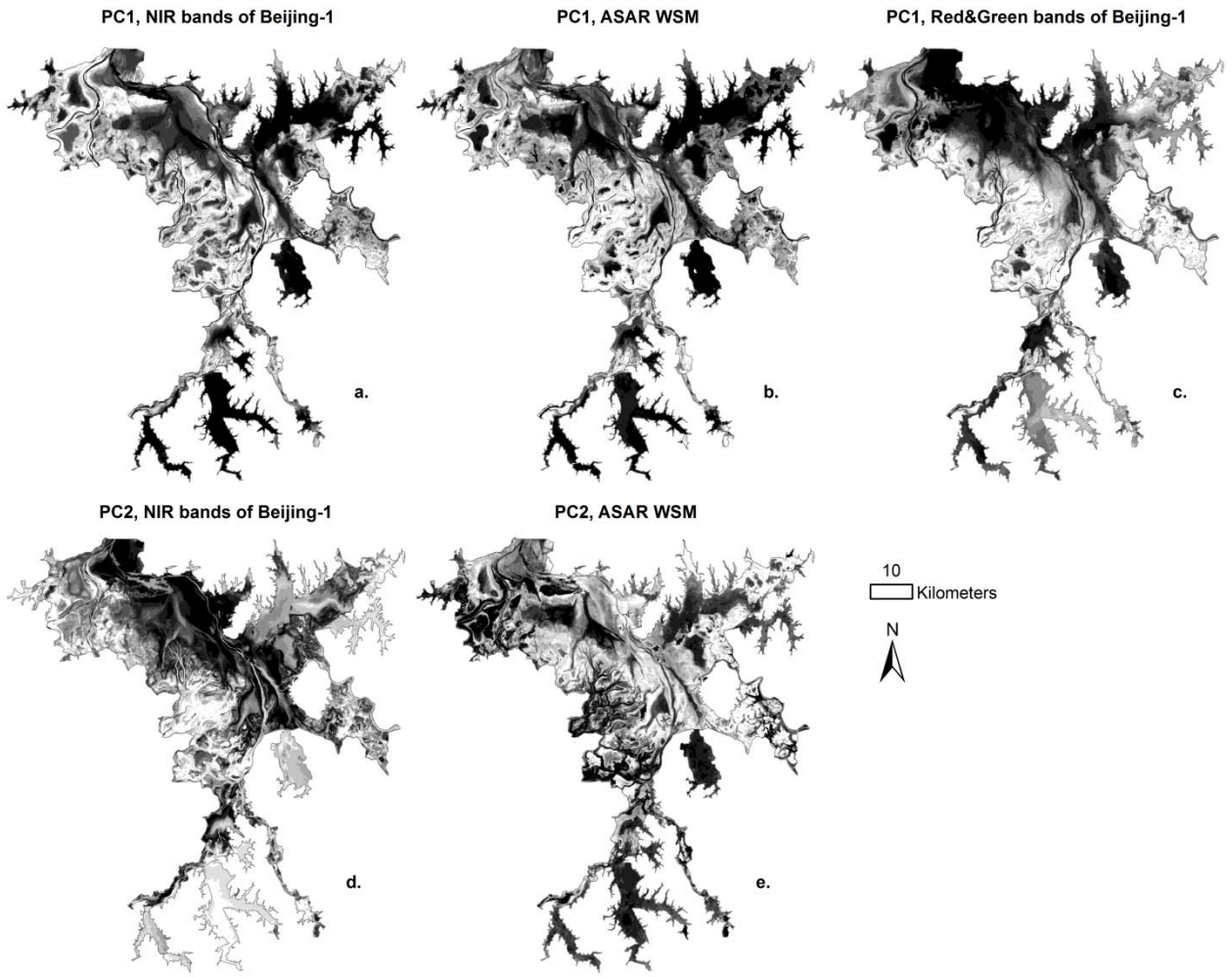

Figure 6. Landscape-level contrasts highlighted by principal component (PC) transformation of multi-date stacks of different band types at the image object level: a) PC1 of Beijing-1 near-infrared band transformation; b) PC1 of ASAR WSM backscatter coefficient transformation; c) PC1 of Beijing-1 combined red and green band transformation; d) PC2 of Beijing-1 near-infrared band transformation; e) PC2 of ASAR WSM backscatter coefficient transformation.

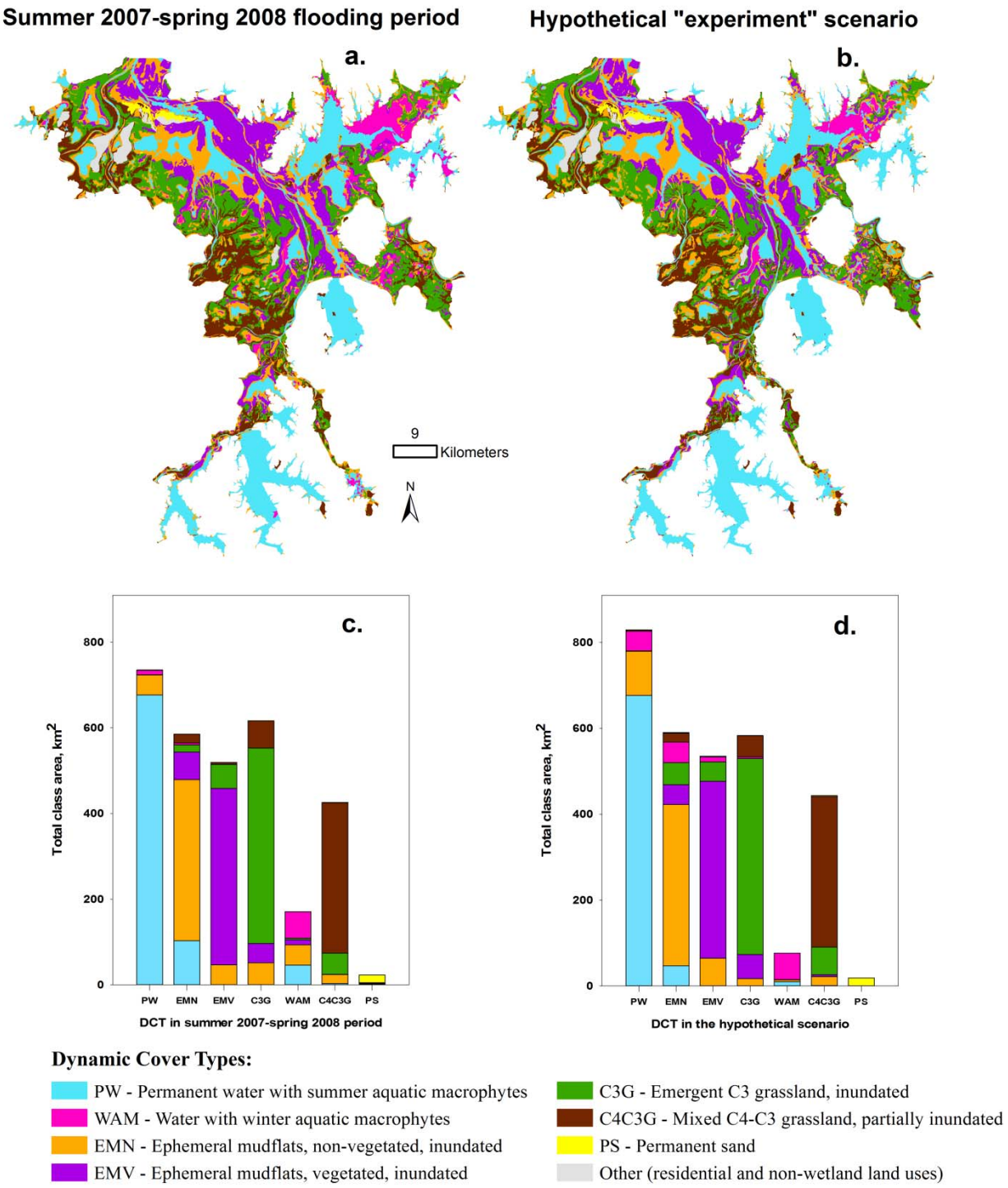

Figure 7. Poyang Lake dynamic cover types (DCTs) and their response to a hypothetical change scenario: a) DCT classification for summer 2007-spring 2008 period; b) DCT classification for a hypothetical "experimental" scenario with spring 2008 images replaced by spring 2007 ones; c) distribution of the area of DCTs predicted for the hypothetical scenario per each class in the summer 2007-spring 2008 period; and d) distribution of the area of DCTs mapped for the summer 2007-spring 2008 period per each class in the hypothetical scenario.

CHAPTER 4. Landscape-level associations of wintering waterbird diversity and abundance with remotely sensed characteristics of seasonal wetlands in a large conservation hotspot

Abstract

Poyang Lake, the largest freshwater lake-wetland system in PR China located in the middle Yangtze River basin, provides critical habitat for large numbers of wintering waterbirds from the East Asian Flyway. Hydrological regulations, uncertain climate effects and residential development impose serious threats to this wetland environment, but landscape drivers of the non-uniform distribution of bird diversity and abundance among permanent-water winter sub-lakes are not well understood. Limited field access and large wetland size create challenges for in situ surveys and call for assessments of potential utility of remote sensing-based indicators of diversity. Using waterbird survey data from late December 2006 and a Landsat TM satellite image from January 6 2007, we examined the relationships among metrics of bird diversity (species richness, Shannon index, number of food guilds and number of size groups) and abundance (total number of birds and the number of tuber-feeding birds) and landscape characteristics of 51 sub-lakes and wetland cover types within 500-m neighborhoods of inundated areas. Independent variables represented sub-lake area, proportions and spectral greenness of habitat cover types, their spectral and patch shape heterogeneity and proportions of cover types associated with human disturbance. Relative importance of individual predictors and their sets was assessed using information-theoretic model selection approach and the Akaike Information Criterion (AIC). Ordinary least squares regression models were diagnosed and corrected for spatial autocorrelation using spatial autoregressive lag and error models. We additionally examined predictive performance of the best models using an independent survey and matching remote sensing image from January 2008. The strongest and most consistent statistical predictors in the best-fit models included Normalized Difference Vegetation Index (NDVI) for mudflat (negative effect) and emergent grassland (positive effect), sub-lake area (positive effect) and proportion of flooded vegetation (negative effect). Significant spatial autocorrelation was detected in linear regression models for most response variables and was associated with local clustering of high and low values in both response variables and selected predictors. Differences in relative support for spatial lag versus spatial error models suggested that spatial dependence in our analysis could result from both model specifications and currently unknown spatially structured ecological relationships among sub-lakes. Model predictions for 2008 survey data had positive and significant (p<0.05) Spearman rank correlation coefficients with actual values for total bird abundance, abundance of tuber-feeding birds and Shannon index, but could not accurately predict magnitude of these variables or species richness, number of food guilds and number of size groups. Unexplained variation in models and the uncertainty of predictions were attributed to several key data limitations, including one-time bird survey per winter season, differences in spectral data quality between satellite images from different years and sensors, and the lack of comprehensive information on ground-based habitat determinants. Despite these challenges, results suggest several potential landscape indicators of waterbird diversity and abundance and new hypotheses on ecological mechanisms underlying their spatial patterns in this landscape.

Introduction

More than 400 waterbird species, including long-distance migrants, critically depend on habitat in low-latitude wetlands, large extents of which have been lost to agriculture, residential sprawl and water storage in recent decades (Millennium Ecosystem Assessment 2005, Fang et al. 2006, Dudgeon et al. 2006, An et al. 2007, Kirby et al. 2008, Gong et al. 2010, Cao et al. 2010, de Boer et al. 2011). A number of remaining sites have been designated as critical conservation targets and wetlands of international importance under the Ramsar Convention (Ramsar 2012). However, understanding of specific factors which underlie non-uniform distributions and "hotspots" of bird diversity within these wetland regions is often still limited. Enhancing this knowledge is important for allocation of management, conservation and research targets within larger wetland complexes and for selection of the meaningful habitat features into predictive models of species and diversity response to various change drivers.

Current uncertainty in understanding the relationships between diversity and wetland habitat is partially driven by the challenges of field observations in wetlands such as constrained site access, limited mobility in very shallow water and soft sediment, the risk of infectious disease and sometimes large site area (Dronova et al. 2011, Feng et al. 2012). However, even in more accessible "upland" terrestrial landscapes temporally frequent and spatially comprehensive field surveys may be logistically challenging and costly. Recognition of these difficulties has stimulated searches for landscape-level indicators of diversity and abundance based on cost-efficient geospatial data and remote sensing images in different biomes (Lavers et al. 1996, Turner et al. 2003, Leyequien et al. 2007, Bergen et al. 2009, Jones et al. In Press). For instance, significant statistical associations of wetland bird species richness and landscape-level variables such as wetland area, proportion of emergent wetland vegetation, water depth or the area of wetlands within a certain distance from sampling sites have been reported in the Rainwater Basin and in the Prairie Pothole Region of the USA (Fairbairn and Dinsmore 2001, Webb et al. 2010). A number of terrestrial studies found strong relationships between bird diversity and remote sensing indices of vegetation greenness, compositional heterogeneity and structure based on active radar and laser remote sensors (e.g., Hurlbert and Haskell 2003, Hawkins 2004, Goetz et al. 2007, Bino et al. 2008, Jones et al. In Press.).

Remote sensing platforms are particularly helpful in landscape-level biodiversity analyses due to instantaneous coverage of large areas, repeated site revisit and collection of spectral data within ecologically relevant spectral bandwidths (Turner et al. 2003, Leyequien et al. 2007). However, to date very few studies have used remote sensing data for analyses of broad-scale migratory bird diversity and habitat use in low-latitude wetland regions. Remote sensing classifications of wetland areas in general suffer from the "salt-and-pepper" speckle due to misallocation of heterogeneous neighbor pixels to very different classes and confusion caused by variable surface wetness and sub-pixel class mixtures (Yu et al. 2006, Dronova et al. 2011). Novel object-based image analysis approaches in combination with sophisticated machine learning algorithms (Jobin et al. 2008, Tian et al. 2008, Blaschke 2009, Pringle et al. 2009, Richmond 2011, Dronova et al. 2012) offer powerful opportunities to enhance the quality of wetland cover interpretation, which have still been substantially under-utilized.

Analyses of landscape patterns in diversity also need to consider potential spatial dependence (autocorrelation) among sampling sites, which may violate the assumptions of independent and identically distributed errors and thus invalidate classical statistical approaches (Tobler 1970, Legendre et al. 1993, Anselin et al. 1996, Hoeting et al. 2006). Specific causes and implications

of spatial dependence are often not known *a priori*, and in some cases its presence may elucidate ecologically meaningful distance-sensitive processes such as dispersal or species interactions (Miller et al. 2007). More often, however, spatial autocorrelation may indicate model misspecification, missing variables or inadequacy of sampling units to represent variables of interest (Dormann et al. 2007). Although multiple methods have been proposed to diagnose and correct for spatial dependence, they are still not applied on a common basis in the analyses of diversity and species distributions (Hoeting et al. 2006, Dormann et al. 2007, Bacaro et al. 2011).

The goal of this study was to explore whether landscape characteristics derived from remote sensing data could explain spatial variation in diversity and abundance of migratory waterbirds at Poyang Lake, the largest freshwater lake in China (Figure 1) and an internationally important wetland conservation site under the Ramsar convention since 1992 (Ramsar 2012). In the winter, this area hosts large numbers of migratory waterbirds from the East Asian Flyway, including 11 endangered and 6 globally threatened species (Qian et al. 2009, IUCN 2012). Of particular conservation concern are large-sized tuber-feeding waterbirds (including critically endangered Siberian White Crane (*Grus leucogeranus*)) dependent on specific types of submerged aquatic macrophytes (SAM) (Wu and Ji 2002, Burnham 2007) for which recent declines have been reported along Central Yangtze River (Fox et al. 2011). Land use change, climatic variation and pending hydrological dam projects raise serious concerns about future ecological integrity of these wetlands and their long-term capacity to sustain wintering birds (Fang et al. 2006, Wu 2008, Barzen et al. 2009, Finlayson et al. 2010, Guo et al. 2012, Zhao et al. 2012). However, critical gaps still exist in the understanding of habitat determinants for individual species and foraging guilds as well as the overall seasonal composition and dynamics of this wetland (Barzen et al. 2009, Dronova et al. 2011). Improving the knowledge of Poyang Lake's environment and its multi-faceted functionality supporting both wildlife and human users of ecosystem services is of the utmost importance for conservation and management in the face of changing climate and water regulations (Wu 2008, Barzen et al. 2009, Guo et al. 2012).

In particular, little is still known about differences in bird habitat quality among permanent water bodies (sub-lakes) that become hydrologically isolated during the low water season and are utilized by wintering waterbirds (Qian et al. 2009). Some of these sub-lakes have been famous as diversity hotspots over multiple years and thus were included in local nature reserves (Wu and Ji 2002, Burnham 2007, Ji et al. 2007). While primary food resources and suitable water depths have been studied for some individual species and foraging guilds (Markkola et al. 1999, Burnham et al. 2007, Barzen et al. 2009), specific reasons behind non-uniform distribution of species diversity among sub-lakes have not been examined thoroughly. Because frequent and spatially extensive acquisition of field data is very difficult due to the large size of Poyang Lake wetlands and limited on-site access, using remote sensing to search for meaningful geospatial indicators of bird diversity is a feasible research venue which has not yet been extensively explored in this area.

This study examined the associations between several metrics of waterbird diversity and abundance based on the pan-lake ground survey in December 2006 and remotely sensed landscape characteristics of the sub-lake neighborhoods extracted from the Landsat TM satellite imagery. Because of the limitations associated with the one-time survey event and the lack of comprehensive field information on wetland status during the survey, this analysis was intended as an exploratory study to provide the first step towards linking Poyang Lake waterbird distributions with broad-scale characteristics of their non-breeding habitat. Our primary objective

was to identify a set of sub-lake characteristics that highlight potentially important landscape indicators of bird diversity and abundance to be tested more thoroughly in future work. Using information-theoretic approach for statistical model selection (Burnham and Anderson 2002), we investigated which sub-lake features and their combinations were most consistently and strongly associated with dependent variables. We additionally examined whether significant spatial autocorrelation was present in models and whether it had any effect on model rank and relative importance of predictor variables. Finally, we assessed the consistency of model performance in application to another Poyang Lake survey from January 2008 and discussed potential challenges in multi-year analysis with remote sensing for this study area.

Methods

Study area and avian community

Poyang Lake is located in the middle Yangtze River basin, Jiangxi Province, PR China (28°25'-29°45'N, 115°48'-116°44'E; Figure 1). Its surface exhibits considerable year-round hydrological variation where water coverage at the highest summer flood stage in July-August can exceed 4000 km^2, while in winter it reduces to less than 1000 km^2 (Shankman et al. 2006, Qi et al. 2009) in rivers, channels and smaller sub-lakes. At these sub-lakes, waterbirds are often observed within 500 m or less of the water boundary along the inundation gradient from water 2-5m deep to higher-elevation emergent grassland (Ji et al. 2007, Barzen et al. 2009, Dronova, field observation). Spatial extent of the waterlogged mudflats and shallow water is often very large, restricting ground and boat access for field surveys to vast portions of Poyang Lake. Because of this challenge, satellite remote sensing data are an extremely important objective and comprehensive source of information on the study area.

The immediate spatial neighborhoods of winter sub-lakes often have gentle slopes with slow change in elevation and belt-shaped zonation of cover types from shallow water to mudflats to emergent grassland dominated by sedges (*Carex* spp.) and various forbs (Barzen et al. 2009, Wang et al. 2012). These emergent plants with C3 photosynthetic pathway (Pearcy and Ehleringer 1984) represent dominant wetland vegetation of the "cool" growing season, while most of the warm-season C4 grasses and aquatic macrophytes are senescent or dormant at this time (Chen et al. 2007, Wang et al. 2012). Some of the submerged aquatic plant species (e.g, *Vallisneria* spp. and *Stuckenia pectinata*) overwinter as tubers buried in lake sediment. Although "invisible" to remote sensors, these tubers provide critical food resources to deep- and shallow-water bird foragers from the tuber-feeding guild (Burnham 2007, Barzen et al. 2009, Fox et al. 2011). At the same time, depending on atmospheric and water temperature, hydrological regime and local vegetation community, some areas can have green photosynthetically active aquatic macrophytes from other taxa even during the cool growing season (Ji et al. 2007, Dronova personal observation), but their specific role in bird habitat has not been extensively studied.

This analysis focused on resident and migratory Poyang Lake waterbirds which in 2003-2008 included up to 87 species (Ji et al. 2007, Qian et al. 2009) from the orders of Podicipediformes, Pelecaniformes, Suliformes, Ciconiformes, Anseriformes, Gruiformes and Chradriiformes. Previous research has suggested six major foraging waterbird guilds among them: 1) tuber feeding; 2) sedge/grass eating; 3) seed eating/dabbling; 4) benthic insect/larvae eating; 5) fish eating and 6) zooplankton eating birds (Barzen et al. 2009). Prevalence of the preferred food types varies by wetland "zones" of deep water, shallow water, mudflat and emergent grassland, which may often cause concentrations of large and diverse bird groups at the sub-lake water

boundary. As a result, most of the historical point-count ground and aerial surveys have used on sub-lakes as units for sampling and reporting waterbird diversity and abundance.

Ground survey of waterbirds in 2006

Our study used the data from the pan-lake ground point-count survey in December 15-25, 2006. This effort was jointly organized by the State Key Lab of Remote Sensing Science (the Chinese Academy of Sciences, Beijing, PR China) and the State Key Lab of Poyang Lake Ecology and Environment at Jiangxi Normal University, Nanchang, China, in collaboration with local nature reserves (Ji et al. 2007, Kwaiser 2009). Identification of bird species and individual counts were performed by field technicians using binoculars and telescopes (Kwaiser 2009, Qian et al. 2009). Surveyed locations covered permanent sub-lakes, water reservoirs near cities and selected vantage points at the shorelines of rivers and channels. We focused on 51 permanent water bodies situated in western, southwestern and southern part of the wetland (Figure 1) that belonged to predominantly "natural" wetland area and were expected to have similar patterns of annual hydrological dynamics and water resource management. In the survey data, bird species and individual counts were reported as sub-lake summaries along with one, rarely two, geolocated GPS point(s) marking the primary spatial position of observers.

There are two key limitations of this dataset. First, count summaries did not include information on how many total observation spots per lake were surveyed, nor provided any record of the ground conditions and vegetation. Thus, given the uncertainty in spatial position of observers relative to birds (Kwaiser 2009), we focused on sub-lakes as the units of statistical analysis. Because of this, however, we could not address the potential non-uniformity of bird and habitat distribution within each sub-lake. Second, each survey location was visited only once, so we could not estimate variation in bird counts and observation error. The latter constraint applies to most historical basin-wide Poyang Lake surveys conducted either aerially or by coordinated ground teams as a one-time effort in a given season (Ji et al. 2007, Qian et al. 2009).

Dependent variables

From the bird counts at 51 selected sub-lakes, we quantified several metrics (Table 1) that were used as dependent variables in the subsequent models of their relationships with landscape characteristics from remote sensing data. These included four alpha-diversity metrics: waterbird species richness (the total number of species per sub-lake); Shannon index; number of foraging guilds defined after Barzen et al. (2009) with maximum value of 6 and number of size groups with the maximum value of 4. We also estimated two abundance variables: total number of waterbirds and the number of tuberfeeders. The latter guild was given special attention in our study because 1) it includes conservation targets of international importance with four out of five species under endangered status (IUCN 2012) and 2) recently reported declines in both the abundance of this guild and availability of tuber-producing aquatic vegetation urge for more thorough investigations of the habitat indicators at different spatial scales (Fox et al. 2011). Most of our diversity and abundance metrics were significantly positively correlated, although the magnitude of Pearson's correlation coefficients varied among their pairs (0.027 – 0.886). To improve the normality of statistical distributions, mathematical transformations were applied to species richness (natural logarithm), number of birds (natural logarithm) and number of tuberfeeders (natural logarithm of the value +1), and from this point on we will refer to discussion of these variables in their transformed versions.

Independent variables based on remote sensing data

Remote sensing image and classification

To generate independent variables as candidate predictors in bird diversity and abundance models, we extracted several landscape characteristics of the sub-lakes and their neighborhoods from a terrain-geocorrected (Level 1T) Landsat 5 TM satellite image of January 6, 2007. Raw digital numbers from six 30-m spatial resolution bands representing visible (bands 1-3), near-infrared (bands 4 and 5) and shortwave-infrared (band 7) portions of the electromagnetic spectrum were corrected for atmospheric noise using 6S algorithm (http://modis-sr.ltdri.org/code.html). We then isolated wetland area using Microsoft Bing aerial layer in ArcGIS 10 (Esri Inc.) and classified it into common cover types that were hypothesized to represent suitable and non-suitable waterbird habitat (Table 2): open water, mudflat, sand, flooded vegetation, green emergent C3 grasses, senescent grasses and burned vegetation.

For this classification, we used the object-based image analysis (OBIA) approach (Benz et al. 2004, Blaschke 2009) where the first step was segmentation of the image into small spectrally homogeneous groups of pixels, i.e., objects, followed by their statistical classification into wetland cover types (Dronova et al. 2011). OBIA was chosen instead of a "traditional" pixel-based methods because 1) it may reduce the "salt-and-pepper" speckle which is common in pixel-based maps of heterogeneous areas; 2) objects approximate landscape patches or patch primitives that are more ecologically relevant spatial units than pixels (Yu et al. 2006, Richmond 2011); and 3) OBIA has been shown to deliver higher classification accuracy than pixel-based methods due to smoothing of the local noise at the object level both in Poyang Lake wetlands (Dronova et al. 2012) and other landscapes (e.g., Johansen et al. 2007, Pringle et al. 2009). Segmentation of the Landsat image into small primitive objects was implemented in eCognition 8.0 software (Trimble Inc.) using a multiresolution segmentation tool which allows flexibility in the output object sizes. Due to the lack of prior information on wetland patch structure, our choice of segmentation parameters prioritized spectral band values in object generation, while parameters controlling object shape and compactness were kept at low values of 0.1 each. For the scale parameter which controls maximum level of heterogeneity and object size (eCognition 8.0 Reference Book), we used a value of 8 which maximized classification accuracy of Poyang Lake vegetation from Landsat data in a previous study (Dronova et al. 2012).

Prior to classification, we labeled objects corresponding to active residential and other human land use areas within the lake neighborhoods interpreted from Microsoft Bing high-resolution aerial image layer in ArcGIS 10 (Esri Inc.). For the "natural" wetland classes, we assigned 222 training/testing objects based on their overlap with field surveys of perennial vegetation (in March 2006, March 2007, December 2007, April 2008) and visual interpretation of the satellite image. Classification was performed with a supervised k-nearest neighbor algorithm in open-source Weka 3.6.5 software (http://www.cs.waikato.ac.nz/ml/weka/; Hall et al. 2009). Due to limited training data and the lack of field habitat assessment close to bird survey, we assessed classification accuracy using 10-times 10-fold cross-validation method (Witten and Frank 2005, Richmond 2011). Resulting overall accuracy was 97.75%, with the primary confusion between turbid shallow water and mudflat, similar to previous studies (Dronova et al. 2011).

From the image classification results, we selected areas corresponding to open water and flooded vegetation which together were expected to approximate the spatial extent of inundated areas. We then constructed 500-m buffer neighborhoods around these sub-lake areas in ArcGIS

10.0. For each sub-lake with its neighborhood we summarized areas of the cover type classes and calculated several metrics that were subsequently used as independent statistical predictor variables in diversity and abundance models (Table 3).

Independent variables as candidates for diversity and abundance indicators

Independent predictor variables (Table 3) were chosen for diversity and abundance models based on two criteria. First, they represented important habitat types and categories of landscape predictors that could be linked with ground-based ecological mechanism of habitat choice by different species and guilds simultaneously. Their general categories (Table 3) were informed by the previous research at Poyang Lake and related studies from other wetlands (e.g., Wu and Ji 2002, Burnham 2007, Barzen et al. 2009, Kwaiser 2009, Fairbairn and Dinsmore 2001, Webb et al. 2010) and terrestrial systems (Leyequien et al. 2007, Bacaro et al. 2011). Spectral indices and shape metrics were calculated separately for different cover types to account for potential differences in patch properties and their ecological relevance.

I expected to find a positive relationship of diversity metrics with sub-lake area and proportions of cover types which theoretically could support diverse foraging guilds and size groups due to their compositional heterogeneity, such as mudflat, flooded vegetation and emergent grassland. We also expected to find a positive relationship between diversity and measures of local heterogeneity of habitat composition and micro-topography represented by spectral and shape diversity of image objects within relevant cover types. In turn, bird abundance metrics were expected to positively correlate with lake area and proportion of green emergent vegetation which may support large mono-specific or mono-guild flocks of floating and grazing waterbirds (Markkola et al. 1999, de Leeuw et al. 2006). Proportions of cover types associated with potential human disturbance and resource removal by burning (Table 3) were expected to have negative statistical effect on diversity and abundance.

Second, potential predictors needed to contribute 'unique' information in order to minimize the conceptual redundancy and statistical multi-collinearity in models. Each category in Table 3 could be represented by more than one landscape index or geospatial metric, and pilot analysis showed that a number of them could be highly correlated even among different categories. For our selected variables (Table 3), most pairwise Pearson correlation coefficients were within 0.06-0.37 and the exceptions did not exceed 0.56. Because these remote sensing-based variables only indirectly represented habitat characteristics on the ground, the primary focus of this analysis was assessing the strength of associations between diversity or abundance and potential "indicators" as either individual variables or their sets.

Model selection and diagnostics for spatial autocorrelation

To examine the strength of statistical associations between the response and independent variables, we used an information-theoretic model selection approach (Burnham and Anderson 2002) because it accounts for both goodness-of-fit and parsimony in comparing models with different predictor sets. For each response variable (Table 1) we constructed multivariate ordinary least squares (OLS) linear regression models with different sets of predictors in MATLAB R2012a software (MathWorks Inc.). Statistical transformations were applied to several variables to improve the normality of their distributions (see note for Table 4). We then ranked these models using the Akaike Information Criterion corrected for the small sample size (AIC_c) following Burnham and Anderson (2002):

$$AIC_c = -2lnL + 2k + \frac{2k(k+1)}{(n-k-1)},$$

where *lnL* is the model log-likelihood, *k* is the number of parameters to be estimated and *n* is the number of observations in the model. Because the number of possible predictor combinations and hence models was large, the final set of candidate models for each response variable included only the models within 2 AIC_c units from the minimum AIC_c, which were likely to have equivalent support based on the framework of Burnham and Anderson (2002).

I also ran several diagnostics for spatial autocorrelation in our variables and models using GeoDa spatial analysis software (Anselin et al. 2006) to examine the effect of potential spatial autocorrelation on model strength, specification and rank. First, we examined spatial dependence in response variables using a global Moran's I statistic to diagnose the overall spatial dependence across the landscape (Anselin et al. 1996) and Anselin's local indicators for spatial association (LISA; Anselin 1995) to search for potential 'hotspots' of diversity, abundance and their candidate predictors. Next, we investigated whether significant spatial autocorrelation occurred in OLS regression models. To implement the diagnostics, a matrix of spatial weights W was calculated based on Euclidean distances between sub-lakes (Anselin et al. 2006) and then used to perform Lagrange Multiplier (LM) tests for spatial dependence in OLS (Anselin 1988). Additionally, the Breusch-Pagan test (Breusch and Pagan 1979) was used to examine heteroskedasticity of residuals. When significant spatial autocorrelation was detected with the *p*-value of the LM test statistics <0.1, we further applied two maximum-likelihood linear spatial autoregressive models in GeoDa (Anselin et al. 2006). The first one was the spatial lag model which accounts for a second-order spatial interaction between localities based on their proximity:

$$y = \mathrm{X}\beta + \rho\mathrm{W}y + \varepsilon \ (1),$$

where β indicates coefficients for the predictor variables X, ρ is the spatial autoregressive coefficient on the matrix of weights W applied to response values from spatial neighbors of each data point and ε is the random error term. The second form of spatial regression was the "spatial error" model which treats spatial autocorrelation as a 'nuisance' and accounts for it in the model error structure to improve the estimates of coefficients on X:

$$y = \mathrm{X}\beta + \lambda\mathrm{W}\varepsilon + \ \varepsilon \ (2),$$

where λ is the estimated spatial autoregressive coefficient for the error term. We then compared coefficients and significance values for individual predictors, model AIC_c and diagnostics for spatial dependence and heteroskedasticity of residuals among OLS and spatial regression outputs. These results were further used to 1) update model ranks for each response variables; and 2) generate predictions for a different survey year and compare with the actual data for model verification, as described in the next section.

Model assessment and model averaging

Ideally, one would like to evaluate the properties of the models using out-of-sample predictions. This is a challenging exercise in the context of Poyang Lake since measurements of response variables in different years are one-time surveys, sometimes using different methods and conventions. Furthermore, cloud-free remote sensing images for a given period during the winter season may be available from different satellite sensors in different years, resulting in disagreements among classifications even under similar ground conditions. Given the dynamic nature of Poyang Lake environment and substantial variation in hydrological conditions from

year to year (Shankman et al. 2006, Feng et al. 2012, Dronova et al. under review), similar states of vegetation greenness and surface wetness may not always match anniversary dates between years and times of bird surveys. Reconciling all these differences would require significant efforts to standardize images from different satellites, possibly by a separate calibration study. Thus comparing models outcomes and independent variables across year may be difficult.

With these limitations in mind, we explored how the highest-rank models of diversity and abundance would perform when applied to another Poyang Lake bird survey. Specifically for this exercise, we used the dataset from the aerial survey of January 3, 2008, organized by Global Environmental Facility (GEF), the International Crane Foundation (ICF) and the Siberian Crane Wetland Project in coordination with Poyang Lake National Nature Reserve, Jiangxi Province, PR China. In this 2008 survey, bird data were also reported by sub-lake, but only 16 sub-lake units were consistent with the 2006 dataset and thus were chosen for verification.

There was no matching cloud-free Landsat TM image for the dates close to 2008 survey, and therefore we extracted geospatial characteristics of the sub-lakes from a January 1, 2008 scene of Beijing-1 microsatellite with one near-infrared, two visible red and green spectral bands and 32-m image spatial resolution. Due to the instrument differences between Landsat and Beijing-1 sensors and the lack of calibration system in the latter (which prevents correction for atmospheric effects), we calibrated red, green and near-infrared bands of Beijing-1image to atmospherically corrected red, green and near-infrared bands of the 2007 Landsat image. This calibration was conducted using band-specific simple linear regression equations estimated from spectral values of the pseudo-invariant targets that were not expected to change between two years: bright sand on top of the high-elevation dunes and dark water in permanent water reservoirs near cities. Beijing-1 image was also segmented into objects in eCognition with segmentation scale value of 5 (producing comparable object size to segmentation of the 2007 Landsat image) and shape and compactness values of 0.1 each, and then classified into wetland cover types (Table 2) using supervised k-nearest neighbor algorithm with the cross-validation overall accuracy of 95.2%.

Model assessment was done as follows. We used regression developed with 2006 survey data to generate 'point' predictions for 16 sub-lake units using their geospatial characteristics from 2008 imagery. These predictions were estimated with the best set of models for each dependent variable averaged by means of the Akaike weights (Burnham and Anderson 2002). For spatial lag model, point predictions were derived using remotely sensed characteristics of all 2008 sub-lake units corresponding to 51 sub-lakes from 2006 by rearranging equation (2):

$$\hat{y} = (I - \rho \mathrm{W})^{-1} X\beta \,,$$

where *I* is the identity matrix for the number of sub-lakes used in regression. However, our comparison of the univariate relationships between response variables and most important predictors in 2006 models detected mismatches in spectral variables despite relative calibration of Beijing-1 image. These mismatches are discussed in more detail in Results section 3.3 below, but they indicated that predictions from models using spectral variables may differ in magnitude from the actual 2008 data. For this reason, we compared final predictions from the weighted models between 2006 and 2008 using non-parametric Spearman rank correlation coefficients.

Results

Spatial patterns of response and predictor variables.

Total number of species varied from 2 to 23 among 51 sub-lakes (Table 1), and the proportional

species turnover (Tuomisto 2010) was equal to 0.86, suggesting that an average sub-lake contained only ~14% of the overall species richness. Preliminary analysis of spatial autocorrelation in response variables suggested low-magnitude positive spatial dependence, where global Moran's I statistic ranged between 0.01 for number of size groups and 0.26 for log-transformed number of tuberfeeders significant with p-value <0.05 only for the latter variable and for Shannon index.

At the same time, LISA statistics showed that spatial autocorrelation in response variables was not uniform across the landscape and concentrated in a few statistically significant local "hotspots" (Figure 2). Specifically, for species richness, Shannon index, number of food guilds, number of size groups and number of birds, there was a cluster of spatially close high values at several lakes within Poyang Lake National Nature Reserve (PLNNR; Figure 2a-c,e). For the number of tuberfeeders, there were two small clusters of high values (one also in PLNNR) and a cluster of low values and also high-low associations in southeastern part the of study area (Figure 2f). For the number of size groups, there were several low-high and high-low clusters indicating negative spatial dependence including PLNNR reserves (Figure 2d). Among predictor variables, the proportion of flooded vegetation and mudflat NDVI both had pronounced clusters of high values in southeastern portion of study area and clusters of low values in PLNNR (Figure 2g,h).

Variable selection in OLS models

Relative importance of independent variables in the univariate OLS models varied among diversity and abundance metrics (Table 4). Spectral greenness (NDVI) of mudflat with a negative effect was consistently among the strongest predictors, while other important variables included total sub-lake area with positive effect and proportion of flooded vegetation with negative effect (Table 4). Combinations of 2-3 of these variables were also frequently included in the lowest-AIC_c multivariate models for each response variable (Table 5). However, none of the univariate models in Table 4 was within 2 AIC_c units from the minimum-AIC_c multivariate models in Table 5, except those with proportion of flooded vegetation and mudflat NDVI for the number of tuberfeeders.

Several variables with lower strength of statistical association in univariate models appeared in the best-fit multivariate models (Table 5). These included: spectral greenness of emergent vegetation with positive effect (multivariate models for all response variables except the number of tuberfeeders), object shape heterogeneity of emergent grassland with a negative effect (species richness, number of food guilds and two abundance metrics); proportion of burned vegetation with a negative effect (number of size groups and two abundance metrics), proportion of emergent grassland with negative (number of food guilds and size groups) or positive effect (number of tuberfeeders), proportion of human land use areas (number of size groups and number of food guilds), but they were frequently not significant at 0.05 level.

The strongest multivariate models for different response variables often included the same sets of predictors. For instance, sub-lake area, proportion of flooded vegetation and NDVI of emergent grassland were selected together in models for all dependent variables except the number of tuberfeeders and formed the key component of all lowest-AIC_c models for number of food guilds and number of size groups (Table 5). In the models for species richness and two abundance metrics, NDVI of mudflat was often included together with heterogeneity of object shape index for emergent grasses. Proportion of burned vegetation was always included with sub-lake area (but not vice versa). At the same time, the overall goodness-of-fit indicated by R^2

statistic was relatively low in most multivariate models (Table 5), especially for number of tuberfeeders with 12 zero values out of 51 sub-lakes, which could reflect both noise in the data and potentially important missing variables. We discuss the latter limitation in section 4.3 below.

Spatial autocorrelation in regression models

Significant spatial autocorrelation was detected in most OLS models for all dependent variables, except the number of size groups (Table 5). Spatial regression successfully corrected this effect in most cases, although it only marginally improved the goodness-of- fit. Most of the changes in AIC_c with spatial regression were within 2 units from the corresponding OLS model (Table 5), in part because both spatial models use one additional parameter relative to OLS (which penalized AIC_c values relative to OLS).

For both species richness and Shannon index, spatial error model had stronger support than spatial lag model when significant spatial autocorrelation was detected (Table 5). For the former response variable, lambda coefficient in spatial error model was significant with p-value<0.01. For Shannon index, lambda in the error model was not significant (p-value>0.1), but the model no longer had significant spatial dependence in residuals. For the number of food guilds and the number of birds, spatial lag model had higher support than spatial error regression (Table 5) in case of significant spatial dependence in OLS. Applying the lag model also slightly changed model ranks and reduced the number of candidate models within 2 units of AIC_c from the minimum (Table 5).

For the number of tuberfeeders, spatial lag models had slightly lower AIC_c than corresponding spatial error models. However, the latter models for this response variable no longer had significant spatial dependence for weight matrix (p-values >0.1), while in spatial lag models there was still unaccounted spatial lag dependence (p-values <0.1). Spatial error model was also more effective at alleviating heteroskedasticity with much higher p-values on the Breusch-Pagan test statistic than with the lag model in this case. Because the difference in AIC_c between lag and error models was less than 2 units for each predictor set (Table 5), spatial error models were used in 2008 predictions for the number of tuberfeeders.

For the number of size groups, LM tests in GeoDa did not detect significant spatial dependence in favor of spatial regression models. All six models here had significant heteroskedasticity based on the structure of this response variable, which could not be removed by spatial regression. Hence, for number of size groups OLS was retained for verification as a more parsimonious option.

Assessment of model performance with 2008 survey

In model assessment, we compared the actual values of response variables for 16 sub-lake units in aerial survey of 2008 with those variables in 2006. Point predictions estimated as Akaike-weighted averages from the highest-support models for diversity metrics did not strongly correlate among the sub-lakes for species richness (Figure 3a), number of food guilds and number of size groups. For Shannon index, there was a generally positive relationship between the actual and predicted values, but the correlation was not significant because of two extreme data points (Figure 3b). With those points excluded, Spearman rank correlation coefficient for Shannon index became higher (0.55) and significant (p-value=0.041). For both number of birds (Figure 3c) and number of tuberfeeders (Figure 3d), there was a significant positive correlation (Spearman rank coefficient values 0.55 and 0.51, p-values 0.027 and 0.044, respectively).

However, the general magnitude of predicted values often differed from the actual 2008 values, and to investigate this issue further, we compared the univariate relationships between response and the strongest predictor variables between 2006/2007 and 2008 datasets (examples for species richness are shown in Figure 4). This comparison revealed that sub-lake area and proportions of cover types were relatively close in magnitude (Figure 4a,b), although some differences among them were expected based on variable hydrology and phenology of Poyang Lake surface among different years (Dronova et al. under review). However, the magnitude of important spectral predictors, specifically, NDVI for mudflat and for emergent grassland, was clearly different between two years (Figure 4c,d). On the one hand, this mismatch could result from true differences in spatial extent and density of green vegetation between survey dates, because winter 2006-2007 was warmer and wetter compared to winter 2007-2008 (Dronova et al. under review). On the other hand, differences in data quality between Landsat TM and Beijing-1 sensors could also play a role because calibration of Beijing-1 data using pseudo-invariant targets may not have accounted for all the atmospheric noise effects on spectral signal. This result highlights a critical caveat for using "similar" remote sensing data from different instruments in multi-temporal analyses of Poyang Lake landscape characteristics. In the future work, more rigorous data calibration may be necessary before spectral indices from different sensors can be used in models of ground variables.

Discussion

Potential indicators of Poyang Lake bird diversity and abundance

Understanding landscape-level variation in biodiversity at different spatial scales is both an important and intriguing challenge in ecology. The degree to which spatial and temporal diversity patterns can be interpreted with indirect but cost-effective remote sensing-based and geospatial "proxies" remains uncertain. Previous studies of bird diversity in different landscapes have identified similar types of indicators related to habitat size, spectral variation representing habitat heterogeneity, spectral indices of vegetation structure and greenness, proximity to human disturbance and other landscape characteristics (e.g., Nøhr and Jørgensen 1997, Fairbairn and Dinsmore 2001, Canepuccia et al. 2007, Bino et al. 2008, Coops et al. 2009a, Webb et al. 2010, Cerezo et al. 2011, Bacaro et al. 2011). However, generality and sufficiency of these proxies across diverse biomes, taxa and guilds or different time periods is not well known, and their performance in statistical models may be limited without including essential ground variables.

Our analysis highlighted several ecologically relevant correlates of waterbird diversity and abundance at Poyang Lake, PR China among landscape characteristics of their wintering habitat based on the ground bird survey and remote sensing data from winter 2006-2007. Strong negative effect of mudflat NDVI on all response variables indicated that mudflats with lower amount of green vegetation (hence more recent post-flood exposure) and/or higher surface wetness on average supported higher bird diversity and abundance. These conditions correspond to "characteristic" Poyang Lake mudflats that represent exposed lake bottomland directly adjacent to water body (Dronova et al. 2011) and may contain large numbers of aquatic invertebrates, vegetation seeds, propagules and buried tubers from summer aquatic macrophytes (Wu and Ji 2002, Liu et al. 2006b, Burnham 2007). Potential variety of food resources together with low depth or lack of surface water on mudflats could make them favorable to birds of different size and foraging preferences, although relative size of sub-lake mudflat area was not an important predictor in our models.

Positive association of vegetation NDVI with bird diversity and total abundance was also consistent with previous terrestrial studies (Nøhr and Jørgensen 1997, Hurlbert and Haskell 2003, Bino et al. 2008, Bacaro et al. 2011). Various plot and ecosystem-level analyses have reported strong correlations between NDVI and plant density, biomass, photosynthetic rates and productivity, canopy leaf area, foliar nutrient and chlorophyll content (e.g., Yoder and Waring 1994; Turner et al. 1999; Ollinger 2011). At Poyang Lake, green emergent sedges with relatively high NDVI are an important food resource to *Anatidae* of the grass-eating guild which forage on grasses in large numbers (Markkola et al. 1999, de Leeuw et al. 2006, Barzen et al. 2009, Zhao et al. 2012) and contribute to both bird diversity and abundance at sub-lakes with this vegetation type. Kwaiser (2009) reported the importance of Poyang Lake sparse vegetation corresponding to sedges in the transitional zone between mudflat and emergent grassland in species-specific habitat models for Tundra Swans (*Cygnus columbianus*) and White-fronted Geese (*Anser albifrons*) based on these 2006 data. However, relative size of emergent grassland was not among the strongest predictors in univariate or multivariate models, suggesting that greenness and uniformity of patch shapes of this cover type was more important than its spatial extent.

Significant negative correlation of most diversity and abundance metrics with the proportion of flooded vegetation poses an interesting question on what features could make the sub-lakes *less* conducive to high diversity and abundance levels. Green aquatic macrophytes occur in Poyang Lake area in winter (Ji et al. 2007), but their ecological services to waterbirds or food organisms from other trophic levels are less well understood than importance of emergent grasses (Markkola et al. 1999, Zhao et al. 2012) or dormant tubers of the warm-season aquatic plants (Burnham 2007, Barzen et al. 2009). Similar to our results, Kwaiser (2009) reported negative effect of Landsat-based wetland vegetation/water class (which was similar to our flooded vegetation) on the abundance and likelihood of presence of tuber-feeding Tundra Swans from the same 2006 survey dataset. Multi-temporal remote sensing data indicates that a number of sub-lakes have the signal of submerged vegetation nearly year-round, including winter (Dronova et al. under review). Based on this phenology pattern, we speculate that plant community composition in these sub-lakes may differ from warm-season tuber-producing macrophytes. Given recent declines in the latter vegetation type across the region (Fox et al. 2011), species composition of winter aquatic vegetation and its potential effects on other plants and habitat quality for birds and lower trophic levels should be more thoroughly investigated in the future.

Among other predictors, statistical importance of sub-lake area was similar to previous studies (e.g., Roshier et al. 2002, Canepuccia et al. 2007, Webb et al. 2010, Cerezo et al. 2011), likely representing the effect of lake size on the amount and potential diversity of food resources and foraging space. Although proportions of cover types directly associated with potential human disturbance within lake neighborhoods were neither frequently nor significantly associated with response variables, we cannot rule out the potential role of human disturbance in bird distributions and its indirect effect on statistical importance of other variables. For instance, larger sub-lake area may provide better opportunities to avoid human presence, while higher greenness of some emergent grasslands may be driven by lower grazing pressure by domestic livestock due to limited wetland access. A variety of human-driven stressors at Poyang Lake such as poaching, fishing, livestock herding (Burnham 2007, Cao et al. 2010, Zhao et al. 2012) may not be captured with remote sensing data alone. Hence, future work should incorporate the information on roads, elevation, and soil characteristics to more explicitly address wetland accessibility to humans in studies of bird spatial distribution and behavior.

Our results also suggest that sets of predictors describing complementary habitat features may be more useful in models of diversity and abundance than single variables. Consistent inclusion of several predictors in the lowest-AIC_c models (Table 5) suggests that not only their individual importance, but also their synergy could illuminate conditions favoring certain diversity levels. Collectively, our results indicate that diversity and total abundance were on average higher in larger sub-lakes with relatively small but heterogeneous component of flooded vegetation, non-vegetated mudflat and green emergent grassland with uniform sub-patches. This description matches several spatially close lakes that have been important diversity hotspots from year to year (Wu and Ji 2002, Burnham 2007, Barzen et al. 2009). In contrast, smaller sub-lakes with more aquatic vegetation in winter and the lack of bare mudflat were associated with lower diversity and abundance and exhibited spatial clustering with respect to these two characteristics. However, the latter conditions should not be immediately interpreted as "non-desirable" for wetland management, since theoretically they might be critical for selected bird species or their diet components, which should be explored in the future work.

Spatial autocorrelation in diversity and abundance models

Significant spatial autocorrelation detected in most of our models presents an important caveat for landscape analyses of bird diversity and abundance in this region, particularly in terms of the risk of violating key assumptions of linear regression and model misspecification. However, specific reasons behind spatial dependence among sub-lakes should be investigated more thoroughly in the future. Differences in support for spatial lag versus spatial error models among our response variables suggest that potential causes for spatial dependence could stem from both the sampling and modeling design and the unknown distance-sensitive ecological processes.

Notably, for species richness, Shannon index and number of tuberfeeders as dependent variables, spatial error regression was the most effective at correcting for spatial autocorrelation. Given large amount of unexplained variation in our models (Table 5), a likely explanation for this result is the absence of important but spatially structured variables (Legendre et al. 2002). A potential candidate could be availability of tubers from warm-season summer aquatic plants that have been previously detected in some of the sub-lakes with high bird abundances and species richness (Burnham 2007) but not sampled in the bird survey of 2006. The hypotheses on spatial dependence in tuber availability could be based on, e.g., similarity in aquatic vegetation communities among proximal sub-lakes belonging to the same hydrological units at higher water stages in the warm growing season.

Alternatively, the importance of spatial error model may question the utility of sub-lakes as sampling units to adequately represent spatial patterns in diversity and abundance in models. Significant clusters of high or low values in most of the response variables and some predictors (Figure 2) suggests some underlying similarity among the corresponding sub-lakes both in avian community and environmental features. For instance, closely located sub-lakes may be utilized by the same bird flocks more frequently than more distant ones, and hence 'function' as a single landscape unit in representing the avian community. Future work should test aggregations of sub-lakes based on basin geomorphology and hydrological connectivity, which may affect similarity among sub-lake resources and cover types.

At the same time, stronger support for spatial lag regression in models for the number of food guilds and the number of birds suggests potential importance of previously unknown second-order spatial interactions in these variables among sub-lakes. While this form of spatial

dependence could not be investigated with available data in our study, future work should explore potential mechanisms of spatial "interaction" among sub-lakes. A candidate hypothesis could be that moderate intra-specific or intra-guild competition for resources and foraging space forces large groups of birds to disperse over spatially close sub-lakes, producing similar avian community composition and autocorrelated magnitudes in bird counts among them. Alternatively, spatial autocorrelation in food resources caused by, e.g., distance-sensitive dispersal of aquatic vegetation, fish and invertebrates could make close sub-lakes attractive to similar bird species and foraging guilds.

Uncertainties in model verification and study limitations

In application to 2008 aerial observation dataset, models derived with 2006 bird ground survey data performed relatively well in representing general differences among lakes, particularly for two bird abundance metrics and Shannon index. Inconsistency among predictions and actual values of response variables in 2008 illustrates the challenges of using remote sensing variables from different data sources and limited availability of cloud-free remote sensing images for this region in general. While wetland classifications of Landsat and Beijing-1 images produced similar magnitudes of sub-lake area and cover type extents, the differences in NDVI and spectral heterogeneity affected the uncertainty in model performance, especially given statistical importance of spectral greenness. The differences between ground and aerial survey methods (including visibility, coverage of sub-lake area and detectability of different-sized birds) could further contribute to error in model predictions for 2008 data in addition to model specification and 2006-based coefficient estimates. Failure of the models to adequately predict numbers of food guilds and size groups and heteroskedasticity of residuals suggests that OLS and spatial regression are not the most optimal methods for these variables. Given their definitions as counts of bird groups rather than individuals, future work should test them as categorical variables predicted by alternative models such as multinomial logistic regression.

It is important to discuss the limitations which affected both model assessment and the overall strength of our analysis. The primary constraint was the single-date nature of the pan-lake bird survey which did not allow to estimate the observation error and to address the uncertainty in sub-lake occupancy by different species within the wintering season. One-time surveys also make it impossible to verify whether bird distribution reflected their "typical" spatial pattern within the winter season or had been affected by a temporary "aggregate shock" e.g., due to prior burning of reeds across the wetland in 2006. Unfortunately, most of the basin-wide Poyang Lake surveys to date have been conducted as a one-time effort per winter, sometimes with different method of observation and timing within the season (Qian et al. 2009). This caveat presents a serious concern for reliable analyses of bird community trends in this wetland and highlights the urgent need for a permanent basin-wide monitoring program with multiple surveys per winter and consistent protocols for different teams and sampling events.

Another limitation was the lack of information on ground variables such as vegetation status, water depth or evidence of human disturbance at the time of bird survey. Large amount of unexplained variation in regression models suggests that useful predictors could be missing from the model structure. For waterbirds specifically, water level may be a key missing variable which determines their spatial location within the study area and access to food resources (Burnham 2007, Barzen et al. 2009). However, field measurements of habitat characteristics may be difficult to perform simultaneously with avian surveys due to both limited access to wetlands and the risk of disturbing the birds. To address this challenge, future research and monitoring should

consider installing wireless sensors to document habitat conditions continuously throughout the low water season (Gong 2007, Burgess et al. 2010).

Summary and implications for the future research

Human regulations of water resources, the uncertainty of climate change effects on future functioning of Poyang Lake ecosystems and ongoing economic development in the middle and central Yangtze region pose serious threats to long-term sustainability of migratory waterbird populations that critically depend on their wintering grounds in this area (Barter et al. 2005, Fang et al. 2006, An et al. 2007, Fox et al. 2011, Zhao et al. 2012). Specific determinants of suitable non-breeding habitats that have historically accommodated large and diverse avian groups are still insufficiently understood, and enhancement of this knowledge is severely constrained by limited field access and large size of these wetlands.

Although predictive models of Poyang Lake bird diversity and abundance in our study did not fully explain variation in response variables based on remote sensing data alone, they suggested several potential landscape predictors and new hypotheses for the future research. In particular, significant negative effect of spectral greenness of mudflats on all response variables may have important implications for conservation and management of Poyang Lake habitats. Non-vegetated seasonal mudflat and shallow water interfaces with low spectral greenness may change their spatial position throughout the low water winter season due to fluctuations in adjacent water bodies and spread of emergent grasses (Dronova et al. 2011, Chapter 3 of this thesis), similar to other periodically inundated wetlands globally (Taft et al. 2002, Canepuccia et al. 2007). Hence, for mudflat and shallow water-dependent birds, projections of sufficient habitat must pre-allocate for potential redistributions of these cover types in the winter season. This may be problematic under scenarios of higher water storage following new dam construction, with the risk of both reduction in available areas and their shifts towards wetland periphery, closer to sources of human disturbance (Barzen 2008, Barzen et al. 2009, Finlayson et al. 2010).

With the one-time bird survey data in this study, it was not possible to examine whether spatial locations of birds had been "tracking" mudflat exposure throughout the winter. However, surveys conducted later in winter season in other years noted higher waterbird aggregations close to Poyang Lake center (Qian et al. 2009) where mudflats are expected to become flood-free later than in peripheral sub-lakes. Sensitivity of waterbird abundance and species richness to hydrological fluctuations and reductions in mudflat availability was also reported in other regions (e.g., Roshier et al. 2002, Taft et al. 2002, Canepuccia et al. 2007). Being directly adjacent to water bodies, mudflat habitats and hence their supported avian guilds may be particularly vulnerable to Poyang Lake hydrological changes caused by shifts in climate and new water control structures (Barzen et al. 2009, Finlayson et al. 2010) and hence must be carefully addressed in management scenarios.

In turn, positive association of spectral greenness of emergent grassland with diversity and abundance metrics reflected the importance of the cool growing season vegetation in habitat services to waterbirds and their food organisms (de Leeuw et al. 2006, Barzen et al. 2009). Future research should test potential sensitivity of this cover type to changes in climate and Poyang Lake hydrological regime, which could affect competitive relationships between C3 sedges and some of the opportunistic C4 grass species that are currently restricted to higher-elevation wetland margins (Dronova et al. 2012, Wang et al. 2012).

Negative correlation between bird diversity and abundance with the proportion of flooded

vegetation should be more thoroughly investigated in future work to explore the composition of cold-season aquatic macrophyte communities and their relationships with tuber-producing warm-season vegetation supporting waterbirds in winter. A number of lakes along central Yangtze River have recently exhibited marked changes both in diversity and specific composition of aquatic macrophyte communities (Fang et al. 2006). These changes include declines in tuber-producing aquatic macrophytes likely affected by pollution, lake eutrophication and changes in water chemistry following economic growth and land use change in the area (Liu et al. 2004, Fang et al. 2006, Xing et al. 2006, Fox et al. 2011). However, no studies to our knowledge have investigated whether significant shifts in aquatic plant communities have occurred specifically in Poyang Lake wetlands in the recent decade (Fang et al. 2006). Such research would be of the utmost importance for understanding trends in food resources and wetland carrying capacity for both the waterbirds and other users of wetland ecosystem services in the region (Fox et al. 2011).

Significant spatial autocorrelation in our models raised interesting questions on model specification as well as on spatial ecological relationships and connectivity among sub-lakes. What are the most ecologically relevant spatial units to sample bird communities and understand their sensitivity to changes in habitat? What aspects of spatio-temporal habitat utilization may underlie snapshot clusters of diversity and abundance that are detected in one-time surveys? And finally, what effective size of protected wetland area is needed to sustain spatial ecological relationships among sub-lakes, especially given the dynamics of wetland surface during the winter season (Dronova et al. 2011, Chapter 3 of this thesis)? These questions and previous studies from other regions (Coops et al. 2009a) suggest that future analyses of spatial and temporal patterns in bird diversity and abundance at Poyang Lake should incorporate landscape dynamics into habitat assessments, instead of using "snapshot" characteristics from single-date images (Crews 2008, McCleary et al. 2008, Chapter 3 of this thesis). Winter habitat quality and availability of food such as tubers and grasses are governed by variation in atmospheric temperature, precipitation, disturbance, flood regime and water column chemistry in the preceding growing season (Burnham 2007). In a previous study (Chapter 3 of this thesis), "dynamic cover types" were used to characterize Poyang Lake wetland zones that exhibit similar pattern of change within an annual flood cycle. Investigating the linkages between spatial bird distributions and wetland ecological regimes represented by dynamic classes could more effectively illuminate habitat preferences and potentially within-season habitat switching, especially if multiple surveys per winter become possible in the future.

In summary, this study provides the first example of linking Poyang Lake waterbird community diversity characteristics with landscape properties of their wetland habitat approximated by remote sensing-based compositional, geometric and spectral variables. Such analyses are urgently needed given recent declines in several important waterbird species along the Yangtze River (Zhao et al. 2012) and threats to wetland hydro-ecological regimes from the upstream Three Gorges Dam and local water control projects (Barzen et al. 2009, Finlayson et al. 2010, Guo et al. 2012). Our results should be interpreted with caution because of the uncertainty associated with one-time bird survey per season, the lack of ground-based habitat descriptions and longer-term data series for multiple years. Nevertheless, our findings highlight the utility of remote sensing data to suggest potential landscape indicators of bird diversity and abundance and develop new ecological and spatial hypotheses for the future work. Challenging field conditions at Poyang Lake and frequent cloudiness will likely remain a constraint for temporal frequency of both bird surveys and imagery from popular sensors in the near future. Therefore, to improve understanding of within-season variation in bird distribution and habitat dynamics, future

research should more rigorously utilize wireless sensor technology for continuous in situ observations and novel wide-swath microsatellite imaging (Dronova et al. 2011, Wang et al. 2012) for more detailed medium-resolution landscape imagery.

Acknowledgements

We acknowledge the waterbird survey data contributions from 1) December 2006 ground survey sponsored by the State Key Lab of Remote Sensing Science (the Chinese Academy of Sciences, Beijing, PR China) and the State Key Lab of Poyang Lake Ecology and Environment at Jiangxi Normal University, Nanchang, China, in collaboration with local nature reserves; and 2) January 2008 survey organized by Global Environmental Facility (GEF), the International Crane Foundation (ICF) and the Siberian Crane Wetland Project in coordination with Poyang Lake National Nature Reserve, Jiangxi Province, PR China (data provided by the International Crane Foundation). We also acknowledge the financial support from the NASA Earth and Space Science Student Fellowship (NNX09AO27H) and services of the Geospatial Innovation Facility, University of California Berkeley for the remote sensing data analysis.

Tables

Table 1. Dependent (response) variables used in regression models and their basic descriptive statistics for 51 sub-lakes from December 2006 Poyang Lake survey.

Variable	Description	min	mean (st.dev.)	max
Species richness	Number of waterbird species per sub-lake	2	9.1(5.44)	23
Shannon index	Diversity index which accounts for both the number of species and evenness of their abundance calculated as $H' = -\sum_{i=1}^{R} p_i \ln p_i$, where p_i is the proportion of individuals from species i in the whole dataset and R is the total number of species in the dataset	0.2	1.1(0.44)	2.03
Number of food guilds	The number of foraging guilds represented per sub-lake, out of 6 groups after Barzen et al. (2009): tuber-feeding, sedge/grass-eating, seed eating/dabbling, benthic insect/larvae eating, fish eating and zooplankton eating birds	1	3.9(1.38)	6
Number of size groups	The number of bird groups out of 4defined by foraging habit (wading versus floating/diving birds) and size (average body mass greater or less than 2 kg for floating birds, average body length greater or less than 0.8 m for waders)	1	3.2(0.98)	4
Total waterbird abundance	Total number of waterbirds per sub-lake	17	7201(16262)	94568
Abundance of tuber feeding birds	The number of birds from the tuber-feeding foraging guild including the species *Grus leucogeranus, Grus monarcha, Grus vipio, Anser cygnoides* and *Cygnus columbianus*	0	2750(8185)	46395

Table 2. Poyang Lake wetland cover types used in satellite image classification.

Cover type name	Description
Water	Inundated areas with water coverage above the ground or vegetation surface: sub-lakes, channels, pools, rivers etc.
Mudflat	Exposed lake bottomland directly adjacent to the water body with sparse (<30%) or no plant cover.
Emergent grassland	Green photosynthetically active emergent wetland vegetation dominated by C3 grasses and forbs
Flooded vegetation*	Green photosynthetically active vegetation with "wet" spectral signal (significantly lower near- and short-wave-infrared range than emergent grasses); includes inundated emergent, floating and submerged aquatic macrophytes and their mixtures
Senescent grasses	Perennial vegetation that maintains dry/senescent biomass during the winter, typically dominated by mixed warm-season C4-grasses and reeds that grow in higher-elevation sub-lake and channel periphery
Burned vegetation	Recently burned grassland with distinct dark soil/ash and little or no vegetation regrowth
Human land use	Areas of active human land use adjacent to Poyang Lake wetlands (residential, agriculture, extraction etc.)

*Due to medium resolution of satellite imagery, lack of vegetation records from the time of the survey and constrained field access to aquatic vegetation beds in general, we were not able to successfully differentiate more specific functional groups of aquatic macrophytes within this category and treated inundated vegetation as a single class. I address this issue in more detail in Discussion section.

Table 3. Independent variables used in regression models of Poyang Lake waterbird abundance and diversity, summarized for 500-m neighborhoods around sub-lakes within the natural wetland area.

Category	Name (model code)	Definition
Area	Total sub-lake unit area (area)	Total area of the sub-lake water body and its 500-m buffer neighborhood, m^2
Prevalence of habitat cover types within sub-lake neighborhood	Percent mudflat (%mudflat)	Proportion of the area classified as mudflat within the sub-lake neighborhood
	Percent emergent vegetation (%emgrass)	Proportion of the area classified as emergent grassland within the sub-lake neighborhood
	Percent flooded vegetation (%floodveg)	Proportion of the area classified as flooded vegetation within the sub-lake neighborhood
Spectral greenness	Normalized Difference Vegetation Index (NDVI) of emergent grassland (ndvi emgrass)	Spectral index of vegetation greenness, here calculated as mean object-level NDVI from Landsat TM bands 3 (Red) and 4 (Near-infrared) within green emergent grass class for each sub-lake: NDVI= (Band 4– Band 3)/(Band 4 + Band 3)
	Normalized Difference Vegetation Index (NDVI) of mudflat (ndvi mudflat)	Calculated using the same formula as above as mean of the objects within the mudflat class
Spectral heterogeneity of habitat cover types	Spectral heterogeneity of mudflat (stdev Red mud)	Standard deviation of the object-level mean values for Landsat TM band 3 (red) among the mudflat class image objects
	Spectral heterogeneity of flooded vegetation (stdev Red floodveg)	Standard deviation of the object-level mean values for Landsat TM band 3 (red) among the flooded vegetation class image objects
	Spectral heterogeneity of emergent vegetation (stdev Red emgrass)	Standard deviation of the object-level mean values for Landsat TM band 3 (red) among the emergent C3 grass image objects
Heterogeneity of primitive patch shapes within habitat cover types	Heterogeneity of shape index for mudflat (stdev SI mud)	Standard deviation of the shape index (the ratio of object with area *A* to perimeter of the square with the same area; eCognition 8.0 Reference Book) for primitive image objects classified as mudflat class within the sub-lake neighborhood
	Heterogeneity of shape index for emergent vegetation (stdev SI emgrass)	Standard deviation of the shape index (the ratio of object with area *A* to perimeter of the square with the same area; eCognition 8.0 Reference Book) for primitive image objects classified as emergent grassland within the sub-lake neighborhood
Potential anthropogenic disturbance within sub-lake neighborhood	Percent of burned vegetation area (%burnveg)	Proportion of the area classified as burnt vegetation within sub-lake neighborhood
	Percent of non-wetland human land use (%human LU))	Proportion of the area representing active human land use (residential or agriculture) within sub-lake neighborhood

Table 4. Relative importance of independent variables in univariate ordinary least squares regression models of diversity and abundance response variables, sorted by Akaike Information Criterion (AIC_c) in ascending order.

Dependent variable:	***Ln(species richness)***		***Shannon index***			***Number of food guilds***	
Independent variable	R^2	AIC_c	***Independent variable***	R^2	AIC_c	***Independent variable***	R^2	AIC_c
Mudflat NDVI	0.29	95.1	Mudflat NDVI	0.15	60.5	Mudflat NDVI	0.21	175.0
Sqrt (%floodveg)	0.18	102.8	Sqrt (%floodveg)	0.12	62.0	Sqrt (%floodveg)	0.12	180.6
Sqrt (%emgrass)	0.08	109.0	Stdev Red floodveg	0.08	64.4	Ln(area)	0.08	182.6
Stdev Red mud	0.08	109.1	NDVI emgrass	0.04	66.6	%human LU	0.06	183.6
Ln(area)	0.05	110.2	Ln(area)	0.04	67.0	NDVI emgrass	0.06	183.9
%human LU	0.04	111.1	Stdev Red emgrass	0.03	67.4	Sqrt (%emgrass)	0.04	184.6
NDVI emgrass	0.03	111.2	Stdev SI emgrass	0.02	67.5	Stdev Red mud	0.03	185.7
Stdev SI emgrass	0.02	111.8	%burnveg	0.02	67.9	Stdev Red floodveg	<0.01	186.8
Stdev Red emgrass	<0.01	112.7	%human LU	<0.01	68.4	%burnveg	<0.01	186.9
Stdev Red floodveg	<0.01	112.8	Stdev Red mud	<0.01	68.5	Sqrt(%mudflat)	<0.01	186.9
Stdev SI mud	<0.01	112.8	Sqrt (%emgrass)	<0.01	68.5	Stdev SI emgrass	<0.01	187.0
%burnveg	<0.01	112.9	Stdev SI mud	<0.01	68.6	Stdev SI mud	<0.01	187.0
Sqrt(%mudflat)	<0.01	112.9	Sqrt(%mudflat)	<0.01	68.6	Stdev Red emgrass	<0.01	187.0

Dependent variable:	***Number of size groups***		***Ln(number of birds)***			***Ln(number of tuber-feeding birds + 1)***	
Independent variable	R^2	AIC_c	***Independent variable***	R^2	AIC_c	***Independent variable***	R^2	AIC_c
Mudflat NDVI	0.15	145.7	Ln(area)	0.2	212.5	Mudflat NDVI	0.09	263.7
NDVI emgrass	0.09	149.0	Mudflat NDVI	0.13	216.8	Sqrt (%floodveg)	0.08	263.9
Ln(area)	0.08	149.7	%burnveg	0.06	220.8	Stdev SI emgrass	0.05	265.6
%human LU	0.07	150.0	Stdev SI emgrass	0.05	221.5	Ln(area)	0.04	266.4
Sqrt (%floodveg)	0.06	150.6	Stdev Red emgrass	0.04	221.7	Stdev Red mud	0.02	267.0
Stdev Red floodveg	0.02	152.8	NDVI emgrass	0.03	222.3	%burnveg	<0.01	267.9
Sqrt (%emgrass)	0.02	152.8	Stdev Red floodveg	0.02	222.8	Sqrt (%emgrass)	<0.01	268.1
Sqrt(%mudflat)	0.02	153.0	Sqrt (%floodveg)	0.02	223.1	Stdev Red emgrass	<0.01	268.1
%burnveg	0.02	153.1	Stdev Red mud	0.01	223.2	Sqrt(%mudflat)	<0.01	268.2
Stdev Red mud	<0.01	153.6	Sqrt (%emgrass)	0.01	223.2	NDVI emgrass	<0.01	268.2
Stdev SI emgrass	<0.01	153.9	%human LU	<0.01	223.7	Stdev Red floodveg	<0.01	268.2
Stdev Red emgrass	<0.01	153.9	Stdev SI mud	<0.01	223.8	%human LU	<0.01	268.3
Stdev SI mud	<0.01	153.9	Sqrt(%mudflat)	<0.01	223.8	Stdev SI mud	<0.01	268.3

Table 5. Multivariate regression models for waterbird diversity and abundance response variables within 2 units of AIC_c from the lowest-AIC_c OLS model. Bold font indicates AIC_c values upon which models were ranked for calculation of the Akaike weights for prediction of 2008 values in model verification.

Models	R^2 OLS	AIC_c OLS	AIC_c Error	AIC_c Lag	Akaike weight
Dependent variable: species richness					
Area - %floodveg + ndvi emgrass – ndvi mudflat	0.50	90.06	**89.47**	92.89	0.61
-%floodveg + ndvi emgrass – ndvi mudflat	0.46	91.27	**90.38**	93.82	0.39
Dependent variable: Shannon index					
-%floodveg + ndvi emgrass + stdev Red floodveg	0.37	52.75	**54.19**	55.29	0.36
Area - %floodveg + ndvi emgrass + stdev Red floodveg	0.40	**53.01***			0.64
Dependent variable: number of food guilds					
Area - %floodveg + ndvi emgrass	0.38	169.73	172.23	**170.45**	0.35
Area - %floodveg + ndvi emgrass – ndvi mudflat	0.41	**170.21***			0.4
Area - %floodveg + ndvi emgrass - %emgrass	0.41	170.29	172.96	**171.18**	0.25
Area - %floodveg + ndvi emgrass + %human LU	0.39	171.55	174.24	172.72	
Area - %floodveg + ndvi emgrass – stdev SI emgrass	0.39	171.73	174.42	172.54	
Dependent variable: number of size groups					
Area - %floodveg + ndvi emgrass	0.33	140.55*			0.25
Area - %floodveg + ndvi emgrass + %human LU	0.35	141.59*			0.15
Area - %floodveg + ndvi emgrass – ndvi mudflat	0.35	141.71*			0.14
Area - %floodveg + ndvi emgrass - %emgrass	0.35	141.72*			0.14
Area - %floodveg + ndvi emgrass - %burnveg	0.35	141.89*			0.13
Area - %floodveg + ndvi emgrass - %mudflat	0.34	142.41*			0.10
Area - %floodveg + ndvi emgrass + stdev Red floodveg	0.34	142.45*			0.10
Dependent variable: total number of birds					
Area + ndvi emgrass – ndvi mudflat – stdev SI emgrass	0.4	207.89	210.56	**209.62**	0.23
Area – ndvi mudflat – stdev SI emgrass	0.35	**209.19***			0.44
Area + ndvi emgrass – ndvi mudflat – stdev SI emgrass - % burnveg	0.41	209.26	211.59	211.47	
Area – ndvi mudflat – stdev SI emgrass - % burnveg	0.38	**209.83***			0.33
Area + ndvi emgrass – ndvi mudflat – stdev SI emgrass - %floodveg	0.41	209.84	212.63	211.55	
Dependent variable: number of tuber feeding birds					
Area - %floodveg	0.16	264.41	**265.17**	263.87	0.36
Area - %floodveg – stdev SI emgrass	0.19	264.79	**266.11**	264.56	0.22
-ndvi mudflat – stdev SI emgrass	0.14	265.19	**265.61**	264.54	0.28
Area - %floodveg - %burnveg	0.17	266.15	267.45	266.03	
Area – ndvi mudflat – stdev SI emgrass	0.17	266.19	**266.97**	265.51	0.14
-ndvi mudflat	0.09	266.25*			
%emgrass – ndvi mudflat – stdev SI emgrass	0.17	266.31*			
-%floodveg	0.08	266.39*			

*Spatial autocorrelation diagnostics not significant with p-value > 0.1.

Figures

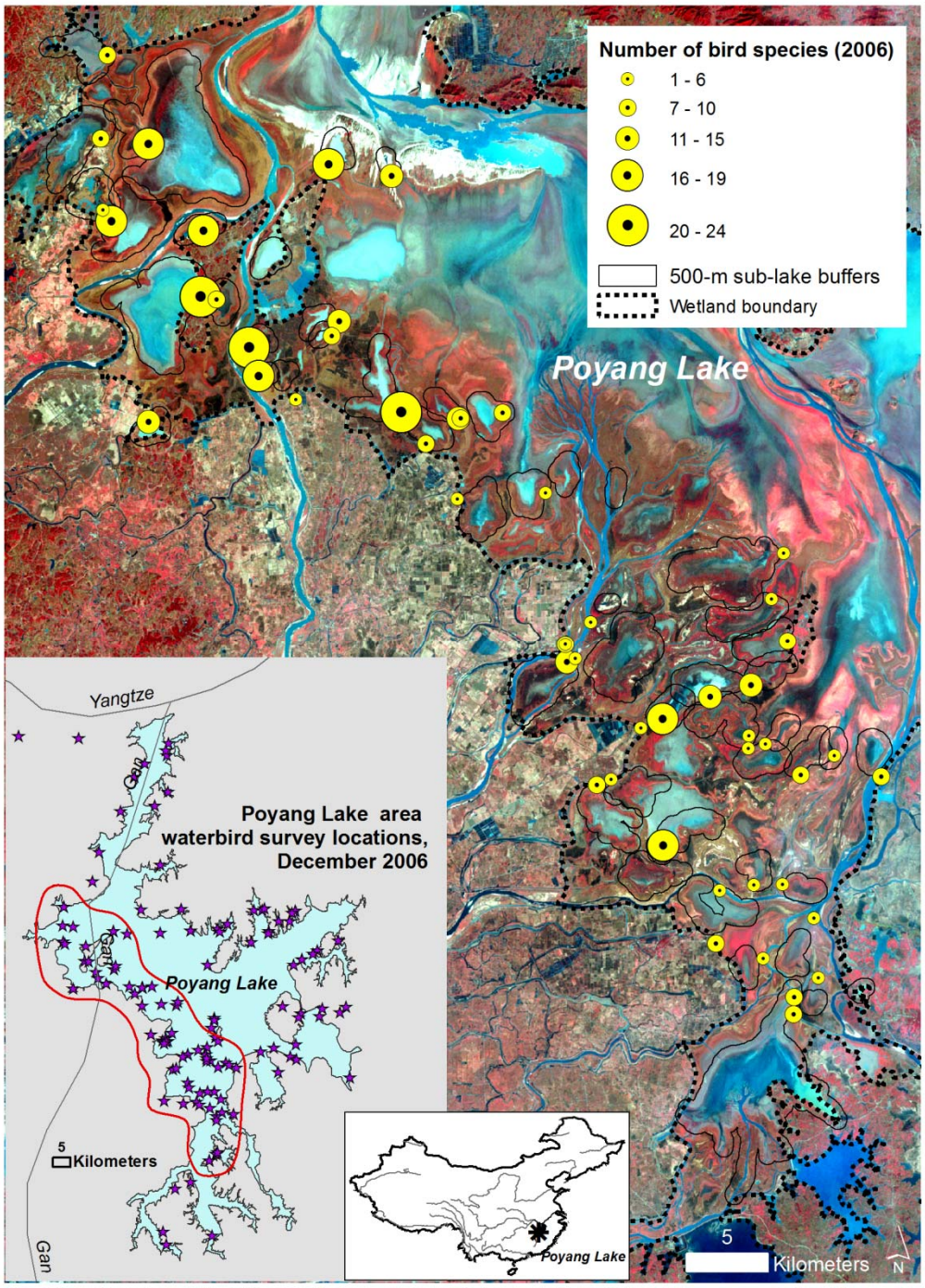

Figure 1. Study area and waterbird survey in December 2006.

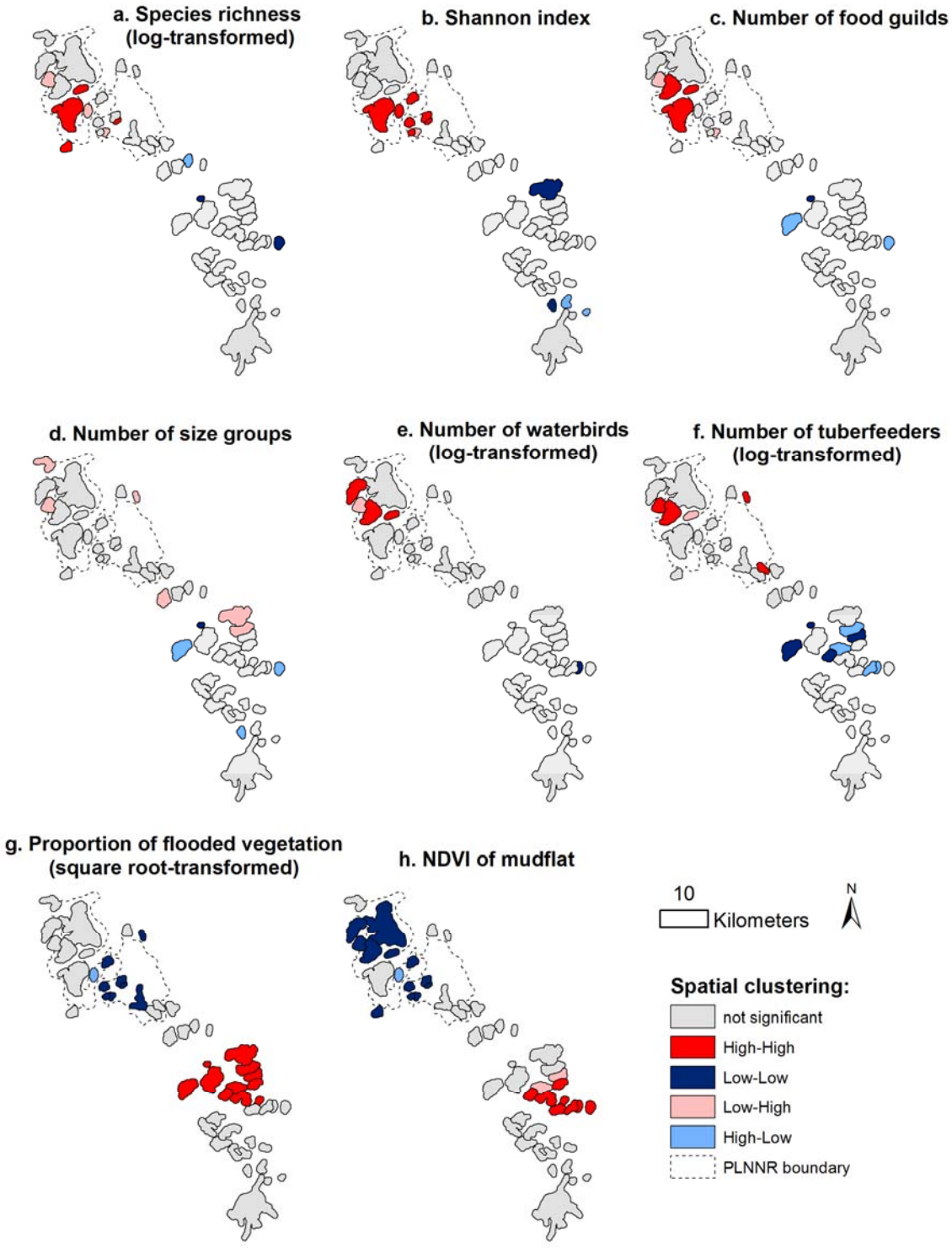

Figure 2. Sub-lake clusters of significant spatial dependence ($p<0.05$) determined using Local Indicators of Spatial Association (LISA). For positive spatial dependence, "High-High" indicates significant clustering of high values in each variable and "Low-Low" – significant clustering of low values. Negative spatial dependence is represented by "High-Low" and "Low-High" significant associations.

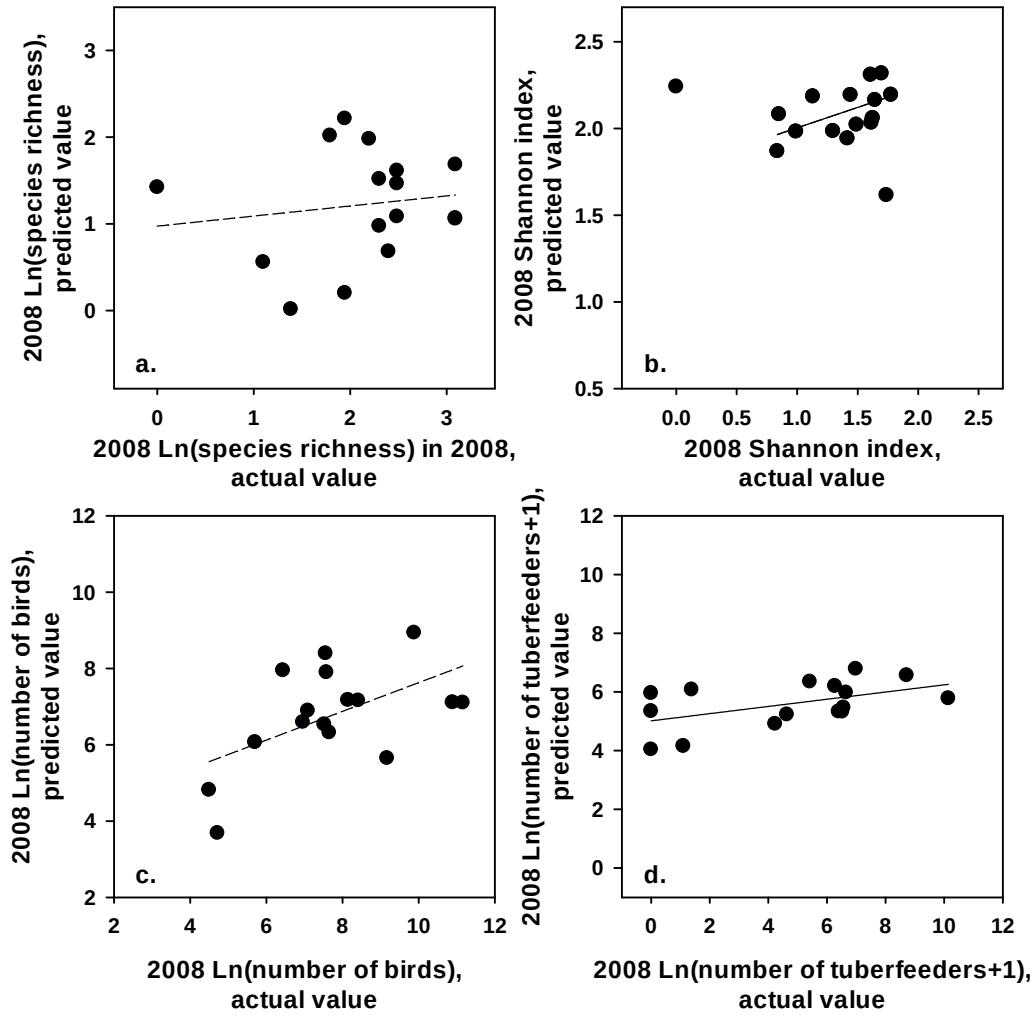

Figure 3. Comparison of the actual and predicted values of selected response variables in 2008 for 16 sub-lake units used in model assessment: a) species richness; b) Shannon index; c) total bird abundance; d) abundance of tuber-feeding birds.

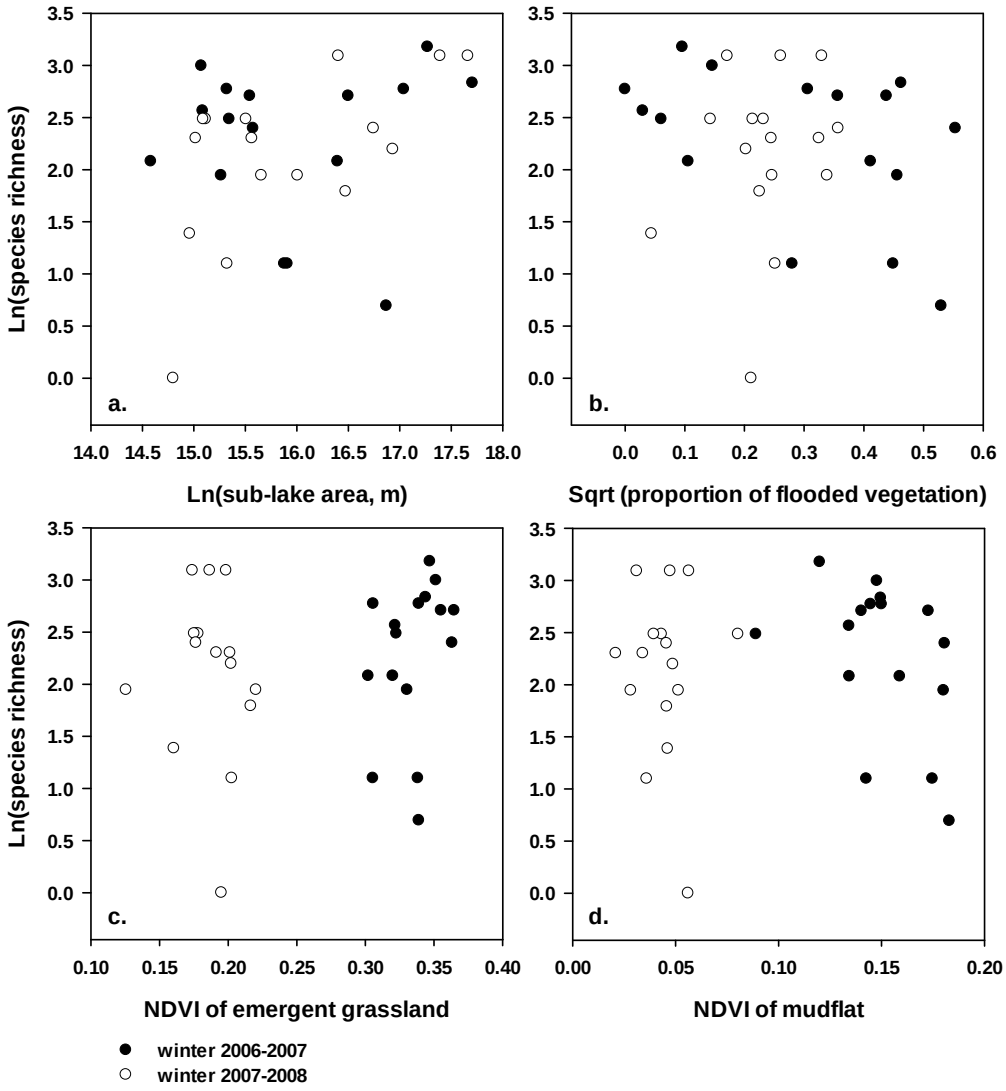

Figure 4. Comparison of the univariate relationships between log-transformed species richness and independent variables for 16 sub-lake units used in model assessment between 2006/2007 and 2008 datasets using a) log-transformed sub-lake and neighborhood area; b) square root-transformed proportion of flooded vegetation cover; c) average normalized difference vegetation index (NDVI) for mudflat and d) average NDVI for emergent grassland.

CHAPTER 5. Conclusions and future research directions

Summary of the key results from thesis chapters

In this dissertation, I investigated the capabilities of satellite remote sensing and novel object-based image analysis (OBIA) methodology to elucidate seasonal composition and dynamics of wetland ecosystems and indicators of habitat for wintering waterbirds in a large conservation hotspot of Poyang Lake, PR China. My results provide new insights about the role of spatial and temporal processes in shaping this unique wetland environment and offer innovative techniques applicable for multi-scale analysis of complex and dynamic landscapes across the globe. In this concluding section, I summarize the key findings from the four dissertation chapters and discuss the important directions for future research.

My first study (Chapter 1) investigated changes in major wetland cover types (water, vegetation, mudflat and sand) and their classification uncertainty during the Poyang Lake low water period from late fall 2007 to early spring 2008. I found that, while hydrological variation strongly affected transitions among classes, the overall dynamics of wetland surface reflected a more complex interplay of vegetation phenology, seasonal turnover of the dominant plant species, grazing disturbance and post-flood mudflat exposure. Signals of these different processes were more effectively highlighted by changes in fuzzy memberships to each class per location, than by changes in spatial extents of the highest-membership classes alone. Classification uncertainty varied by both image date and by cover type, generally decreasing from transitional post-flooding wetland state in November 2007 to early spring and being consistently the highest for dynamic and heterogeneous mudflat in all images. Vulnerability to flooding and high classification uncertainty makes mudflat habitats an important target for the future work. Tthe accuracy of Poyang Lake analyses in the low water season may be sensitive to the timing of available cloud-free remote sensing data. However, for spatially dynamic and heterogeneous cover types, classification uncertainty may not be fully resolved even with advanced machine-learning methods and customized algorithms. This shortcoming stimulated exploration of alternative methods for Poyang Lake change analysis (Chapter 3).

To more thoroughly investigate the benefits of OBIA for remote sensing-based wetland analysis, in Chapter 2 I examined sensitivity of Poyang Lake plant functional type (PFT) classification accuracy to the choice of image segmentation scale, machine-learning classification method and a more general versus more specific PFT class definition. Results suggested that OBIA may improve classification accuracy relative to pixel-based methods even for heterogeneous wetland vegetation and with medium-resolution Landsat imagery. Both the overall and class-specific accuracy values increased from close-to-pixel object scales to coarser levels, regardless of the classification algorithm, likely due to smoothing of the local heterogeneity and approximation of the vegetation patches by image objects. In contrast to general PFTs, specific classes differed in their highest-accuracy object scale values which calls for more research on drivers of their unique patch structure and disturbance agents. The 29-35% disagreement between the area of each general PFT and its respective subclasses further suggested that ecological classifications based on plant functional traits alone may not sufficiently capture spectral and spatial hierarchy among plant types on a landscape. Future research should test the benefits of integrating spectral and geometric properties of vegetation patches with functional ecological traits, similar to the recently proposed concept of the “optical” functional types (Ustin and Gamon 2010).

Analysis of change among wetland cover types in Chapter 1 highlighted the challenges on resolving classification uncertainty for Poyang lake mudflats and mixed transitional cover types regardless of the image date. In Chapter 3, I explored an alternative change analysis approach by classifying Poyang Lake wetland into "dynamic cover types" (DCTs) defined as sequences of common transitions observable in a given flood period. This analysis identified major steps in seasonal wetland change driven by flooding and vegetation phenology and spatial differences in change schedules across the large and heterogeneous study area. Comparison of DCTs from the actual flood period with a hypothetical quasi-experimental scenario of a warmer, wetter low water season revealed both a "hydrological" response with class shifts away from expanding permanent water bodies and more complex location-specific redistributions of vegetation types and mudflats. These outcomes imply that changes in flooding patterns may have non-uniform effects on different ecosystems and habitats and call for a thorough investigation of more specific hydrological and climatic change scenarios for this landscape. The possibility to disentangle short-term ecological "regimes" from longer-term landscape changes via DCT framework suggests a promising research strategy for landscape ecosystem modeling, conservation and ecosystem management. Extension of this approach to multi-year change assessments should carefully consider the limitations related to temporal frequency of remote sensing data, complementary characteristics of different sensors and the benefits of wireless in situ sensors to supply continuous reference information for areas with problematic access.

The analyses conducted in Chapters 1-3 revealed important characteristics of the Poyang Lake low water season which may affect suitability of wetland habitat for wintering birds. In the final Chapter 4, I investigated which landscape characteristics of the permanent sub-lakes extracted from the Landsat satellite image were most closely associated with spatial variation in waterbird diversity and abundance in the ground survey of December 2006. In the best-fit models selected using the Akaike Information Criterion, on average higher bird diversity and abundance were associated with larger sub-lake size, higher spectral greenness of emergent grassland and lower spectral greenness of mudflat as well as lower proportion of flooded/aquatic vegetation. At the same time, predictive performance of even the best-fit models was penalized by large amounts of unexplained variation and inconsistencies among bird survey and remote sensing data from another year. Significant spatial autocorrelation in most linear regression models raised concerns about missing predictor variables, the utility of sub-lakes as spatial units for sampling and modeling of bird diversity, but it also suggested the new hypotheses on potential spatial interactions in distributions of waterbird groups or their foraging resources among the sub-lakes. The key limitations of the study included one-time pan-lake bird survey event per winter season and the lack of comprehensive field data on important habitat variables such as water levels and vegetation composition. These challenges indicate that future bird monitoring programs should take more rigorous steps to standardize the protocols of bird surveys and collection of field- and remote sensing-based habitat variables in different years.

Needs for the future research and monitoring at Poyang Lake

The future of Poyang Lake wetland ecosystems and biodiversity is disturbingly uncertain due to the growing complexity of landscape change drivers and anthropogenic pressures in this region (Fang et al. 2006, Barzen et al. 2009, Harris and Hao 2010, Fox et al. 2011). The most urgent research needs are based on the potential near-future modification of Poyang Lake hydrological regimes by now operating Three Gorges dam upstream Yangtze River (Guo et al. 2012), planned local water control structures (Finlayson 2010, Harris and Hao 2010) and climate change.

Thorough analysis of the future wetland change scenarios would ideally require development of reliable and spatially explicit hydrological, ecosystem and habitat models. This, in turn, would require filling the important gaps in current data (e.g., construction of a seamless high-resolution bathymetry and digital elevation layer), systematic sampling of environmental variables over Poyang Lake basin and stronger collaboration among different domestic and international research groups. Results of my dissertation suggest several research directions to expand the understanding of Poyang Lake ecological environment and its response to change drivers.

One particularly important research venue concerns the insufficiently understood feedbacks between flooding and functional performance of wetland plants. My analysis and previous studies suggest that taxonomic and functional composition of Poyang Lake vegetation is strongly associated with landscape inundation status as well as with seasonal patterns of submersion per location (Wu and Ji 2002, Chen et al. 2007, Wang et al. 2012). Similarly, temporal variation in flood regimes may affect the interactions between wet C3 sedges and less flood-tolerant opportunistic C4 grasses currently restricted to wetland margins (Dronova et al. 2012). Assessing specific timing of phenological changes and flood-driven seasonal turnover of plant functional types would be extremely useful in modeling responses of ecosystem productivity, nutrient fluxes and greenhouse gas emissions to hydrological and climatic change (Keenan et al. 2012). Enhancing the understanding of flooding-vegetation feedbacks is also critical for monitoring and modeling bird habitat suitability and temporal variation in winter food resources that are shaped by ecosystem dynamics of the preceding growing season (Barzen et al. 2009).

A related key direction for the future work is the assessment of potential recent shifts in species composition of Poyang Lake aquatic and wetland vegetation communities. Considerable changes in dominant vegetation have been reported for a number of smaller lakes in the central Yangtze region over the last decade, including decline of tuber-producing warm-season aquatic macrophytes, replacement of historical dominants by previously less common species and eutrophication-induced shifts from macrophytes to algae (Fang et al. 2006, Xing et al. 2006, Fox et al. 2011). The known dominant plant types of Poyang Lake has been linked with important habitat and food for fish, invertebrates resident and migratory birds and forage for domestic livestock in local villages (Wu and Ji 2002, Wang et al. 2012). Changes in wetland plant communities may thus have far-reaching consequences not only for ecosystem function directly controlled by vegetation, but also for upper trophic levels and valuable ecosystem services to humans. Because many sub-lakes are hydrologically isolated for substantial part of the year, sampling efforts to assess vegetation shifts may need to be more spatially and temporally rigorous than in previous surveys (Zeng et al. 2007, Burnham et al. 2011, Wang et al. 2012).

In order to better understand habitat requirements and threats for the wintering waterbirds, more work is needed on investigating spatio-temporal patterns of habitat use by species and foraging guilds as well as on consolidating current bird survey programs and protocols. Limited data reporting and the lack of repeated pan-lake surveys per winter season contribute to the uncertainty in habitat modeling and constrain applicability of current records to robust projections of future bird population and habitat changes. Given persisting challenges of limited field access and logistical constraints to frequent surveys, future studies should continue exploring remote sensing-based indicators of bird habitat utilization and diversity. One strategy to enhance predictive capacity of landscape models would be to combine remote sensing proxies with field descriptors of habitat dynamics assessed prior to bird arrival (Burnham et al. 2011). In addition, future work should more thoroughly investigate ecological meaning of spatial

autocorrelation in distributions of birds and their habitat characteristics to better understand landscape connectivity and spatial interactions among hydrological sub-units. Improved understanding of the spatial linkages among waterbird communities and their suitable habitats is of critical importance for conservation management of the local protected areas, but this knowledge may be difficult to obtain by field surveys in this challenging wetland landscape.

These suggested directions for future work address immediate research needs elucidated by this thesis and other recent studies (e.g., Burnham 2007, Wu 2008, Barzen et al. 2009, Wang et al. 2012, Guo et al. 2012). On a more general note, comprehensive studies of Poyang Lake ecosystem mechanisms and dynamics continue to be hampered by insufficient data availability, the lack of consistent monitoring programs and limited coordination among parallel studies by different research groups. A potential solution to this problem could be the establishment of a unified information repository to facilitate data sharing and collaboration among contributing parties. Ideally, this effort should also incorporate a unified monitoring program coordinating both the bird surveys and field and remote sampling of ecosystem variables.

Because high cost and limited feasibility of frequent field surveys at Poyang Lake will remain a constraint in the near future, ecological monitoring and research should consider alternative strategies for systematic data collection. First, temporal frequency of ground observations may be enhanced by an integrated network of wireless sensors (Gong 2007, Burgess et al. 2010). To ensure basin-wide representation in these observations, installation and maintenance of wireless sensors could be coordinated among >20 current field ecological monitoring stations in this area. Second, an extremely useful monitoring effort would be an establishment of the regular airborne wetland survey program to maintain the continuity of seasonal remote sensing observations for periods of prolonged cloudiness when optical satellite data become useless. It is particularly important to provide the aerial survey opportunity for the warm summer growing season of aquatic vegetation which produces critical food resources for the migratory waterbirds later in the season (Burnham 2007, Barzen et al. 2009, Burnham et al. 2011). Repeated collection of airborne remote sensing data over Poyang Lake wetlands would provide invaluable source of information for diverse research initiatives in the region and would greatly facilitate continuous long-term projects by the local universities and environmental monitoring institutes.

Research needs for integration of the object-based remote sensing image analysis and landscape ecology

In this section I discuss several research directions for enhancing the utility of remote sensing in complex and dynamic landscapes such as the Poyang Lake study area. An especially important future task is to formalize the criteria of the "optimal" representation of heterogeneous landscape patches by image objects. In particular, more straightforward and flexible approaches are needed to determine image segmentation parameters which maximize the accuracy of patch boundary delineation and cover type identification across diverse classes simultaneously. Previous studies proposed semi-automated algorithms for pre-classification testing of segmentation outputs using either known object properties (Clinton et al. 2010a) or measures of local spectral variance sensitive to contrasts among patches (Dragut et al. 2010). These techniques have been successful for target objects of similar type and size, and future work should advance them to handle higher variability in object (patch) parameters among classes and provide greater flexibility for using multiple spectral bands and ancillary geospatial datasets in class delineation. For more reliable outcomes, it is also important to more closely integrate machine-based segmentation and

classification algorithms with ecological and biophysical optical properties of cover types derived from field measurements or high-resolution images (Ustin and Gamon 2010).

Another important future objective is to develop more standardized approaches for assessing propagation of classification uncertainty among different levels of hierarchical classifications. The OBIA framework is particularly useful for hierarchical landscape analyses where different layers of nested objects with matching boundaries can be easily generated to represent levels of landscape complexity (Burnett and Blaschke 2003, Tuxen and Kelly 2008, Kim et al. 2011, Ouyang et al. 2011). However, the caveats associated with propagation of classification error among hierarchical levels (Townsend and Walsh 2001) or mismatches between the MAPPED class hierarchy and the actual patch structure have not been yet explicitly discussed in OBIA applications. Mismatches among general and specific plant functional type maps in Chapter 2 suggested that the overall classification error would accumulate if the output class boundaries from one hierarchical level were used to constrain class assignment for another level. However, nested spatial structure of different-level patches and the uncertainty assessment framework developed in Chapter 1 can be useful for spatially explicit quantitative assessments of changes in error among class levels. At the same time, it is important to recognize the informative value of classification error to suggest follow-up questions and hypotheses for future research and to guide the choice of spatial resolution, object scale and quality of training/test samples.

An interesting and important direction for the future work is extension of the dynamic cover type framework to address long-term ecosystem change. The first step towards this goal should be a thorough assessment of the intrinsic "reference" variation of dynamic classes (Zhong et al. 2011) that needs to be disentangled from long-term directional change trajectories. It is also necessary to examine what minimum temporal frequency of remote sensing data is required to reliably represent transition types for given landscape and research objectives (Lobell and Asner 2004, Crews 2008, Ozdogan 2010, Zhong et al. 2011). On the one hand, precise timing of transitions is important for understanding ecosystem response to climate change (Keenan et al. 2012), but on the other hand, excessive data frequency may result in noise and class confusion (McCleary et al. 2008, Zhong et al. 2011). Given limited availability of cloud-free imagery in humid regions such as Poyang Lake study area, future studies should consider novel wide-swath microsatellites such as the Surrey constellation (http://www.sstl.co.uk/) and DEIMOS-1 (http://www.deimos-imaging.com) providing both frequent revisit and medium spatial resolution, as well as fusion of multi-spectral imagery with complementary benefits of radar instruments.

Obtaining sufficient representative training and validation DCT samples will be a challenge for most landscapes because frequent field surveys are often costly even for accessible sites. Alternatively, *in situ* wireless sensor technology can be used to collect both environmental variables (e.g., temperature, water levels) and temporally frequent images of the sample sites (Gong 2007, Burgess et al. 2010). Wireless sensor technology has been useful for continuous observations of vegetation phenology in diverse biomes and detection of precise timing of change events (Richardson et al. 2009, Sonnentag et al. 2012), and hence could greatly facilitate DCT analyses across large and inaccessible wetland areas.

Finally, future work should adapt the DCT framework to identify "novel" change types which may occur due to short-term disturbance, unprecedented shifts in climate and hydrology, human management and restoration activities, or alien species invasions. Unsupervised image classification approaches and multi-temporal independent components analysis (Ozdogan 2010,

Zhong et al. 2011) can be applied to detect considerable deviations from known transitions suggesting previously unknown dynamics. Developing diagnostics of the novel change types for the long-term DCT analysis would be extremely useful for early detection of vulnerable and non-resilient ecosystem states, signatures of undocumented disturbance, starting points of invasions or insect/disease outbreaks and novel types of communities adapting to shifting environment. The important benefit of DCTs is the possibility to generalize and compare change signatures among different locations, which may offer significant future shortcuts for rapid change assessments under shifting climate and cascade effects in ecosystem states across wide regions.

LITERATURE CITED

Addink, E.A., de Jong, S.M., & Pebesma, E.J. (2007). The importance of scale in object-based mapping of vegetation parameters with hyperspectral imagery. *Photogrammetric Engineering and Remote Sensing, 73*, 905-912

An, S.Q., Li, H.B., Guan, B.H., Zhou, C.F., Wang, Z.S., Deng, Z.F., Zhi, Y.B., Liu, Y.H., Xu, C., Fang, S.B., Jiang, J.H., & Li, H.L. (2007). China's natural wetlands: Past problems, current status, and future challenges. *Ambio, 36*, 335-342

Andreoli, R., Yesou, H., Li, J., Desnos, Y.L., Shifeng, H., & De Fraipont, P. (2007). Poyang Hu (Jiangxi Province, P.R. of China) area variations between January 2004 and June 2006 using ENVISAT low and medium resolution time series. *Geographic Information Sciences 13,* 24-35

Anselin, L. (1988). Lagrange Multiplier Test Diagnostics for Spatial Dependence and Spatial Heterogeneity. *Geographical Analysis, 20*, 1-17

Anselin, L. (1995). Local Indicators of Spatial Association - LISA. *Geographical Analysis, 27*, 93-115

Anselin, L., Bera, A.K., Florax, R., & Yoon, M.J. (1996). Simple diagnostic tests for spatial dependence. *Regional Science and Urban Economics, 26*, 77-104

Anselin, L., Syabri, I., & Kho, Y. (2006). GeoDa: An introduction to spatial data analysis. *Geographical Analysis, 38*, 5-22

Arbiol, R., Zhang, Y., & Palá, V. (2006). Advanced classification techniques: a review. ISPRS Commission VII Mid-term Symposium "From Pixel to Processes"', Enschede, NL, 8-11 May 2006

Artigas, F.J., & Yang, J.S. (2005). Hyperspectral remote sensing of marsh species and plant vigour gradient in the New Jersey Meadowlands. *International Journal of Remote Sensing, 26*, 5209-5220

Assendorp, D. (2010). Classification of pattern and process in small-scale dynamic ecosystems; with cases in the Dutch coastal dunes. PhD Dissertation, University of Amsterdam, the Netherlands, 172 pp.

Baatz, M., & Schäpe, M. (2000). Multiresolution segmentation – An optimization approach for high-quality multi-scale image segmentation. IN: Strobl, J., Blaschke, T., Griesebner, G. (Eds.), Angewandte Geographische Informations-Verarbeitung XII. Wichmann Verlag, Karlsruhe, pp.12-23.

Bacaro, G., Santi, E., Rocchini, D., Pezzo, F., Puglisi, L., & Chiarucci, A. (2011). Geostatistical modelling of regional bird species richness: exploring environmental proxies for conservation purpose. *Biodiversity and Conservation, 20*, 1677-1694

Baker, C., Lawrence, R., Montague, C., & Patten, D. (2006). Mapping wetlands and riparian areas using Landsat ETM+ imagery and decision-tree-based models. *Wetlands, 26*, 465-474

Baret, F., & Guyot, G. (1991). Potentials and limits of vegetation indexes for LAI and aPAR assessment. *Remote Sensing of Environment, 35*, 161-173

Bartlett, M.K., Ollinger, S.V., Hollinger, D.Y., Wicklein, H.F., & Richardson, A.D. (2011). Canopy-scale relationships between foliar nitrogen and albedo are not observed in leaf reflectance and transmittance within temperate deciduous tree species. *Botany-Botanique, 89*, 491-497

Barzen, J. (2008). Phase 1 Report: How development projects may impact wintering waterbirds at Poyang Lake. Unpublished report submitted to Hydro-ecology Institute of the Yangtze Water Resources Commission. International Crane Foundation, Baraboo, Wisconsin, USA. 14 pp. http://www.savingcranes.org/images/stories/Phase%201%20Report_English.pdf

Barzen, J., Engels, M., Burnham, J., Harris, J., & G. Wu. (2009). Phase 2 Report: Potential impacts of a water control structure on the abundance and distribution of wintering waterbirds at Poyang Lake. Unpublished report submitted to Hydro-ecology Institute of the Yangtze Water Resources Commission. International Crane Foundation, Baraboo.Wisconsin, USA. 54 pp.
http://www.savingcranes.org/images/stories/pdf/conservation/Phase%202%20Report_English.pdf
Benz, U.C., Hofmann, P., Willhauck, G., Lingenfelder, I., & Heynen, M. (2004). Multi-resolution, object-oriented fuzzy analysis of remote sensing data for GIS-ready information. *ISPRS Journal of Photogrammetry and Remote Sensing, 58*, 239-258
Berberoglu, S., Yilmaz, K.T., & Ozkan, C. (2004). Mapping and monitoring of coastal wetlands of Cukurova Delta in the Eastern Mediterranean region. *Biodiversity and Conservation, 13*, 615-633
Bergen, K.M., Goetz, S.J., Dubayah, R.O., Henebry, G.M., Hunsaker, C.T., Imhoff, M.L., Nelson, R.F., Parker, G.G., & Radeloff, V.C. (2009). Remote sensing of vegetation 3-D structure for biodiversity and habitat: Review and implications for lidar and radar spaceborne missions. *Journal of Geophysical Research-Biogeosciences,* G00E06, doi:10.1029/2008JG000883
Bino, G., Levin, N., Darawshi, S., Van Der Hal, N., Reich-Solomon, A., & Kark, S. (2008). Accurate prediction of bird species richness patterns in an urban environment using Landsat-derived NDVI and spectral unmixing. *International Journal of Remote Sensing, 29*, 3675-3700
Blaschke, T. (2010). Object based image analysis for remote sensing. *ISPRS International Journal of Photogrammetry and Remote Sensing 65*, 2-16
Blaschke, T., Lang, S., Lorup, E., Strobl, J., & Zeil, P. (2000). Object-oriented image processing in an integrated GIS/remote sensing environment and perspectives for environmental applications. In: A. Cremers, & K. Greve (Eds.), *Environmental Information for Planning, Politics and the Public* (Vol. 2 pp. 555-570). Marburg: Metropolis.
Bonan, G., Levis, S., Kergoat, L., & Oleson, K. (2002). Landscapes as patches of plant functional types: An integrating concept for climate and ecosystem models. *Global Biogeochemical Cycles, 16*, 1021
Borsotti, M., Campadelli, P., & Schettini, R. (1998). Quantitative evaluation of color image segmentation results. *Pattern Recognition Letters, 19*, 741-747
Bunting, P., & Lucas, R. (2006). The delineation of tree crowns in Australian mixed species forests using hyperspectral Compact Airborne Spectrographic Imager (CASI) data. *Remote Sensing of Environment, 101*, 230-248
Burgess, S.S.O., Kranz, M.L., Turner, N.E., Cardell-Oliver, R., & Dawson, T.E. (2010). Harnessing wireless sensor technologies to advance forest ecology and agricultural research. *Agricultural and Forest Meteorology, 150*, 30-37
Burnett, C., & Blaschke, T. (2003). A multi-scale segmentation/object relationship modelling methodology for landscape analysis. *Ecological Modelling, 168*, 233-249
Burnham, J. W. (2007). Environmental drivers of Siberian crane (*Grus leucogeranus*) habitat selection and wetland management and conservation in China. Madison, University of Wisconsin: 108 pp.
Burnham, J., Barzen, J., Li, F., & Zeng N. (2011). Long Term Ecological Monitoring and its Application at Poyang Lake, People's Republic of China. In: Prentice C. (Editor). Conservation of Flyway Wetlands in East and West/Central Asia. Proceedings of the Project

Completion Workshop of the UNEP/GEF Siberian Crane Wetland Project, 14-15 October 2009, Harbin, China. Baraboo (Wisconsin), USA: International Crane Foundation.
Burnham, K.P., & Anderson, D.R. (2002). Model selection and multimodel inference: a practical information-theoretic approach. New York: Springer. 488 pp.
Canepuccia, A.D., Isacch, J.P., Gagliardini, D.A., Escalante, A.H., & Iribarne, O.O. (2007). Waterbird response to changes in habitat area and diversity generated by rainfall in a SW Atlantic coastal lagoon. *Waterbirds, 30*, 541-553
Cao, L., Zhang, Y., Barter, M., & Lei, G. (2010). *Anatidae* in eastern China during the non-breeding season: Geographical distributions and protection status. *Biological Conservation, 143*, 650-659
Cao, M.K., & Woodward, F.I. (1998). Dynamic responses of terrestrial ecosystem carbon cycling to global climate change. *Nature, 393*, 249-252
Caruana, R. & Niculescu-Mizil, A. (2006). An empirical comparison of supervised learning algorithms. In Proceedings of the 23rd International Conference on Machine Learning. Vol. 148 of ACM International Conference Proceeding Series. Pittsburgh, Pennsylvania, pp. 161–168
Castaneda, C., & Ducrot, D. (2009). Land cover mapping of wetland areas in an agricultural landscape using SAR and Landsat imagery. *Journal of Environmental Management, 90*, 2270-2277
Cerezo, A., Conde, M.C., & Poggio, S.L. (2011). Pasture area and landscape heterogeneity are key determinants of bird diversity in intensively managed farmland. *Biodiversity and Conservation, 20*, 2649-2667
Chabrier, S., Emile, B., Rosenberger, C., & Laurent, H. (2006). Unsupervised performance evaluation of image segmentation. *EURASIP Journal on Applied Signal Processing*, *2006,* 1-12
Chambers, J.Q., Asner, G.P., Morton, D.C., Anderson, L.O., Saatch, S.S., Espirito-Santo, F.D.B., Palace, M., & Souza, C. (2007). Regional ecosystem structure and function: ecological insights from remote sensing of tropical forests. *Trends in Ecology & Evolution, 22*, 414-423
Chen, H.G., & Lin, D.D. (2004). The prevalence and control of schistosomiasis in Poyang Lake region, China. *Parasitology International, 53*, 115-125
Chen, S., Su., X., Fang, L., & Chen, L. (2007). *Carex* dynamics as an Environmental Indicator in the Poyang Lake Wetland Area: Remote Sensing Mapping and GIS Analysis. *Geographic Information Sciences, 13*, 44-50
Chubey, M.S., Franklin, S.E., & Wulder, M.A. (2006). Object-based analysis of Ikonos-2 imagery for extraction of forest inventory parameters. *Photogrammetric Engineering and Remote Sensing, 72*, 383-394
Clinton, N., Holt, A., Scarborough, J., Yan, L., & Gong, P. (2010a). Accuracy Assessment Measures for Object-based Image Segmentation Goodness. *Photogrammetric Engineering and Remote Sensing, 76*, 289-299
Clinton, N.E., Potter, C., Crabtree, B., Genovese, V., Gross, P., & Gong, P. (2010b). Remote Sensing-Based Time-Series Analysis of Cheatgrass (Bromus tectorum L.) Phenology. *Journal of Environmental Quality, 39*, 955-963
Collins, J.B., & Woodcock, C.E. (1996). An assessment of several linear change detection techniques for mapping forest mortality using multitemporal landsat TM data. *Remote Sensing of Environment, 56*, 66-77

Conchedda, G., Durieux, L., & Mayaux, P. (2008). An object-based method for mapping and change analysis in mangrove ecosystems. *ISPRS Journal of Photogrammetry and Remote Sensing, 63*, 578-589

Cook, C. D. K. (1996). Aquatic plant book. SPB Academic Publishing, Amsterdam. 228 pp.

Coops, N.C., Wulder, M.A., & Iwanicka, D. (2009a). Exploring the relative importance of satellite-derived descriptors of production, topography and land cover for predicting breeding bird species richness over Ontario, Canada. *Remote Sensing of Environment, 113*, 668-679

Coops, N.C., Wulder, M.A., & Iwanicka, D. (2009b). Large area monitoring with a MODIS-based Disturbance Index (DI) sensitive to annual and seasonal variations. *Remote Sensing of Environment, 113*, 1250-1261

Coppin, P., Jonckheere, I., Nackaerts, K., Muys, B., & Lambin, E. (2004). Digital change detection methods in ecosystem monitoring: a review. *International Journal of Remote Sensing, 25*, 1565-1596

Coppin, P., Nackaerts, K., Queen, L., & Brewer, H. (2001). Operational monitoring of green biomass change for forest management. *Photogrammetric Engineering and Remote Sensing, 67*, 603-611

Crews, K.A. (2008). "Landscape dynamism: disentangling thematic versus structural change in northeast Thailand", pp.99-118, in R. J. Aspinall and M. J. Hill (Eds) Land use change: science, policy and management, CRC Press, New York, 250 pp.

Crist, E.P., & Cicone, R.C. (1984). A Physically-Based Transformation of Thematic Mapper Data - the Tm Tasseled Cap. *IEEE Transactions on Geoscience and Remote Sensing, 22*, 256-263

Davidson, A., & Csillag, F. (2003). A comparison of three approaches for predicting C4 species cover of northern mixed grass prairie. *Remote Sensing of Environment, 86*, 70-82

Davranche, A., Lefebvre, G., & Poulin, B. (2010). Wetland monitoring using classification trees and SPOT-5 seasonal time series. *Remote Sensing of Environment, 114*, 552-562

de Boer, W.F., Cao, L., Barter, M., Wang, X., Sun, M.M., van Oeveren, H., de Leeuw, J., Barzen, J., & Prins, H.H.T. (2011). Comparing the Community Composition of European and Eastern Chinese Waterbirds and the Influence of Human Factors on the China Waterbird Community. *Ambio, 40*, 68-77

De Chant, T., & Kelly, M. (2009). Individual Object Change Detection for Monitoring the Impact of a Forest Pathogen on a Hardwood Forest. *Photogrammetric Engineering and Remote Sensing, 75*, 1005-1013

de Leeuw, J., Si, Y., Zeng, Y.D., Lei, G., Li, L., & Liu, Y. (2006). Mapping flood recessional grasslands used by overwintering geese: a multi-temporal remote sensing application. ISPRS Mid-Term Symposium Remote Sensing, Enschede, the Netherlands.

DeFries, R.S., Field, C.B., Fung, I., Justice, C.O., Los, S., Matson, P.A., Matthews, E., Mooney, H.A., et al. (1995). Mapping the Land-Surface for Global Atmosphere-Biosphere Models - toward Continuous Distributions of Vegetations Functional-Properties. *Journal of Geophysical Research-Atmospheres, 100*, 20867-20882

Desclee, B., Bogaert, P., & Defourny, P. (2006). Forest change detection by statistical object-based method. *Remote Sensing of Environment, 102*, 1-11

Ding, W.X., Cai, Z.C., & Tsuruta, H. (2005). Plant species effects on methane emissions from freshwater marshes. *Atmospheric Environment, 39,* 3199–3207

Dobrowski, S.Z., Safford, H.D., Cheng, Y.B., & Ustin, S.L. (2008). Mapping mountain

vegetation using species distribution modeling, image-based texture analysis, and object-based classification. *Applied Vegetation Science, 11*, 499-508

Dormann, C.F., McPherson, J.M., Araujo, M.B., Bivand, R., Bolliger, J., Carl, G et al. (2007). Methods to account for spatial autocorrelation in the analysis of species distributional data: a review. *Ecography, 30*, 609-628

Dorren, L.K.A., Maier, B., & Seijmonsbergen, A.C. (2003). Improved Landsat-based forest mapping in steep mountainous terrain using object-based classification. *Forest Ecology and Management, 183*, 31-46

Dragut, L., Tiede, D., & Levick, S. (2010). ESP: a tool to estimate scale parameters for multiresolution image segmentation of remotely sensed data. *International Journal of Geographical Information Science*, *24*, 859-871

Dronova, I., Gong, P., & Wang, L. (2011). Object-based analysis and change detection of major wetland cover types and their classification uncertainty during the low water period at Poyang Lake, China. *Remote Sensing of Environment, 115*, 3220-3236

Dronova, I., Gong, P., Clinton, N., Wang, L., Fu, W., Qi, S., & Liu, Y. (2012). Landscape analysis of wetland plant functional types: the effects of image segmentation scale, vegetation classes and classification methods. *Remote Sensing of Environment, 127*, 357-369

Dronova, I., Zhong, L., & Gong, P. Characterizing surface change types in a large inundated wetland using independent components analysis. In preparation for submission.

Duckworth, J.C., Kent, M., & Ramsay, P.M. (2000). Plant functional types: an alternative to taxonomic plant community description in biogeography? *Progress in Physical Geography, 24*, 515-542

Dudgeon, D., Arthington, A.H., Gessner, M.O., Kawabata, Z.I., Knowler, D.J., Leveque, C., Naiman, R.J., Prieur-Richard, A.H., Soto, D., Stiassny, M.L.J., & Sullivan, C.A. (2006). Freshwater biodiversity: importance, threats, status and conservation challenges. *Biological Reviews, 81*, 163-182

Eastman, J.R., & Fulk, M. (1993). Long Sequence Time-Series Evaluation Using Standardized Principal Components (Reprinted from Photogrammetric Engineering and Remote-Sensing , Vol 59, Pg 991-996, 1993). *Photogrammetric Engineering and Remote Sensing, 59*, 1307-1312

ECognition Developer 8 Reference Book. (2009). 276 pp.

Fairbairn, S.E., & Dinsmore, J.J. (2001). Local and landscape-level influences on wetland bird communities of the prairie pothole region of Iowa, USA. *Wetlands, 21*, 41-47

Fang, J., Wang, Z.H., Zhao, S.Q., Li, Y.K., Tang, Z.Y., Yu, D., Ni, L.Y., Liu, H.Z., Xie, P., Da, L.J., Li, Z.Q., & Zheng, C.Y. (2006). Biodiversity changes in the lakes of the Central Yangtze. *Frontiers in Ecology and the Environment, 4*, 369-377

Feng, L., Hu, C.M., Chen, X.L., Cai, X.B., Tian, L.Q., & Gan, W.X. (2012). Assessment of inundation changes of Poyang Lake using MODIS observations between 2000 and 2010. *Remote Sensing of Environment, 121*, 80-92

Finlayson, M., Harris, J., McCartney, M., Young, L., & Chen, Zh. (2010). Report on Ramsar visit to Poyang Lake Ramsar site, P.R. China 12-17 April 2010. Report prepared on behalf of the Secretariat of the Ramsar Convention. 34 pp. http://www.ramsar.org/pdf/Poyang_lake_report_v8.pdf Accessed on 09/30/2010.

Foley, J.A., DeFries, R., Asner, G.P., Barford, C., Bonan, G., Carpenter, S.R., Chapin, F.S., et al. (2005). Global consequences of land use. *Science, 309*, 570-574

Fox, A.D., Cao, L., Zhang, Y., Barter, M., Zhao, M.J., Meng, F.J., & Wang, S.L. (2011).

Declines in the tuber-feeding waterbird guild at Shengjin Lake National Nature Reserve, China - a barometer of submerged macrophyte collapse. *Aquatic Conservation-Marine and Freshwater Ecosystems, 21*, 82-91

Friend, A.D., Arneth, A., Kiang, N.Y., Lomas, M., Ogee, J., Rodenbeckk, C., Running, S.W., Santaren, J.D., Sitch, S., Viovy, N., Woodward, F.I., & Zaehle, S. (2007). FLUXNET and modelling the global carbon cycle. *Global Change Biology, 13*, 610-633

Fung, T., Wong, F.K., Leung, Y. & Dai, M. (2009). Mangrove species mapping using Quickbird Image in the Maipo Ramsar Site, Hong Kong. Paper presented at the Annual Meeting of the Association of American Geographers

Gibbs, J.P. (2000). Wetland loss and biodiversity conservation. *Conservation Biology, 14*, 314-317

Gilmore, M.S., Wilson, E.H., Barrett, N., Civco, D.L., Prisloe, S., Hurd, J.D., & Chadwick, C. (2008). Integrating multi-temporal spectral and structural information to map wetland vegetation in a lower Connecticut River tidal marsh. *Remote Sensing of Environment, 112*, 4048-4060

Gitay H. & Noble, I. R. (1997). What are functional types and how should we seek them? In 'Plant functional types: their relevance to ecosystem properties and global change'. (Eds T. M. Smith, H. H. Shugart, F. I. Woodward) pp. 3-19 (Cambridge University Press, Cambridge)

Goetz, S., Steinberg, D., Dubayah, R., & Blair, B. (2007). Laser remote sensing of canopy habitat heterogeneity as a predictor of bird species richness in an eastern temperate forest, USA. *Remote Sensing of Environment, 108*, 254-263

Gong P. (2007). Wireless sensor network as a new ground remote sensing technology for environmental monitoring. *Journal of Remote Sensing, 11,* 545-551

Gong, P., Niu, Z.G., Cheng, X.A., Zhao, K.Y., Zhou, D.M., Guo, J.H., Liang, L., et al. (2010). China's wetland change (1990-2000) determined by remote sensing. *Science China-Earth Sciences, 53*, 1036-1042

Gong, Z.M., Wen, C.Y., & Mital, D.P. (1996). Decentralized robust controller design for a class of interconnected uncertain systems: With unknown bound of uncertainty. *IEEE Transactions on Automatic Control, 41*, 850-854

Gopal, S., & Woodcock, C.E. (1994). Theory and methods for accuracy assessment of thematic maps using fuzzy sets. *Photogrammetric Engineering and Remote Sensing 60,* 181–188

Grenier, M., Demers, A.M., Labrecque, S., Benoit, M., Fournier, R.A., & Drolet, B. (2007). An object-based method to map wetland using RADARSAT-1 and Landsat ETM images: test case on two sites in Quebec, Canada. *Canadian Journal of Remote Sensing, 33*, S28-S45

Grimm, N.B., Foster, D., Groffman, P., Grove, J.M., Hopkinson, C.S., Nadelhoffer, K.J., Pataki, D.E., & Peters, D.P.C. (2008). The changing landscape: ecosystem responses to urbanization and pollution across climatic and societal gradients. *Frontiers in Ecology and the Environment, 6*, 264-272

Guglielmini, A.C., & Satorre, E.H. (2004). The effect of non-inversion tillage and light availability on dispersal and spatial growth of Cynodon dactylon. *Weed Research, 44*, 366-374

Guan, Y., Lin, W., Zhou, F. & Zeng, N. (2008). Monitoring dynamics of grassland vegetation in Poyang Lake National Nature Reserve, using MODIS imagery. *The International Archives of the Photogrammetry, Remote Sensing and Spatial Information Sciences, Beijing, 37 (B8),* 1337-1342

Guo, H., Hu, Q., Zhang, Q., & Feng, S. (2012). Effects of the Three Gorges Dam on Yangtze

River flow and river interaction with Poyang Lake, China: 2003-2008. *Journal of Hydrology, 416*, 19-27
Hajek, F. (2008). Process-based approach to automated classification of forest structures using medium format digital aerial photos and ancillary GIS information. *European Journal of Forest Research, 127*, 115-124
Hall, M., Frank, E., Holmes, G., Pfahringer, B., Reutemann, P, & Witten, I.H. (2009). The WEKA Data Mining Software: An Update; SIGKDD Explorations, Vol.11, Iss.1.
Hame, T., Heiler, I., & San Miguel-Ayanz, J. (1998). An unsupervised change detection and recognition system for forestry. *International Journal of Remote Sensing, 19*, 1079-1099
Han, M., Cheng, L., & Meng, H. (2003). Application of four-layer neural network on information extraction. *Neural Networks, 16*, 547-553
Haralick, R.M., Shanmugam, K., Dinstein, I., 1973. Textural features for image classification. *IEEE Transactions on Systems, Man and Cybernetics, 3,* 610–621
Harris, J. & Z. Hao. (2010). An Ecosystem Approach to Resolving Conflicts Among Ecological and Economic Priorities for Poyang Lake Wetlands. Unpublished report. IUCN, Gland, Switzerland. http://cmsdata.iucn.org/downloads/iucn_poyang_report_august_2010_final.pdf
Hawkins, B.A. (2004). Summer vegetation, deglaciation and the anomalous bird diversity gradient in eastern North America. *Global Ecology and Biogeography, 13*, 321-325
Hess, L.L., Melack, J.M., Novo, E.M.L.M., Barbosa, C.C.F., & Gastil, M. (2003). Dual-season mapping of wetland inundation and vegetation for the central Amazon basin. *Remote Sensing of Environment, 87*, 404-428
Hestir, E.L., Khanna, S., Andrew, M.E., Santos, M.J., Viers, J.H., Greenberg, J.A., Rajapakse, S.S., & Ustin, S.L. (2008). Identification of invasive vegetation using hyperspectral remote sensing in the California Delta ecosystem. *Remote Sensing of Environment, 112*, 4034-4047
Heyman, O., Gaston, G.G., Kimerling, A.J., & Campbell, J.T. (2003). A per-segment approach to improving aspen mapping from high-resolution remote sensing imagery. *Journal of Forestry, 101*, 29-33.
Hilker, T., Coops, N.C., Wulder, M.A., Black, T.A., & Guy, R.D. (2008). The use of remote sensing in light use efficiency based models of gross primary production: A review of current status and future requirements. *Science of the Total Environment, 404*, 411-423
Hoeting, J.A., Davis, R.A., Merton, A.A., & Thompson, S.E. (2006). Model selection for geostatistical models. *Ecological Applications, 16*, 87-98
Horowitz, M. (1972). Spatial growth of *Cynodon dactylon* (L) Pers. *Weed Research, 12*, 373-383
Houlahan, J.E., Keddy, P.A., Makkay, K., & Findlay, C.S. (2006). The effects of adjacent land use on wetland species richness and community composition. *Wetlands, 26*, 79-96
Hu, Q., Feng, S., Guo, H., Chen, G.Y., & Jiang, T. (2007). Interactions of the Yangtze River flow and hydrologic processes of the Poyang Lake, China. *Journal of Hydrology, 347,* 90–100
Hui, F.M., Xu, B., Huang, H.B., Yu, Q., & Gong, P. (2008). Modelling spatial-temporal change of Poyang Lake using multitemporal Landsat imagery. *International Journal of Remote Sensing, 29*, 5767-5784
Hurlbert, A.H., & Haskell, J.P. (2003). The effect of energy and seasonality on avian species richness and community composition. *American Naturalist, 161*, 83-97
IUCN. (2012). *The IUCN Red List of Threatened Species. Version 2012.2*. http://www.iucnredlist.org Accessed on 17 October 2012.
Ji, W., Zeng, N., Wang, Y., Gong, P., Bing, X., & Bao, S. (2007). Analysis on the Waterbirds Community Survey of Poyang Lake in Winter. *Geographic Information Sciences, 13,* 51-64

Jiang, L.G., Bergen, K.M., Brown, D.G., Zhao, T.T., Tian, Q., & Qi, S.H. (2008). Land-cover change and vulnerability to flooding near Poyang Lake, Jiangxi Province, China. *Photogrammetric Engineering and Remote Sensing, 74*, 775-786

Jobin, B., Labrecque, S., Grenier, M., & Falardeau, G. (2008). Object-based classification as an alternative approach to the traditional pixel-based classification to identify potential habitat of the grasshopper sparrow. *Environmental Management, 41*, 20-31

Johansen, K., Coops, N.C., Gergel, S.E., & Stange, Y. (2007). Application of high spatial resolution satellite imagery for riparian and forest ecosystem classification. *Remote Sensing of Environment, 110*, 29-44

Johnston, R.M., & Barson, M.M. (1993). Remote-Sensing of Australian Wetlands - an Evaluation of Landsat Tm Data for Inventory and Classification. *Australian Journal of Marine and Freshwater Research, 44*, 235-252

Jones, T.G., Coops, N.C, Arcese, P., & Sharma, T. (2012). Describing avifaunal richness with functional and structural bio-indicators derived from advanced airborne remotely sensed data. International Journal of Remote Sensing, In Press.

Judd, C., Steinberg, S., Shaughnessy, F., & Crawford, G. (2007). Mapping salt marsh vegetation using aerial hyperspectral imagery and linear unmixing in Humboldt Bay, California. *Wetlands, 27*, 1144-1152

Kao-Kniffin, J., Freyre, D.S., & Balser, T.C. (2010). Methane dynamics across wetland plant species. *Aquatic Botany 93*, 107-113

Keenan, T.F., Baker, I., Barr, A., Ciais, P., Davis, K., Dietze, M., Dragon, D., Gough, C.M. et al. (2012). Terrestrial biosphere model performance for inter-annual variability of land-atmosphere CO2 exchange. *Global Change Biology, 18*, 1971-1987

Khanna, S., Santos, M.J., Ustin, S.L., & Haverkamp, P.J. (2011). An integrated approach to a biophysiologically based classification of floating aquatic macrophytes. *International Journal of Remote Sensing, 32*, 1067-1094

Kim, M., Warner, T.A., Madden, M., & Atkinson, D.S. (2011). Multi-scale GEOBIA with very high spatial resolution digital aerial imagery: scale, texture and image objects. *International Journal of Remote Sensing, 32*, 2825-2850

Kirby, J.S., Stattersfield, A.J., Butchart, S.H.M., Evans, M.I., Grimmett, R.F.A., Jones, V.R., O'Sullivan, J., Tucker, G.M., & Newton, I. (2008). Key conservation issues for migratory land- and waterbird species on the world's major flyways. *Bird Conservation International, 18*, S49-S73

Knight, A.W., Tindall, D.R., & Wilson, B.A. (2009). A multitemporal multiple density slice method for wetland mapping across the state of Queensland, Australia. *International Journal of Remote Sensing, 30*, 3365-3392

Kwaiser, K.S. (2009). Accounting for observation uncertainty in species-habitat models: A case study using bird survey data from Poyang Lake, China. University of Michigan, Ann Arbor. 101 pp.

Kwoun, O.I., & Lu, Z. (2009). Multi-temporal RADARSAT-1 and ERS Backscattering Signatures of Coastal Wetlands in Southeastern Louisiana. *Photogrammetric Engineering and Remote Sensing, 75*, 607-617

Laba, M., Blair, B., Downs, R., Monger, B., Philpot, W., Smith, S., Sullivan, P., & Baveye, P.C. (2010). Use of textural measurements to map invasive wetland plants in the Hudson River National Estuarine Research Reserve with IKONOS satellite imagery. *Remote Sensing of Environment, 114*, 876-886

Laliberte, A.S., & Rango, A. (2009). Texture and Scale in Object-Based Analysis of Subdecimeter Resolution Unmanned Aerial Vehicle (UAV) Imagery. *IEEE Transactions on Geoscience and Remote Sensing, 47*, 761-770

Laliberte, A.S., Rango, A., Havstad, K.M., Paris, J.F., Beck, R.F., McNeely, R., & Gonzalez, A.L. (2004). Object-oriented image analysis for mapping shrub encroachment from 1937 to 2003 in southern New Mexico. *Remote Sensing of Environment, 93*, 198-210

Lavers, C., Haines, Young, R. & Avery, M. (1996). The habitat associations of dunlin (*Calidris alpina*) in the Flow Country of northern Scotland and an improved model for predicting habitat quality. *Journal of Applied Ecology, 33,* 279-290

Lawrence, R.L., & Ripple, W.J. (1999). Calculating change curves for multitemporal satellite imagery: Mount St. Helens 1980-1995. *Remote Sensing of Environment, 67*, 309-319

Legendre, P. (1993). Spatial autocorrelation - trouble or new paradigm. *Ecology, 74*, 1659-1673

Legendre, P., Dale, M.R.T., Fortin, M.J., Gurevitch, J., Hohn, M., & Myers, D. (2002). The consequences of spatial structure for the design and analysis of ecological field surveys. *Ecography, 25*, 601-615

Lenssen, J., Menting, F., van der Putten, W.H., & Blom, K. (1999). Control of plant species richness and zonation of functional groups along a freshwater flooding gradient. *Oikos, 86*, 523-534

Levine, M.D., & Nazif, A.M. (1985). Dynamic Measurement of Computer Generated Image Segmentations. *IEEE Transactions on Pattern Analysis and Machine Intelligence, 7*, 155-164

Leyequien, E., Verrelst, J., Slot, M., Schaepman-Strub, G., Heitkonig, I.M.A., & Skidmore, A. (2007). Capturing the fugitive: Applying remote sensing to terrestrial animal distribution and diversity (vol 9, pg 1). *International Journal of Applied Earth Observation and Geoinformation, 9*, 224-224

Li, J. (2009). Scientists Line Up Against Dam That Would Alter Protected Wetlands. *Science, 326,* 508-509

Li, L., Ustin, S.L., & Lay, M. (2005). Application of multiple endmember spectral mixture analysis (MESMA) to AVIRIS imagery for coastal salt marsh mapping: a case study in China Camp, CA, USA. *International Journal of Remote Sensing, 26*, 5193-5207

Li, R., & Liu, J. (2002). Wetland vegetation biomass estimation and mapping from Landsat ETM data: a case study of Poyang Lake. *Journal of Geographic Sciences 12,* 35-41

Liira, J., Feldmann, T., Maemets, H., & Peterson, U. (2010). Two decades of macrophyte expansion on the shores of a large shallow northern temperate lake-A retrospective series of satellite images. *Aquatic Botany, 93*, 207-215

Liu, D.S., & Xia, F. (2010). Assessing object-based classification: advantages and limitations. *Remote Sensing Letters, 1*, 187-194

Liu, G.H., Li, W., Li, E.H., Yuan, L.Y., & Davy, A.J. (2006a). Landscape-scale variation in the seed banks of floodplain wetlands with contrasting hydrology in China. *Freshwater Biology, 51*, 1862-1878

Liu, G.H., Li, W., Zhou, J., Liu, W.Z., Yang, D., & Davy, A.J. (2006b). How does the propagule bank contribute to cyclic vegetation change in a lakeshore marsh with seasonal drawdown? *Aquatic Botany, 84*, 137-143

Liu, M. (2009). Monitoring ephemeral vegetation in Poyang Lake using MODIS Remote Sensing Images. M.Sc. Thesis, the International Institute for Geo-information Science and Earth Observation, the Netherlands. 65 pp. *www.itc.nl/library/papers_2009/msc/nrm/liu.pdf*

Liu, X.P., Kelin, W., & Geli, Z. (2004). Perspectives and policies: Ecological industry

substitutes in wetland restoration of the Middle Yangtze. *Wetlands, 24*, 633-641
Lobell, D.B., & Asner, G.P. (2004). Cropland distributions from temporal unmixing of MODIS data. *Remote Sensing of Environment, 93*, 412-422
Lodge, D.M. (1991). Herbivory on Fresh-Water Macrophytes. *Aquatic Botany, 41*, 195-224
Lu, D., Mausel, P., Brondizio, E., & Moran, E. (2004). Change detection techniques. *International Journal of Remote Sensing, 25*, 2365-2407
Lunetta, R.S., Ediriwickrema, J., Johnson, D.M., Lyon, J.G., & McKerrow, A. (2002). Impacts of vegetation dynamics on the identification of land-cover change in a biologically complex community in North Carolina, USA. *Remote Sensing of Environment, 82*, 258-270
Mallinis, G., Koutsias, N., Tsakiri-Strati, M., & Karteris, M. (2008). Object-based classification using Quickbird imagery for delineating forest vegetation polygons in a Mediterranean test site. *ISPRS Journal of Photogrammetry and Remote Sensing, 63*, 237-250
Marie, T., Lai, X., Huber, C., Chen, X., Uribe, C., Huang, S., Lacaux, J-P., Lafaye, M., & Yesou, H. (2010). Monitoring temporal evolution of the presence intermediate host of the Schistosomiasis and its risk transmission based on DRAGON times series in Poyang Lake area, Jiangxi province, P.R. China. *In:* ESA SP 686, *Proceedings of "Living Planet Symposium"*, 27 June – 2 July 2010, Bergen, Norway.
Markkola, J., Iwabuchi, S, Gang, L., Aarvak, T., Tolvanen, P., & Øien, I.J. (1999). Lesser White-fronted Goose Survey at the East Dongting and Poyang Lakes in China. In P. Tolvanen, I.J. Øien & K. Ruokolainen (Eds.), *Fennoscandian Lesser White-fronted Goose Conservation Project Annual Report 1999* (pp.9-15). Helsinki, Finland: WWF
Mas, J.F. (1999). Monitoring land-cover changes: a comparison of change detection techniques. *International Journal of Remote Sensing, 20*, 139-152
McCarthy, J., Gumbricht, T., & McCarthy, T.S. (2005). Ecoregion classification in the Okavango Delta, Botswana from multitemporal remote sensing. *International Journal of Remote Sensing, 26*, 4339-4357
McCleary, A.L., Crews-Meyer, K.A., & Young, K.R. (2008). Refining forest classifications in the western Amazon using an intra-annual multitemporal approach. *International Journal of Remote Sensing, 29*, 991-1006
McFeeters, S.K. (1996). The use of the normalized difference water index (NDWI) in the delineation of open water features. *International Journal of Remote Sensing, 17*, 1425-1432
Melillo, J.M., Mcguire, A.D., Kicklighter, D.W., Moore, B., Vorosmarty, C.J., & Schloss, A.L. (1993). Global Climate-Change and Terrestrial Net Primary Production. *Nature, 363*, 234-240
Mertens, B., & Lambin, E.F. (2000). Land-cover-change trajectories in southern Cameroon. *Annals of the Association of American Geographers, 90*, 467-494
Michishita, R., Xu, B., & Gong, P. (2008). A decision tree classifier for the monitoring of wetland vegetation using ASTER data in the Poyang Lake region, China. *The International Archives of the Photogrammetry, Remote Sensing and Spatial Information Sciences, 37B8,* 315-321.
Michishita, R., Gong, P., & Xu, B. (2012). Spectral mixture analysis for bi-sensor wetland mapping using Landsat TM and Terra MODIS data. *International Journal of Remote Sensing, 33*, 3373-3401
Millennium Ecosystem Assessment. (2005). Ecosystems and Human Well-being: Wetlands and Water Synthesis. World Resources Institute, Washington, DC
Miller, R. L., & Fujii, R. (2010). Plant community, primary productivity, and environmental conditions following wetland re-establishment in the Sacramento-San Joaquin Delta,

California. *Wetlands Ecology and Management, 18*, 1-16
Miller, J., Franklin, J., & Aspinall, R. (2007). Incorporating spatial dependence in predictive vegetation models. *Ecological Modelling, 202*, 225-242
Mitchell, S.F., & Perrow, M.R. (1998). Interactions between grazing birds and macrophytes. In: E. Jeppesen, M. Søndergaard, K. Christoffersen (Eds.), *The Structuring Role of Submerged Macrophytes in Lakes* (pp. 175–196). New York: Springer
Mitsch, W.J., & Gosselink, J.G. (2000). The value of wetlands: importance of scale and landscape setting. *Ecological Economics, 35*, 25-33
Na, X.D., Zhang, S.Q., Zhang, H.Q., Li, X.F., Yu, H., & Liu, C.Y. (2009). Integrating TM and Ancillary Geographical Data with Classification Trees for Land Cover Classification of Marsh Area. *Chinese Geographical Science, 19*, 177-185
National Climatic Data Center, U.S. Department of Commerce. http://www.ncdc.noaa.gov/oa/mpp/freedata.html. Global Summary of the Day (GSOD) data. Accessed June 28, 2011.
Nicholls, R.J., Hoozemans, F.M.J., & Marchand, M. (1999). Increasing flood risk and wetland losses due to global sea-level rise: regional and global analyses. *Global Environmental Change-Human and Policy Dimensions, 9*, S69-S87
Niu, Z.G., Gong, P., Cheng, X., Guo, J.H., Wang, L., Huang, H.B., Shen, S.Q., Wu, Y.Z., Wang, X.F., Wang, X.W., Ying, Q., Liang, L., Zhang, L.N., Wang, L., Yao, Q., Yang, Z.Z., Guo, Z.Q., & Dai, Y.J. (2009). Geographical characteristics of China's wetlands derived from remotely sensed data. *Science in China Series D-Earth Sciences, 52*, 723-738
Nøhr, H. & Jørgensen, A.F. (1997). Mapping of biological diversity in Sahel by means of satellite image analyses and ornithological surveys. *Biodiversity and Conservation, 6,*545-566
Ollinger, S.V. (2011). Sources of variability in canopy reflectance and the convergent properties of plants. *New Phytologist, 189*, 375-394
Ordoyne, C., & Friedl, M.A. (2008). Using MODIS data to characterize seasonal inundation patterns in the Florida Everglades. *Remote Sensing of Environment, 112*, 4107-4119
Ouyang, Z.T., Zhang, M.Q., Xie, X., Shen, Q., Guo, H.Q., & Zhao, B. (2011). A comparison of pixel-based and object-oriented approaches to VHR imagery for mapping saltmarsh plants. *Ecological Informatics, 6*, 136-146
Ozdogan, M. (2010). The spatial distribution of crop types from MODIS data: Temporal unmixing using Independent Component Analysis. *Remote Sensing of Environment, 114*, 1190-1204
Ozesmi, S.L., & Bauer, M.E. (2002). Satellite remote sensing of wetlands. *Wetlands Ecology and Management, 10*, 381-402
Parmesan, C. (2006). Ecological and evolutionary responses to recent climate change. *Annual Review of Ecology Evolution and Systematics, 37*, 637-669
Pearcy, R.W., & Ehleringer, J. (1984). Comparative Ecophysiology of C-3 and C-4 Plants. *Plant Cell and Environment, 7*, 1-13
Pezeshki, S.R. (2001). Wetland plant responses to soil flooding. *Environmental and Experimental Botany, 46*, 299-312
Pringle, R.M., Syfert, M., Webb, J.K., & Shine, R. (2009). Quantifying historical changes in habitat availability for endangered species: use of pixel- and object-based remote sensing. *Journal of Applied Ecology, 46*, 544-553
Qi, S.H., Brown, D.G., Tian, Q., Jiang, L.G., Zhao, T.T., & Bergen, K.A. (2009). Inundation Extent and Flood Frequency Mapping Using LANDSAT Imagery and Digital Elevation

Models. *Giscience & Remote Sensing, 46*, 101-127
Qian, F., Yu, C. & Jiang, H. (2009). Ground and aerial surveys of wintering waterbirds in Poyang Lake basin. Proceedings of the UNEP/GEF Siberian Crane Wetland Project – Project Completion Workshop. 14-15 October 2009, Harbin, China. 13 p. http://www.scwp.info/proceedings/Final%20Papers/8%20%20Aerial%20and%20Ground%20Surveys%20of%20Wintering%20Waterbirds%20in%20Poyang.pdf Accessed 24 October 2012
Ramsar. (2009). Ramsar Sites Database. Accessed 24 October 2012. http://ramsar.wetlands.org/Database/Searchforsites/tabid/765/language/en-US/Default.aspx
Randerson, J.T., Hoffman, F.M., Thornton, P.E., Mahowald, N.M., Lindsay, K., Lee, Y.H., Nevison, C.D., Doney, S.C., Bonan, G., Stockli, R., Covey, C., Running, S.W., & Fung, I.Y. (2009). Systematic assessment of terrestrial biogeochemistry in coupled climate-carbon models. *Global Change Biology, 15*, 2462-2484
Rebelo, L.M., Finlayson, C.M., & Nagabhatla, N. (2009). Remote sensing and GIS for wetland inventory, mapping and change analysis. *Journal of Environmental Management, 90*, 2144-2153
Ribed, P.S., & Lopez, A.M. (1995). Monitoring Burnt Areas by Principal Components-Analysis of Multitemporal Tm Data. *International Journal of Remote Sensing, 16*, 1577-1587
Richardson, A.D., Braswell, B.H., Hollinger, D.Y., Jenkins, J.P., & Ollinger, S.V. (2009). Near-surface remote sensing of spatial and temporal variation in canopy phenology. *Ecological Applications, 19*, 1417-1428
Richmond, O.M.W. (2011). *Inferring ecological relationships from occupancy patterns for California Black Rails in the Sierra Nevada foothills*. PhD Dissertation, University of California Berkeley. 107 pp.
Rokitnicki-Wojcik, D., Wei, A.H., & Chow-Fraser, P. (2011). Transferability of object-based rule sets for mapping coastal high marsh habitat among different regions in Georgian Bay, Canada. *Wetlands Ecology and Management, 19*, 223-236
Roshier, D.A., Robertson A.I. & Kingsford R.T. (2002). Responses of waterbirds to flooding in an arid region of Australia and implications for conservation. *Biological Conservation, 106,*399-411.
Sanchez-Hernandez, C., Boyd, D.S., & Foody, G.M. (2007). Mapping specific habitats from remotely sensed imagery: Support vector machine and support vector data description based classification of coastal saltmarsh habitats. *Ecological Informatics, 2*, 83-88
Sculthorpe, C.D. (1967). *The Biology of Aquatic Vascular Plants*. Edward Arnold Publishers, Limited, London. 1985 reprint, Koeltz Scientific Books, Königstein, West Germany.
Seto, E., Xu, B., Liang, S., Gong, P., Wu, W.P., Davis, G., Qiu, D.C., Gu, X.G., & Spear, R. (2002a). The use of remote sensing for predictive modeling of schistosomiasis in China. *Photogrammetric Engineering and Remote Sensing, 68*, 167-174
Seto, K.C., Woodcock, C.E., Song, C., Huang, X., Lu, J., & Kaufmann, R.K. (2002b). Monitoring land-use change in the Pearl River Delta using Landsat TM. *International Journal of Remote Sensing, 23*, 1985-2004
Shankman, D., Keim, B.D., & Song, J. (2006). Flood frequency in China's Poyang Lake region: Trends and teleconnections. *International Journal of Climatology, 26*, 1255-1266
Shen, G.Z., Guo, H.D., & Liao, J.J. (2008). Object oriented method for detection of inundation extent using multi-polarized synthetic aperture radar image. *Journal of Applied Remote Sensing, 2*, 023512, doi:10.1117/1.2911669
Singh, A. (1989). Digital change detection techniques using remotely sensed data. *International*

Journal of Remote Sensing, 10, 989–1003
Soares, V. P., & Hoffer, R. M. (1994). Eucalyptus forest change classification using multi-data Landsat TM data. *Proceedings, International Society of Optical Engineering (SPIE), 2314,* 281–291
Sonnentag, O., Hufkens, K., Teshera-Sterne, C., Young, A.M., Friedl, M., Braswell, B.H., Milliman, T., O'Keefe, J., & Richardson, A.D. (2012). Digital repeat photography for phenological research in forest ecosystems. *Agricultural and Forest Meteorology, 152*, 159-177
Taft, O.W., Colwell, M.A., Isola, C.R., & Safran, R.J. (2002). Waterbird responses to experimental drawdown: implications for the multispecies management of wetland mosaics. *Journal of Applied Ecology, 39*, 987-1001
Thuiller, W., Albert, C., Araujo, M.B., Berry, P.M., Cabeza, M., Guisan, A., Hickler, T., Midgely, G.F., Paterson, J., Schurr, F.M., Sykes, M.T., & Zimmermann, N.E. (2008). Predicting global change impacts on plant species' distributions: Future challenges. *Perspectives in Plant Ecology Evolution and Systematics, 9*, 137-152
Tian, B., Zhou, Y.X., Zhang, L.Q., & Yuan, L. (2008). Analyzing the habitat suitability for migratory birds at the Chongming Dongtan Nature Reserve in Shanghai, China. *Estuarine Coastal and Shelf Science, 80*, 296-302
Tobler, W. R. (1970). A computer movie simulating urban growth in the Detroit region. *Economic Geography*, *46*, 234–40.
Townsend, P.A., & Walsh, S.J. (2001). Remote sensing of forested wetlands: application of multitemporal and multispectral satellite imagery to determine plant community composition and structure in southeastern USA. *Plant Ecology, 157*, 129-149A
Turner, D.P., Cohen, W.B., Kennedy, R.E., Fassnacht, K.S., & Briggs, J.M. (1999). Relationships between leaf area index and Landsat TM spectral vegetation indices across three temperate zone sites. *Remote Sensing of Environment, 70*, 52-68
Turner, D.P., Ollinger, S.V., & Kimball, J.S. (2004). Integrating remote sensing and ecosystem process models for landscape- to regional-scale analysis of the carbon cycle. *Bioscience, 54*, 573-584
Turner, W., Spector, S., Gardiner, N., Fladeland, M., Sterling, E., & Steininger, M. (2003). Remote sensing for biodiversity science and conservation. *Trends in Ecology & Evolution, 18*, 306-314
Tuxen, K., & Kelly, N.M. (2008). Multi-scale functional mapping of tidal wetlands: an object-based approach. Chapter in Object-based Image Analysis: Spatial concepts for knowledge driven remote sensing applications. Pp. 415-442 in Thomas Blaschke, Stefan Lang and Geoffrey Hay (Editors). *Springer Lecture Notes in Geoinformation and Cartography*
Tzotsos, A. (2006). A support vector machine approach for object based image analysis. Proceedings of the 1st International Conference on Object-based Image Analysis (OBIA 2006).
Ustin, S.L., & Gamon, J.A. (2010). Remote sensing of plant functional types. *New Phytologist, 186*, 795-816
Vågen, T.G. (2006). Remote sensing of complex land use change trajectories - a case study from the highlands of Madagascar. *Agriculture Ecosystems & Environment, 115*, 219-228
Vierling, L. A., Baldocchi, D. D., Coops, N. C., Eitel, J., Friedl, M. A., Gamon, J. A., Garrity, S. R., Hilker, T., Huemmrich, K. F., Richardson, A. D., Schaaf, C., Sonnentag, O., Tweedie, C. E. (2011). Beyond Greenness: Towards a Continuous Phenology of Vegetation. American

Geophysical Union, Fall Meeting 2011, abstract #B43A-0273, poster presentation.
Walker, S., Wilson, J.B., Steel, J.B., Rapson, G.L., Smith, B., King, W.M., & Cottam, Y.H. (2003). Properties of ecotones: Evidence from five ecotones objectively determined from a coastal vegetation gradient. *Journal of Vegetation Science, 14*, 579-590
Wang, L., Dronova, I., Gong, P., Yang, W., Li, Y., & Liu, Q. (2012). A new time-series vegetation-water index of phenological-hydrological trait across species and functional types for Poyang Lake wetland ecosystem. *Remote Sensing of Environment, 125,* 49-63
Wang, L., Sousa, W.P., & Gong, P. (2004). Integration of object-based and pixel-based classification for mapping mangroves with IKONOS imagery. *International Journal of Remote Sensing, 25*, 5655-5668
Wang L., Gong P., & Dronova, I. Aquatic PFT classification using time series Envisat ASAR data and Beijing-1 imagery over Poyang Lake, China. Under review.
Webb, E.B., Smith, L.M., Vrtiska, M.P., & Lagrange, T.G. (2010). Effects of Local and Landscape Variables on Wetland Bird Habitat Use During Migration Through the Rainwater Basin. *Journal of Wildlife Management, 74*, 109-119
Weismiller, R.A., Kristof, S.J., Scholz, D.K., Anuta, P.E., & Momin, S.A. (1977). Change Detection in Coastal Zone Environments. *Photogrammetric Engineering and Remote Sensing, 43*, 1533-1539
Wetzel, R.G. (2001). Limnology: Lake and River Ecosystems. Third Edition. Academic Press.
Witten, I.H., & Frank, E. (2005). Data Mining: Practical Machine Learning Tools and Technology, (2nd ed.), Elsevier, San Francisco
Wright, C., & Gallant, A. (2007). Improved wetland remote sensing in Yellowstone National Park using classification trees to combine TM imagery and ancillary environmental data. *Remote Sensing of Environment, 107*, 582-605
Wu, G. (2008). Impact of human activities on water level and clarity and underwater light climate of *Vallisneria spiralis* L. in Poyang Lake, China. Wageningen University 2008. ITIC Dissertation. 117 pp.
Wu Y, Ji W. (2002). Researches on Jiangxi Poyang Lake National Nature Reserve. Beijing: China Forestry Press.
Wu, Z. Y., P. H. Raven & Hong, D. Y., eds. (1994-). Flora of China. Science Press, Beijing, and Missouri Botanical Garden Press, St. Louis. [http://www.efloras.org/]
Xiao, J.F., Zhuang, Q.L., Baldocchi, D.D., Law, B.E., Richardson, A.D., Chen, J.Q., Oren, R., et al. (2008). Estimation of net ecosystem carbon exchange for the conterminous United States by combining MODIS and AmeriFlux data. *Agricultural and Forest Meteorology, 148*, 1827-1847
Xing, Y.P., Xie, P., Yang, H., Wu, A.P., & Ni, L.Y. (2006). The change of gaseous carbon fluxes following the switch of dominant producers from macrophytes to algae in a shallow subtropical lake of China. *Atmospheric Environment, 40*, 8034-8043
Yoder, B.J., & Waring, R.H. (1994). The Normalized Difference Vegetation Index of Small Douglas-Fir Canopies with Varying Chlorophyll Concentrations. *Remote Sensing of Environment, 49*, 81-91
Yu, Q., Gong, P., Clinton, N., Biging, G., Kelly, M., & Schirokauer, D. (2006). Object-based detailed vegetation classification with airborne high spatial resolution remote sensing imagery. *Photogrammetric Engineering and Remote Sensing, 72*, 799-811
Yu, Q., Gong, P., Tian, Y.Q., Pu, R.L., & Yang, J. (2008). Factors affecting spatial variation of classification uncertainty in an image object-based vegetation mapping. *Photogrammetric*

Engineering and Remote Sensing, 74, 1007-1018
Zedler, J.B., & Kercher, S. (2004). Causes and consequences of invasive plants in wetlands: Opportunities, opportunists, and outcomes. *Critical Reviews in Plant Sciences, 23*, 431-452
Zeng, Y., Liu Y., Liu Y., & de Leeuw J. (2007). Mapping grass communities based on multi-temporal Landsat TM imagery and environmental variables. Geoinformatics 2007: Remotely Sensed Data and Information, edited by Weimin Ju, Shuhe Zhao. Proceedings of SPIE Vol. 6752 67521K-1.
Zhang, W., Cao, X., & Peng, J. (2008). Analyzing the 2007 drought of Poyang Lake Watershed with MODIS-derived normalized difference water deviation index. *Proceedings SPIE 7083, 70831G,* Remote Sensing and Modeling of Ecosystems for Sustainability V, San Diego, CA, 13 August 2008. doi 10.1117/12.797552
Zhang, S.Q., Na, X.D., Kong, B., Wang, Z.M., Jiang, H.X., Yu, H., Zhap, Z.C., Li, X.F., Liu, C.Y., & Dale, P. (2009). Identifying Wetland Change in China's Sanjiang Plain Using Remote Sensing. *Wetlands, 29*, 302-313
Zhao, M.J., Cong, P.H., Barter, M., Fox, A.D., & Cao, L. (2012). The changing abundance and distribution of Greater White-fronted Geese *Anser albifrons* in the Yangtze River floodplain: impacts of recent hydrological changes. *Bird Conservation International, 22*, 135-143
Zhao, X., Stein, A., & Chen, X.L. (2011). Monitoring the dynamics of wetland inundation by random sets on multi-temporal images. *Remote Sensing of Environment, 115*, 2390-2401
Zheng, J.M., Wang L.Y., Li S.Y., Zhou J.X., & Sun, Q.X. (2009). Relationship between community type of wetland plants and site elevation on sandbars of the East Dongting Lake, China. *Forestry Studies in China, 11*, 44-48.
Zheng, Y. (2009). Prediction of the distribution of C3 and C4 plant species from a GIS-based model: a case study in Poyang Lake, China. M.Sc. Thesis, ITC, Enschede, the Netherlands.
Zhong, L.H., Hawkins, T., Biging, G.S., & Gong, P. (2011). A phenology-based approach to map crop types in the San Joaquin Valley, California, *International Journal of Remote Sensing, 32,* 7777-7804